



International Journal of

Young Scientist Research

Vol 5, No1, Dec 2021

ISSN: 2588-5111

Contents

Falling Tower	3
Irreversible Cartesian Diver	4
The Intelligent Diagnosis and Treatment.....	11
Magnetic Field	16
Epidemiology (Covid-19)	19
Genotoxic and Cytogenic Effect of Four Loko in Human Cells.....	23
Augmented Reality as a Didactic Tool in Education	27
The Effect of Salt on Ice Melting (33-35)	33
Slope Warning System	36
The Effect of Biofilters on Water Quality Parameters and.....	38
Nephron Model For Course Teaching Material Purpose.....	44
The Coefficient of Restitution of Rebounding Capsules	48
ZEPHYROS a Habitat on Mars	51
A New Sampler Invention.....	53

Young Scientist Research

Editor in Chief:

Dr. Dina Izadi

Physics Education, National Polytechnic Institute
IPN, Mexico

Researcher & President, AYIMI & ADIB
info@ayimi.org
dinaocean@gmail.com

Associated Editors

Dr. Masoud Torabi Azad

Professor, Physical Oceanography,
Islamic Azad University &
Board Member, AYIMI
torabi_us@yahoo.com

Nona Izadipannah

Geophysicist, Scientific Committee &
Board Member, AYIMI
daisyip67@gmail.com

Dr. Cesar Eduardo Mora Ley

Professor, Physics Education, National
Polytechnic Institute, IPN, and
CICATA Principal , Mexico
ceml36@gmail.com

Dorna Izadipannah

Microbiologist, Scientific Committee &
Board Member, AYIMI
dorna_izadipannah@yahoo.com

Dr. Carmen del Pilar Suarez Rodriguez

Faculty Member, Physics Education,
UASLP, Universidad Autónoma
de San Luis Potosi, Mexico
pilar.suarez@uaslp.mx

Aria Izadi

Mechanical Engineering at
Sheffield Hallam University, UK
aria.izadi.uk@gmail.com

Ümit Karademir,

Dr. Cansu İlke KURU ,

Dr. Meltem Gönülol Çelikoğlu and

Belit Karaca

Buca Municipality Kızılçullu Science and
Art Center, Turkey
info@bucaimsef.org

Designers:

Dorna Izadipannah
Nona Izadipannah

Address:

Unit 14, No.32, Malek Ave., Shariati St.

Post Code: 1565843537

Tel:+9821-77507013, 77522395

YOUNG SCIENTIST RESEARCH
Journal in Science Education
ISSN: 2588-5111

WELCOME TO THE INTERNATIONAL JOURNAL of YOUNG SCIENTIST RESEARCH

Young Scientist Research is a research journal based on scientific projects and we are pleased to present our students' work in scientific activities. This open-access journal includes young students' research in any field of science which publishes full-length and abstract research on any aspects of applied sciences in relation to work presented in both national and international conferences, competitions and tournaments of all types.

Programs that have educational opportunities for high school students to present their distinguished projects from regional, national and international events such as International Conference of Young Scientists (ICYS), International / Persian Young Physicists' Tournament (IYPT/ PYPT), International / Iran Physics' Tournament (IPT/ IRPT), International Music , Science , Engineering Fair (IMSEF).

New manuscripts sent to the Journal will be handled by the Editorial Office who checks compliance with the guidelines to authors. Then a rapid screening process at which stage a decision to reject or to go to full review is made.

By submission of a manuscript to the Journal, all authors warrant that they have the authority to publish the material and that the paper, or one substantially the same, has neither been published previously, nor is being considered for publication elsewhere.

This journal belongs to Ariaian Young Innovative Minds Institute, AYIMI, and one to two issues are published in a year. All details are on the YOUNG SCIENTIST RESEARCH Journal website (<http://journal.ayimi.org>)

Editor in Chief
Dr. Dina Izadi
Researcher & President of
AYIMI , International Research Institute
ADIB, Cultural and Artistic Institute
<http://www.ayimi.org>
<http://adib.ayimi.org>
<http://journal.ayimi.org>
Email: info@ayimi.org
Unit 14, No. 32, Malek Ave., Shariati St.,
Post Code: 1565843537
Young Scientist Research Journal, ISSN: 2588-5111
Tehran/ Iran



CURRENT ISSUE
Vol 5 NO 1 DEC 2021

COPYRIGHT © INTERNATIONAL JOURNAL OF YOUNG
SCIENTIST RESEARCH (<http://journal.ayimi.org>)

FALLING TOWER

Sahar Semsarha ,Farzanegan2 high school, Tehran/ Iran, sahar.sems@gmail.com

ABSTRACT

This research is about the motion of identical discs that are stacked on top of each other when we apply a sudden horizontal force to the bottom disc, the tower might remain standing. We are going to investigate in which cases the tower will remain standing and rigid, not rigid or it will fall. Is it affected by the friction between the discs or other parameters?

Key Words Tower, Discs, Force, Friction

ARTICLE INFO

Participated in O-IYPT2020

Accepted in country selection by Ariaian Young

Innovative Minds Institute , AYIMI

http://www.ayimi.org_info@ayimi.org

1 Introduction

This experiment is about the motion of identical discs that are stacked on top of each other if we apply a sudden horizontal force to the bottom disc, the tower might remain standing.

When the sudden force is applied to the tower, other discs will start to move versus each other. If the center of mass of the discs passes through the last point of the bottom disc more than a critical time, the tower will topple because of the torque which is applied to the discs of the tower (Fig.1).

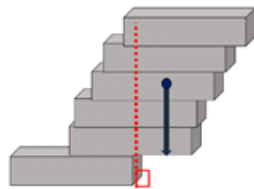


Fig. 1: Falling tower modeling (passing through the last point of the bottom disc)

Three kinds of movement have been observed in experimental results. The first kind was when we applied the sudden force to the bottom disc and the tower remain standing and also the movement between the discs of the tower is insignificant so we can consider it as a rigid body. The second kind is when the tower will remain standing but the movement between the discs of the tower is significant. This situation show the tower had the tendency to fall down and the third was when the tower topple (Fig. 2 a-c).

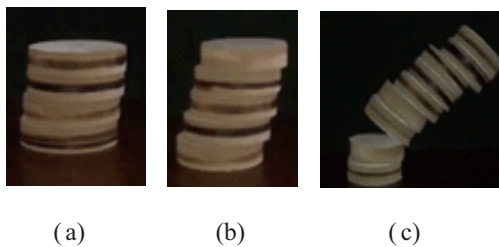


Fig. 2: a) Rigid body tower, b) Not Rigid body tower
c) Falling tower

In this paper, we are going to investigate in which cases the tower will remain standing and rigid, not rigid or it will fall.

2 Theory and Experiment

In experimental setup, the sudden force has been applied to the bottom disc with a ruler and some wooden discs are used as tower. The thickness of the discs was 1.5cm with different diameters (4,6,8,10cm).

2-1 Pattern of the Tower

When the sudden force is applied to the bottom disc the force will be transferred to the other discs as well but this transformation will happen with delay, so the first disc will start to move sooner than the other discs and it makes the distance between first discs to be shorter rather than the last discs as the pattern is observed in Figure (3).

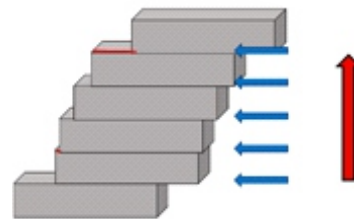


Fig. 3: Pattern of the tower after transformation

2-2 Rigid Body Tower

We need to prevent this transformation with delay to have a rigid body tower. To avoid this transformation, the second disc must not start to move and accelerate. So the summation of the forces affecting the second disc must be zero (Fig. 4).

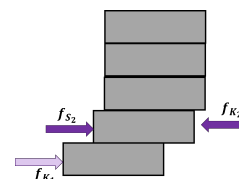


Fig. 4: Second disc free diagram

According to equations (1-3) the static friction affecting the disc from the upper discs and the kinetic friction from the lower disc must be equal to each other.

$$f_{K2} = mg\mu_k(n - 1) \tag{1}$$

$$f_{S2} < mg\mu_s(n - 2) \tag{2}$$

$$f_{K2} = f_{S2} \tag{3}$$

so:

$$\frac{n - 1}{n - 2} < \frac{\mu_s}{\mu_k} \tag{4}$$

By decreasing the amount of S the second disc will move less so the possibility of staying rigid will increase as well (Eq. 4). S have been investigated in different cases (Fig. 5).

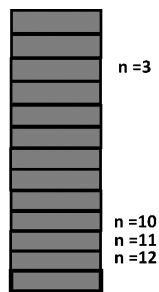


Fig. 5: Investigating the number of the discs

As much as the number of the discs increases, S will decrease (Eq. 5). Also the inertia of the tower will increase as well so in high tower, hitting the bottom disc makes the angular acceleration of the tower less (Eq.6). So increasing the number of the discs increases the possibility of staying rigid as well (Fig. 6).

$$\frac{n - 1}{n - 2} \Rightarrow \frac{11}{10} < \frac{10}{9} < \frac{9}{8} < \frac{2}{1} < \frac{\mu_s}{\mu_k} \tag{5}$$

$$\tau = I\alpha \tag{6}$$



Fig. 6: The second disc doesn't move a lot because of the high number of the discs

But when the number of the discs decrease, the pattern can be observed. According to Figure (7) the acceleration of the discs are equal to each other. So when the amount of S increases the tower will not stay rigid.

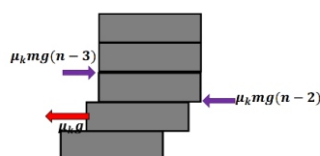


Fig. 7: Final pattern of the tower with low number of the discs

2-3 Falling Tower

The toppling will happen in not rigid cases after the pattern is observed. The center of mass of this pattern must

be investigated.

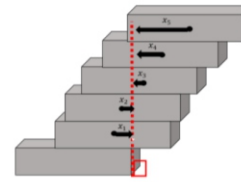


Fig. 8: Place of the center of mass

If the summation of x is more than zero (that means the center of mass of the tower passes through the last point of the bottom disc is more than a critical time), the tower will topple when it is still over the bottom disc (Eq.7).

$$\frac{\sum_2^n x}{n - 1} > 0 \tag{7}$$

When the tower is coming down, it will hit the bottom disc for a short time This phenomenon will change the angle of the tower and it makes the torque to be applied to the disc of the tower. Torque makes the discs of the tower to move versus each other so the place of the center of mass must be investigated again.

If the equation (7) become more than zero in figure (9) the tower will topple in the moment that it hits the ground. Otherwise the tower will remain standing in a not rigid pattern (Fig. 10).

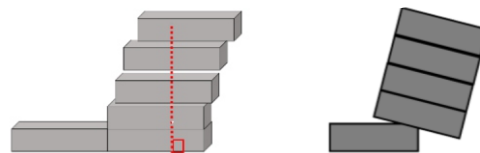


Fig. 9 : Changing the angle of the tower



Fig.10: not rigid tower

3 Effective Parameters

Some effective parameters are introduced in this section. also the effect of the parameters on possibility of toppling has been explained.

3-1 Friction Coefficient between the Discs

According to Fig. (11), the acceleration given to discs is equal to $\mu_k g$.

When we increase μ_k the acceleration given to each disc will increase. That makes the second disc to have a greater velocity. So the distance between the discs will increase and a not rigid pattern can be observed and this increases the possibility of toppling.

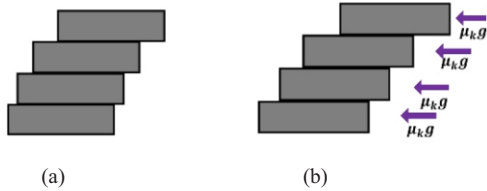


Fig. 11: a) Lower friction modeling, b) Higher friction modeling

3-2 Mass of the Discs

From equation (7) we concluded when mass of each disc increases the inertia of the tower increase. So the angle of the tower doesn't change when it hits the bottom disc and the possibility of toppling decreases.

3-3 Radius of Each Disc

In cases that the radius of each disc is high, the tower will be stable. The duration that the center of mass of the tower passes through the last point of the bottom disc will less than a critical time. But when the radius decreases the center of mass passes through the red line sooner so the tower will topple (Fig. 12).

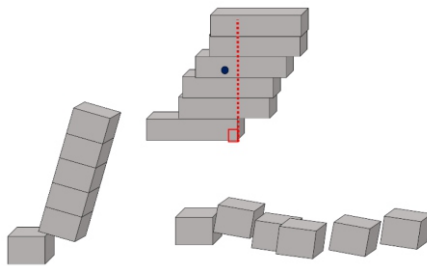


Fig. 12: Different radius of the discs

3-4 Speed of the Hand

When the speed of the hand is low, the duration that the tower and the bottom disc are touched with each other will increase (Eq. 8). So the second disc will have a greater velocity and not rigid pattern will be observed and that makes the tower to topple.

$$\mu_k g \Delta T = v \tag{8}$$

4 Experimental Procedures

4-1 Number of the Discs and Radius of each Disc

Different number of the discs have been investigated (4 cm diameter) of each disc (Fig. 13).

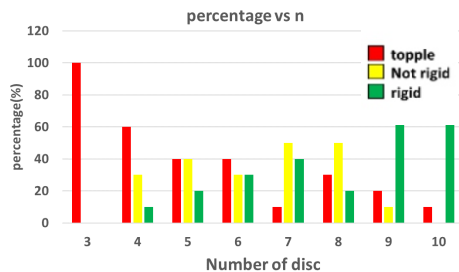


Fig. 13: Possibility of toppling per Number of the discs(4cm)

As much as the number of the discs increases the S will decrease and it makes the tower to remain standing. It is also the same in figure (13) the possibility of staying rigid increases with number of the discs. When the radius of each disc increases, possibility of toppling increases with the number of the discs (Fig. 14).

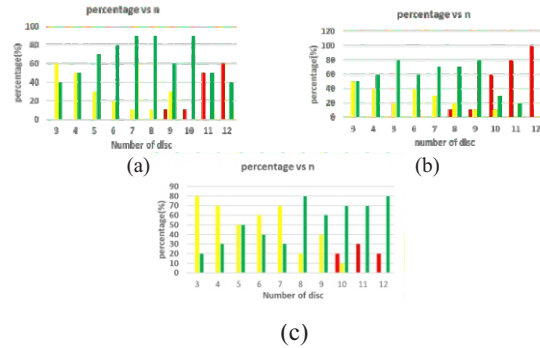


Fig. 14: . Possibility of toppling per Number of the discs, a) 8cm; b)10 cm; c) 6 cm

When the radius of the discs increases, the tower will have a stable situation so increasing the number of the discs will make it stable to a critical point. After that critical point, the effect of the speed of the hand will be important. When the speed of the hand is low the tower will topple because the second disc will have a high velocity otherwise the tower will remain standing.

4-2 Changing the Friction Coefficient

Some papers have been attached to the discs to change the friction coefficient. Therefore, when the friction coefficient is high the acceleration of the discs increases and the possibility of toppling increases as well and this matches the charts.

4-3 Height of Each Disc

Two discs have been attached to each other to increase the height of each disc. When the height of each disc increases, n will decrease so S decrease and the tower will topple (Fig. 15).

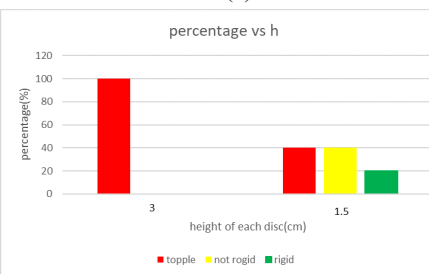
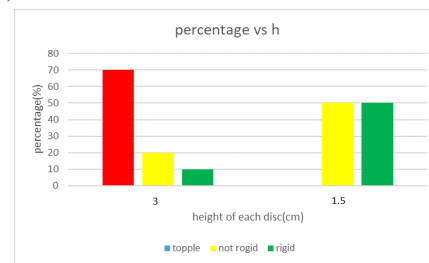


Fig. 15: F32. Possibility of toppling per height of the discs , a) 6cm; b) 4 cm

In all , discs in 3cm height had a higher possibility of toppling rather than 1.5 cm.

[6] <https://www.youtube.com/watch?reload=9&v=PcGIUZZWoVc>

5 Ratio

A variable has been defined to conclude the effect of height and radius of the discs.

$$\text{ratio} = \frac{\text{height of the tower}}{\text{Diameter of the bottom disc}}$$

It can be concluded that by increasing the ratio, the possibility of toppling increases as well but the slope is decreasing after a while (Fig. 16) . That is because of the inertia. When the number of the discs is higher than a critical number, the inertia of the tower affects the tower a lot so the tower will not rotate when it hits the bottom disc. So the possibility of toppling will start to decrease again when the number of the discs increases.

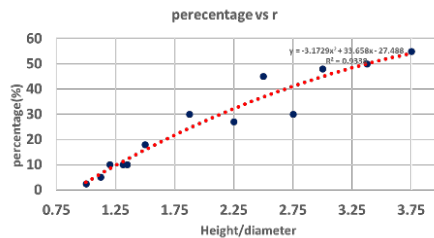


Fig 16: Possibility of toppling in each ratio

6 Conclusion

Three kinds of movement have been observed in this phenomenon. Rigid body, not rigid body and toppling. The pattern of the tower has been explained. These kinds of movement have been explained according to the theory. We found in which cases there is a rigid body or not rigid body and also in which cases the tower will topple.

Some affective parameters have been investigated theoretically and experimentally and possibility of toppling have been investigated too.

When we increase μ_k the acceleration given to each disc will increase. That makes the second disc to have a greater velocity. So the distance between discs will increase and a not rigid pattern can be observed and this increases the possibility of toppling.

In cases that the radius of each disc is high, the tower will be stable. The duration that the center of mass of the tower passes through the last point of the bottom disc will be less than a critical time. But when the radius decreases the center of mass passes through the red line sooner so the tower will topple.

When the height of each disc increases, n will decrease in so S decreases and the tower will topple.

References

- [1] D.Halliday , R.Resnick ,J.Walker. Fundamentals of Physics. John Wiley & Sons. (1923)
- [2] The Feynman Lectures on Physics Vol I. Addison Wesley. Richard Feynman (1970).
- [3] "Memoir on Heat", Académie Royale des Sciences pp. Lavoisier, A.L. & Laplace, P.S. (1780)
- [4] On the shoulders of merchants: exchange and the mathematical conception of nature in early modern Europe. Hadden, Richard W. (1994).
- [5] Michael Weiss and John Baez. "Is Energy Conserved in General Relativity?". Retrieved 5 Jan 2017

IRREVERSIBLE CARTESIAN DIVER

Mouzhah Moinian , Farzanegan 7 high school, Tehran/ Iran, reymah2001@yahoo.com

ABSTRACT

This problem wants to investigate a simple Cartesian diver which is placed in a long vertical tube filled with water. Increasing the pressure in the tube forces the Cartesian diver to sink. When it reaches a certain depth, it never returns to the surface even if the pressure is changed back to its initial value. We are going to find how it depends on relevant parameters such as pressure, depth, initial velocity and other parameters.

Key Words: Cartesian diver, Pressure, Depth, Velocity

ARTICLE INFO

Participated in IYPT2021 , Georgia, Tbilisi

Accepted in country selection by Ariaian Young

Innovative Minds Institute , AYIMI

http://www.ayimi.org_info@ayimi.org

1 Introduction

The problem statement says “ A simple Cartesian diver (e.g. an inverted test tube partially filled with water) is placed in a long vertical tube filled with water. Increasing the pressure in the tube forces the Cartesian diver to sink. When it reaches a certain depth, it never returns to the surface even if the pressure is changed back to its initial value. Investigate this phenomenon and how it depends on relevant parameters.”

In our initial observation, when we squeeze the bottle, the diver sinks to the bottom of the bottle and after crossing a certain depth, it spontaneously sinks and doesn't come back to the surface when we decrease or release the pressure.

What happens to a simple Cartesian diver? The behavior of a Cartesian diver is unique and doesn't occur with normal buoys, but why?

When we squeezed the bottle, the air inside the diver compressed and water enters the diver. So part of the initial volume of the air that is inside the diver gets replaced by water. As we know, the density of water is much bigger than the density of air. Thus, the density of our diver increases, which causes our diver to sink.

When we release the pressure, water comes out of the diver. So the volume of the air increases and reaches its initial value. As a result, the density of our diver returns to its initial value. So our diver returns to its first position that was floating on the surface of the water.

The density of our diver changes due to the external pressure, so by increasing the pressure, the diver sinks. Now let's take a look at our diver. Here we have the initial length of air and water columns in our diver (Fig. 1).

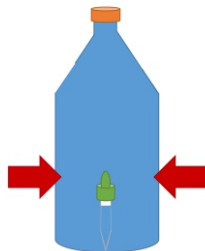


Fig.1: by increasing the pressure, the diver sinks

Air is compressible water is not. So by the rise of the total pressure, the air inside the diver compresses, and its volume decreases. So it allows more water to come inside of the diver. Thus the volume of water inside of the diver increases. As a result, the density of our diver rapidly increases, and it causes our diver to sink.

An irreversible Cartesian diver is a simple Cartesian diver with this difference; it remains at the bottom of the bottle, even when the pressure is released.

2 Theory and Methods

These are our assumptions:

- The air bubble in the diver feels only the ambient pressure plus the pressure exerted on the surface of water.
- The temperature of the water and the air trapped in the diver is constant during the experiment.
- Water is practically incompressible, so its density is constant and does not change with depth.
- The trapped air behaves like an ideal gas.

At first glance, we have the forces acting on our diver: The buoyant force, the diver's weight, and the dissipative force proportional to velocity (Fig. 2).

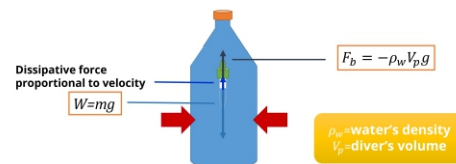


Fig. 2: Forces acting on the diver

Both of our theories show that we have a certain depth in a bottle of an irreversible Cartesian diver, which is called “Critical depth”. When the diver goes beyond that depth, it spontaneously sinks and doesn't come back to the surface when the pressure is released.

But in a simple Cartesian diver, the bottle usually isn't long enough. So the diver always remains above that depth. So when it reaches the bottom of the bottle, the buoyant force will return it to the surface when we release the pressure. If we don't consider the drag force, we will realize that beyond the critical depth, the buoyant force that applied to our diver is lower than the diver's weight. So it

diver at the bottom and the buoyant force won't be enough to overcome it and return the diver to the surface when the pressure is released (Fig. 3).

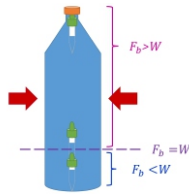


Fig. 3: The condition for never returning

So we wrote this equation of motion, without considering the drag force.

$$ma = mg - \rho_w V_p g \tag{1}$$

$$m\ddot{h} = mg - \frac{\rho_w nRTg}{P_a + \rho_w gh} \tag{2}$$

Now let's investigate the behavior of the diver in different pressures. Suppose we have this test tube, in P_0 pressure. The length of air column inside of it is l_0 and the length of the test tube is L . And suppose we have this bottle that the pressure of the air inside it is P . We place the test tube inside the bottle. The new length of air column in the diver is l , which is obviously smaller than l_0 . We have x , that is the distance between the end of the diver and the free water level and α that is part of the of the air column in the diver that is submerged. We suppose our diver is the trapped air plus the test tube's glass (Fig. 4).

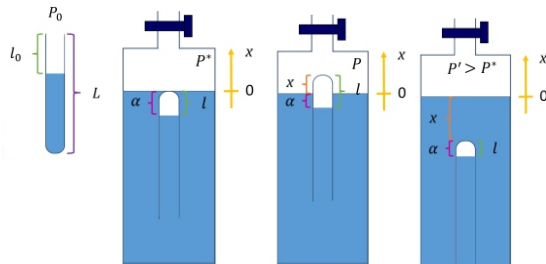


Fig. 4: The behavior of diver in different pressure

When we increase the pressure of the air inside of the bottle, x become lower until at a point, it equals to 0, at that point, the pressure is the “critical pressure”; that is defined as the pressure in which the end of the diver is at the same level as the liquid's surface. If we increase the pressure pass the critical pressure, our diver spontaneously and completely will sink.

Now let's discuss the first static equilibrium of our diver; when the pressure of the air inside of the bottle is P and in equilibrium position α is α_e (Fig. 5).

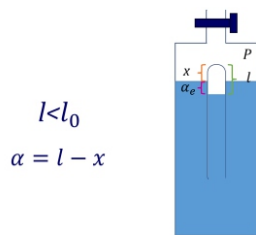


Fig. 5: The equilibrium position

The mass of the trapped air inside of the diver is negligible compared to the mass of the test tube so according to

Archimedes' principle, we can rewrite this equation. The first term is the buoyant force exerted on air that is submerged and the second term is the buoyant force exerted on glass that is submerged.

$$mg = \underbrace{A\alpha_e \rho_w g}_{\text{Buoyant force exerted on air that is submerged.}} + \underbrace{V \left(1 - \frac{x_e}{L}\right) \rho_w g}_{\text{Buoyant force exerted on glass that is submerged.}} \tag{3}$$

Now we have the equilibrium equation when P is P^* and α_e^* is equal to l . So we can write this equation as equilibrium in critical pressure. This quantity depends only on geometrical parameters and on the two densities (Fig.6).

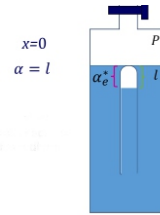


Fig. 6: Equilibrium with critical pressure

$$\alpha_e^* = \frac{V}{A} \left(\frac{\rho_{glass}}{\rho_w} - 1 \right) = L \left(\frac{d_{external}^2}{d_{internal}^2} - 1 \right) \left(\frac{\rho_{glass}}{\rho_w} - 1 \right) \tag{4}$$

- $x_e \ll L \rightarrow$ We can ignore x_e
- $\alpha_e \approx \alpha_e^*$

We suppose x_e is much smaller than L so we can neglect it and then α_e is approximately equal to α_e^* and we suppose the trapped air inside of the diver behaves like an ideal gas, and temperature is constant during the experiment (Fig. 7). So according to Pascal's principle and Boyle's law we can rewrite what we wrote in the previous step.

$$\frac{P^*}{P_0} \approx \frac{l_0}{\alpha_e^*} \tag{5}$$

$\alpha_e \rho_w g \ll P$ so it is neglected.

$$mg = V \rho_{glass} g = A \alpha_e \rho_w g + V \left(1 - \frac{x_e}{L}\right) \rho_w g \tag{6}$$

$$P_0 l_0 A = (P + \alpha_e \rho_w g)(\alpha_e + x_e) A \tag{7}$$

$$x_e = \frac{P_0 l_0}{P + \alpha_e \rho_w g} - \alpha_e \tag{8}$$

$$P_0 l_0 = (P^* + \alpha_e^* \rho_w g) \alpha_e^* \tag{9}$$

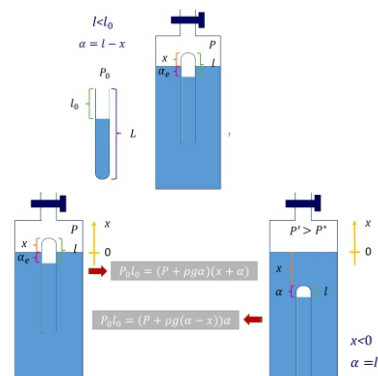


Fig. 7: First static equilibrium

Now let's take a look at the dynamics of our diver. In order to derive the equation of motion, we have to use Newton's second law. There are 4 forces acting on our diver: The buoyant force on air, the buoyant force on glass, the diver's weight and the dissipative force.

$$m \frac{d^2x}{dt^2} = \begin{cases} A\alpha(x)\rho_w g + V(1 - \frac{x}{L})\rho_w g - V\rho_{glass}g - b\dot{x}, & x > 0 \\ A\alpha(x)\rho_w g + V\rho_w g - V\rho_{glass}g - b\dot{x}, & x \leq 0 \end{cases} \quad (10)$$

Buoyant force exerted on air that is submerged.
 Buoyant force exerted on glass that is submerged.
 Weight of the diver
 Dissipative force proportional to velocity

Now we have a differential equation should be solved to reach $x(t)$, where b is the constant coefficient of velocity, and for a cylinder, C_D is 0.82, according to our reference.

$$b = \frac{1}{2} \rho_w C_D A$$

↓
In a cylinder

$$C_D = 0.82$$

x_e is approximately equal to 0. So $\alpha(t)$ is smaller than α_e^* . The net force that is acting on the diver, might become negative and it causes the diver to sink.

$$\alpha(t) < \frac{V}{A} \left(\frac{\rho_{glass}}{\rho} - 1 \right) = \alpha_e^* \quad (11)$$

Our diver sinks when it reaches the no return depth. In that depth, x is equal to x_{nr} and α is equal to α_e^* . So x_{nr} is calculated

$$|x_{nr}| = \frac{1}{\rho g} \left(\frac{P_0 l_0}{\alpha_e^*} - P \right) - \alpha_e^* \longrightarrow |x_{nr}| + \alpha_e^* = \frac{\Delta P}{\rho g} \quad (12)$$

By simulations and using tracker, the ordinary differential equation is solved. So we used this library in python by the initial conditions: x and v_0 .

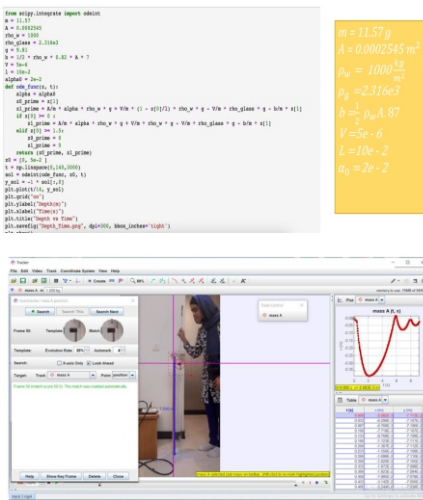


Fig. 8: using Simulation and tracker to solve equation

3 Experiments and Results

In this experimental setup, we used a cylindrical tube as the bottle, with 1 meter height and 10 centimeters diameter, a removable lead, at the top of the cylinder, a test tube, as the diver, that we marked it with black tape so that we are able to track it with Tracker, a pump, to apply pressure on the liquid's surface, a three-way stopcock, to control the air admittance, a one-way stopcock, to control and maintain the pressure, a medical digital manometer and a ruler. So we are mechanically applying pressure on the water's surface and we are able to measure it.

Also several test tubes were used in our experiments (Fig. 9).

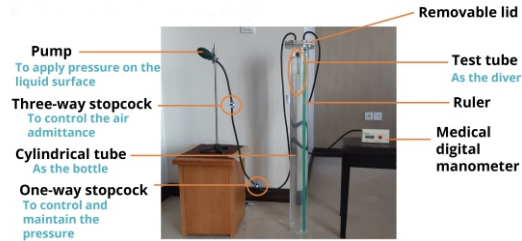


Fig. 9: Experimental setup

In this experiment, we are displacing the diver from its first static equilibrium a little; it creates some damped oscillations in the diver, around its equilibrium point.



Fig 10: Damped oscillations of the diver around its equilibrium point

In other part of experiment, we have the irreversible Cartesian diver. When we increase the pressure, the diver sinks, even if we keep the pressure constant, when we reach P^* and when we release the pressure, the diver remains at the bottom of the cylinder.

Here we used several identical test tubes, with different l_0 .

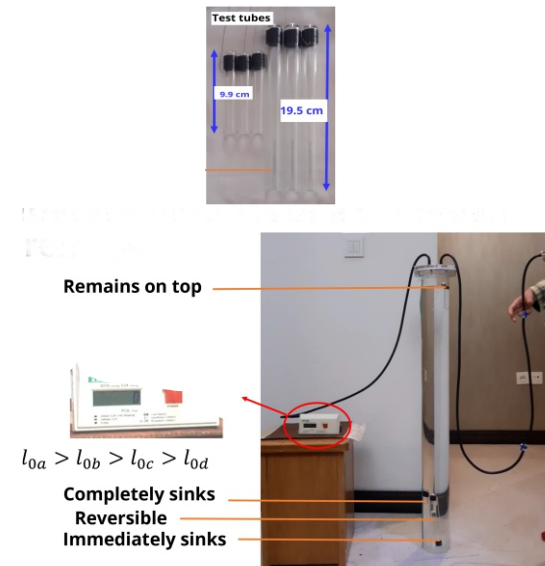


Fig. 11: Different motions of a Cartesian diver with different l_0

The diver d immediately sinks when we put it in the cylinder and when we increase the pressure, the diver c sinks. By increasing the pressure further, the diver b sinks too; because its critical pressure is lower than the diver a and higher than the diver c. But the diver a remains on top because its critical pressure is too much that we are not able to apply it. When we release the pressure, the diver b returns to the surface, but the positions of other divers won't change.

For the next experiment, we used one diver, with a specific l_0 but varying its initial velocities in constant pressure. Here are the graphs of the depths versus time when the initial velocities of our diver are :

$$(v_1 < v_2 < v_3)$$

With initial velocity v_1 , the diver goes down but because it doesn't reach the no return depth, it returns to the surface and has some damped oscillations around its equilibrium point.

v_2 is bigger, so the diver goes deeper but it doesn't sink completely and has a similar motion to the first situation, because it doesn't reach the no return depth either. But in the next situation, the diver crosses that depth and completely sinks and doesn't return to the surface. If we compare these graphs with those from the simulation, there is a good agreement between the theory and experiment (Fig. 12).

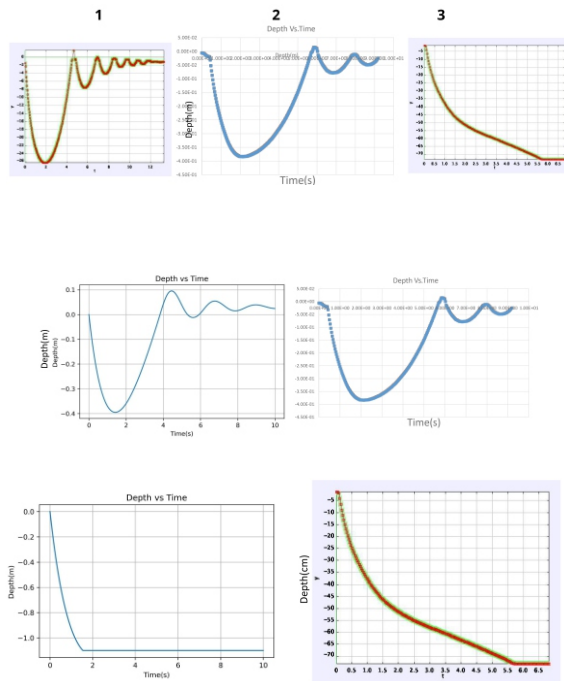


Fig 12: Different motions in the diver with different initial velocities

For the next experiment, we used one diver, but changing its l_0 and measuring the critical pressure for its amounts it is found they have a linear correlation (Fig. 13).

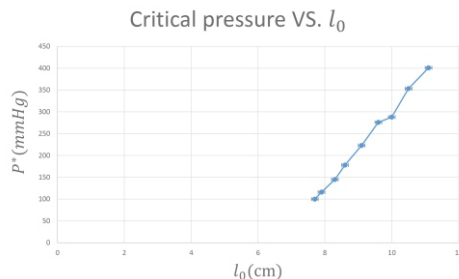


Fig 13: Linear relation in a diver between critical pressure and l_0

In comparison between the theory and the experiment for each of these two α_e^* and $\alpha_e^* + |x_{nr}|$ we can find a good agreement (Fig. 14).

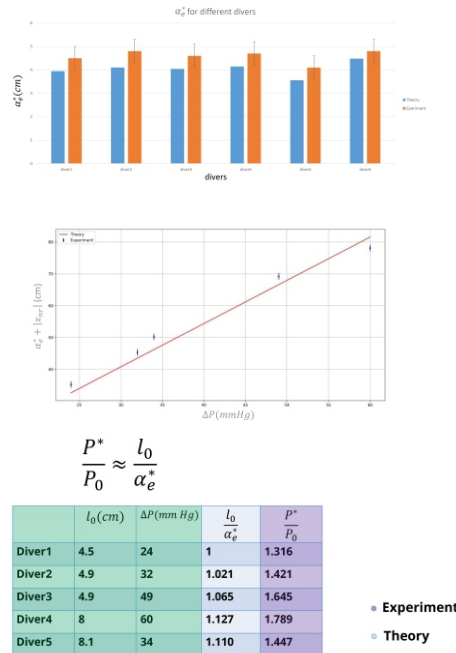


Fig 14: Comparison between theory and experiment

4 Conclusions

In this research we wanted to make a Cartesian diver that doesn't come back to the surface when the pressure is released, and to find the relevant parameters. Our theory said these following parameters are important and by adjusting them, we can have a Cartesian diver that when it goes below a certain depth, it never returns to the surface. But the irreversible Cartesian diver also can be achieved by some other ways, for example by using two liquids in the bottle with different densities, using absorbent material in the diver, etc.

When the external pressure is changed and the diver goes below a certain depth at the same time, we can have an irreversible Cartesian diver. That critical depth depends on the pressure and the initial amount of water in the diver.

When we give a small perturbation to a diver at its equilibrium point, it has some damped oscillations around its equilibrium point.

By using identical divers but with different initial conditions (l_0 , initial velocity, etc.) we can observe different motions.

The diver completely sinks when it reaches its no return depth and when the pressure is rose to the critical pressure it spontaneously sinks and also we observed a good agreement between the theory and the experiments.

References

[1] Planinsic, G., Kos, M., & Jerman, R. (2003). Two-liquid Cartesian diver. *Physics Education*, 39(1), 58–64.

[2] Güémez, J. & Fiolhais, Carlos & Fiolhais, M.. (2002). The Cartesian diver and the fold catastrophe. *American Journal of Physics –AMER J PHYS.* 70. 710-714. 10.1119/1.1477433.

[3] Luca, R. D., & Ganci, S. (2011). A lot of good physics •in the Cartesian diver. *Physics Education*, 46(5), 528–532.

[4] Güémez, J., Fiolhais, C., & Fiolhais, M. (2003). A Demonstration Apparatus for the Cartesian Diver. *The Physics Teacher*, 41(8), 495–496.

The Intelligent Diagnosis and Treatment of Postural Deformities by Analyzing the Given Data from Kinect Camera

SeyedehSara Jalilishani, sarajalili33@gmail.com

ABSTRACT

Postural deformities are common abnormalities related to the skeleton form, with growing prevalence among people. In the constructed system we have created a method by which any individual can diagnose and treat their postural deformities intelligently with the least requirement of an orthopedic doctor's supervision. In the implementation of the project we used Kinect camera, a gaming device provided by Microsoft company, because it has functional features with a reasonable price. The Kinect camera is capable of body tracking, joint coordinating and motion capturing.

Key words: Postural deformities, Kinect, diagnosis, treatment, skeleton

ARTICLE INFO

Winner of Gold Medal, ICYS 2018, Belgrade, Serbia
 Supervisor: Hossein Azizinaghsh
 Accepted in country selection by Ariaian
 Young Innovative Minds Institute, AYIMI

<http://www.ayimi.org>, info@ayimi.org

1 Introduction

In postural deformities, there is an imbalance in the loads imposed on different areas. Where loads exceed normal physiological limits consistently and over prolonged periods of time, structural changes occur in the skeletal bones. These structural changes cause postural deformities, such as: genu valgum, genu verum, asymmetric shoulders, Kyphosis and etc. [1]. These deformities are spreading among people and mostly among students and workforces because of the environment they work in.

1-1 Postural Deformities in Workforces

A research was done in Romania to present the risk factors in hand-arm tasks leading to neck and upper limb musculoskeletal disorders (MSDs) among workforces. In this research the relative occurrence of the type of work-related health problem was calculated and as shown, workforces mainly suffered from disorders related to the skeleton structure (Fig. 1).

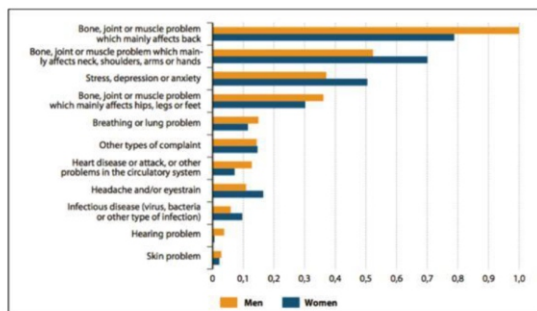


Fig.1: Relative occurrence of the type of work-related health problem[2].

1-2 Postural deformities in students

A research was done to identify the prevalence and the main risk factors of poor posture among school children in Czech Republic. As shown in the table, in average about 40 percent of the students suffered from having a poor posture (Table 1).

Table 1: Trends in the Incidence of Poor Body Posture and Its Component in Relation to Age in Czech School Children [3]

Study parameter	7 Year-Olds (n = 1097)		11 Year-Olds (n = 1190)		15 Year-Olds (n = 1236)		p Value	Trend by Age
	Frequency	%	Frequency	%	Frequency	%		
Poor posture	361	32.91	463	40.59	498	40.29	,0,001*	Increase [†]
Protruding scapulae	614	55.97	620	52.10	512	41.42	,0,001*	Decrease
Increased lumbar lordosis	352	32.09	393	33.03	365	29.53	0.304	Without trend
Round back	281	25.62	388	32.61	432	34.95	,0,001*	Increase
Scoliosis	17	1.55	59	4.96	129	10.44	,0,001*	Increase

1-3 Kinect Camera

The Kinect sensor for Xbox360 (from now on Kinect 1.0) is an active camera. Unlike other human-based control devices lunched by other firms it allows users to play and completely control the console without having to hold any kind of device, but only by the use of voice and gesture. The Kinect is a low-cost sensor that allows the real-time measurement of depth information (by triangulation) and the acquisition of RGB and IR images at a frame rate up to 30 fps. It is composed of an RGB camera, an IR camera, an IR-based projector, a microphone array, a tilt motor and a 3-axis accelerometer (Fig.2).

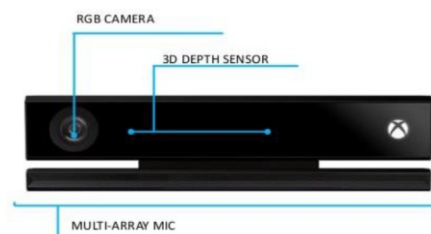


Fig. 2 : Kinect for Xbox one

The implementation of this project requires specific data from the user's body such as the coordination of the joints and their orientation that this camera provides alongside other features like motion capturing and gesture building used for implementing other phases of the projects. Since the project is based on a medical purpose its necessary that it imparts sufficient accuracy. Given that Kinect camera is

low-cost, portable and does not require any sensors to be attached to the body, it could provide numerous advantages when compared to established marker- or wearable sensor based system. The Kinect V2 has the potential to be used as a reliable and valid clinical measurement tool [6].

2 Objectives and Importance of the Project

The objectives of this project are:

- Decreasing the costs for diagnosing and treating the deformities by using the proper equipment and methods
- Accelerating the whole amelioration process by gathering the phases in one system
- Reducing the requirement of an orthopedic doctor by increasing the accuracy of the system as far as possible

As mentioned before postural deformities are increasing among people and becoming a serious issue in school children and workforces. Diagnosing and treating these deformities instantaneously not only prevents further damages caused on your health but also saves money and time. Yet many people neglect the importance of diagnosing and treating these deformities for reasons like: the heavy fees for doctor's referral, not being able to spare some time for the amelioration process, living in a disadvantaged area and etc. The designed system can solve these problems by costing less than visiting a doctor, being accessible and having visual attraction that increases the user's interest in doing the amelioration process.

3 Methodology

This research is in the form of a software, created using the Unity game engine which was proper for creating a 3D concept. The environment of this system is designed as a doctor's office to increase the interaction between the user and the program (Fig. 3).



Fig. 3: Experimental environment

Having this system in unity, one of the things we were able to do was creating a hypothetical skeleton of the user's body with 3D objects using the Kinect camera. The main feature of this camera which was the most practical for our purpose was the body tracking feature. When the user stands in a proper distance from the camera, it tracks the body of the user, the tracked body comes with some data that is also received from the user's body such as the coordination and the orientation of the 25 joints .

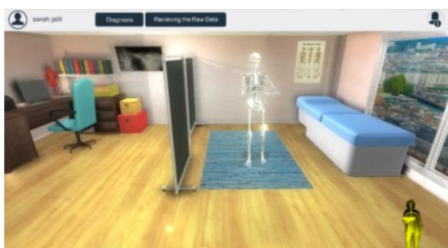


Fig 4: The drawn skeleton

Having the coordination of the joints in three dimension (x, y and z) we were able to draw a skeleton of the user's body in 3D by having a rigged skeleton object and setting its joints' coordination to the coordination that was received from the user's body (Fig. 4).

Having the skeleton in 3D had medical purposes, for instance if the doctor or the user wants to examine the skeleton they can zoom in and examine it closely (Fig. 5).

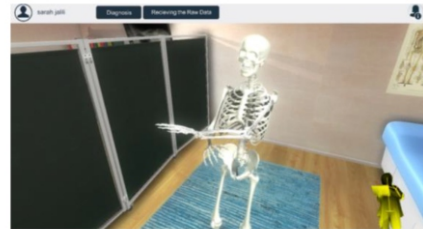


Fig. 5: Zooming in the skeleton

3-1 Creating a Profile for the Patient

Before entering the program users will go through a profiling process in which some personal information will be received from them and will be held in a profile with a profile number that will be also provided for the users. As the profile is created an email will be send to the patient's doctor so that the doctor would have access to this data. The reason for sending this personal info to the doctor which includes the patient's name, height, weight and age, is that in some cases the doctor needs to be able to check if the deformity is caused because the patient is overweight or it's because of the patient's age or etc. After the final diagnosis the intensity of the user's deformity will also be send to the doctor via an email (Figs. 6-8).

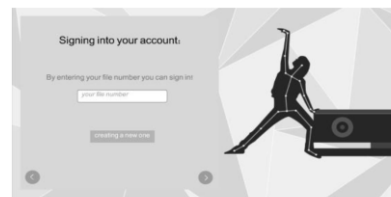


Fig. 6: Entering in the user's account

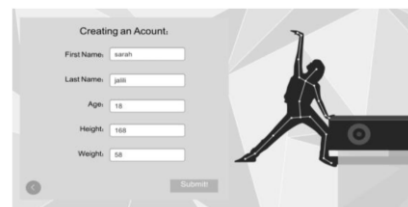


Fig. 7: Receiving the personal info

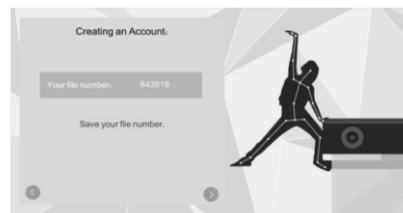


Fig. 8: providing a profile number

The amelioration process is divided into two parts: the diagnosis and the treatment. The diagnosis phase includes the diagnosis of three deformities: wry neck, asymmetric shoulders and genu verum. The diagnosis of these deformities is mostly based on the coordination of the joints received by the Kinect camera. Having the joints' coordination of the user's body we could do the diagnosis by comparing the position of the user's joints with the standard position they must have.

3-2 Diagnosis of the Asymmetric Shoulders

In standard posture the shoulders are supposed to be in the same axis meaning that their variable y must be almost equal, as much as the subtraction of their y variable increases the intensity of the deformity also increases (Fig. 9).

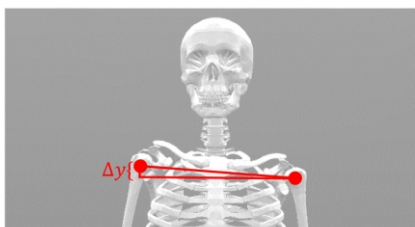


Fig. 9: As shown in the figure Δy is the determinative variable for the intensity of the asymmetric shoulders, as the Δy increases the shoulders will be more in an asymmetric position

Having Δy we could diagnose the deformity by comparing the given data from user's body and medical references in which the standard of these data is discussed.

3-3 Diagnosis of Wry Neck

In Wry Neck the patient's neck is not in a straight line and the neck is bended toward his/her left or right shoulder. The method for diagnosing this deformity is to compare the x variable of the head and the neck of the user's body (Fig.10).

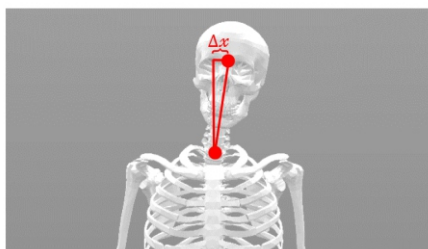


Fig 10: As shown in the figure Δx is the demonstrative variable for the intensity of the wry neck, as Δx increases the neck is more bended towards the right or left shoulders

This deformity is also diagnosed by comparing the Kinect's data and the discussed data in the medical references.

3-4 Diagnosis of Genu Verum

In this deformity when the patient is standing in a standard position (legs closed) the distance between the knees will be calculated using the x variable of left and right knees, based on this distance the deformity will be diagnosed by comparing this distance to standards available references (Fig. 11).

3-5 Drawing the Live Charts

Using the methods declared above we were able to diagnose three deformities. To provide the user with this diagnosis, we showed the diagnosis done on each frame on a live chart. The data of these live charts that includes the intensities of these deformities, will be updated each frame. Each chart has four possible data, zero, one, two or three; and each number states an intensity except for number zero which will be discussed later. When one is shown it means that the deformity is not seen in the person's body, two means the deformity is clearly seen in the user's body, when the data of chart is three the deformity is highly intense in the user's body (Fig. 12).

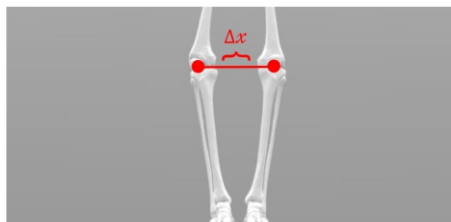


Fig. 11: As shown in the figure Δx is the demonstrative variable for the intensity of the genu verum, as Δx increases the knees are more distanced from each other and the intensity of this deformity also increases.

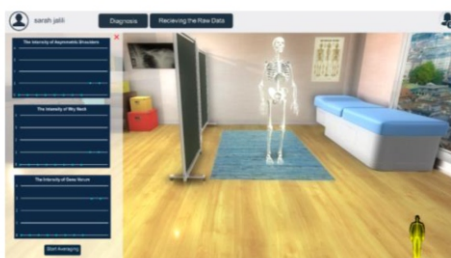


Fig. 12 : The drawn live charts for the intensities of the user's deformities

3-6 The calibration process

Two parameters will affect the results during the diagnosis process: the posture that the user is having and the distance that the user has from the camera. The user must stand in a normal posture in front of the camera, meaning the user's body must be held in an upright position, so if the user stands in a T-pose or has the arms crossed or legs open, we wouldn't be led to a valid diagnosis. Another parameter is the distance of the user from the computer, Kinect camera has an exact scope that if the user doesn't stand in it (getting too close to the camera), the skeleton of the body wouldn't be drawn accurately so there will be an error in our diagnosis too (Fig. 13).

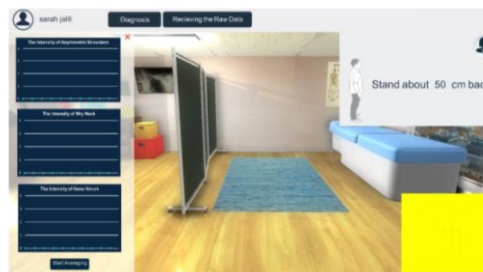


Fig.13: The user is standing in an improper distance from the camera so an alter is shown, the skeleton is disabled and the intensity of the deformities are shown zero.

Therefore, we added the calibration process. In this process when the user enters the diagnosis phase before doing the final diagnosis the posture and the position of the user will be checked to declare whether the user is in the proper distance and having a normal posture or not, if the user is standing too close to the camera or has an invalid posture he/she will get an alter for that and the data of the live charts will change to zero and the skeleton of the user wouldn't be drawn anymore until the user changes his/her posture (Fig. 14).

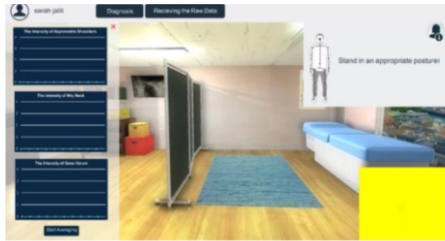


Fig. 14: while the person is standing in an improper posture the same sequence of actions will happen but the distance of the user is prioritized from the posture of the person.

3-7 The Marker-Based Method

Kinect camera's body recognition is a marker-less process which is done using machine learning. Any device using this method can come with inaccuracies. Accuracy of Kinect V2 landmark movements was moderate to excellent and depended on movement dimension, landmark location and performed task. Signal to noise ratio provided information about Kinect V2 landmark stability and indicated larger noise behavior in feet and ankles [7]. These joints don't effect the diagnosis of the deformities except for genu valgum which is diagnosed using ankles' x variable. In this condition for the ankles' joints the suggested method was the marker-based method. In this method specific markers will be attached on the user's ankles and the coordination of these markers will be calculated using an image processing procedure. During the diagnosis of this deformity the coordination of the markers will be used instead of the coordination that are calculated by Kinect camera. As the accuracy of the marker-based method is way more than the marker-less method, this method was discussed for the solution to this problem.

4 Averaging Process

Another method that was used for increasing the accuracy of the system was the averaging method. Kinect camera receives about 30 frames per second depending on different parameters. Doing the final diagnosis based on the data of one frame wouldn't be accurate enough, so to have a valid diagnosis we averaged the data of the user's body (the coordination of the joints) in 90 frames and did the diagnosis based on the averaged data (Figs. 15-17).

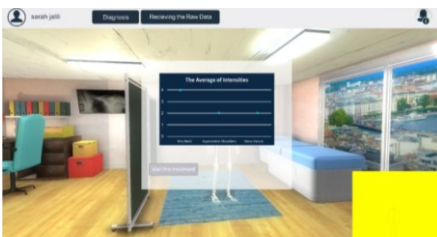


Fig. 15: The final diagnosis that is based on the averaged data

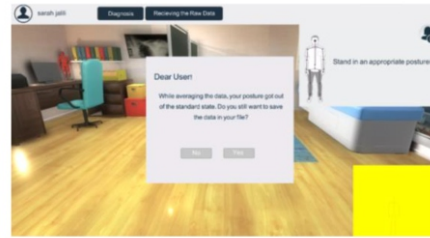


Fig. 16 : If the user's posture gets out of the valid form during the averaging process an alter will pop on to check whether the user wants to save the data of the averaging or wants to do the process all over again

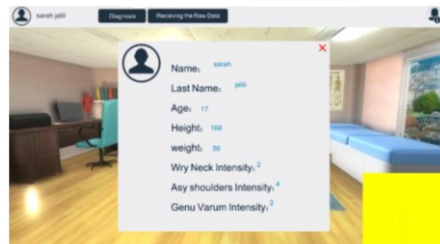


Fig.17: as the final diagnosis finishes the intensities of the patient's deformities will be saved in the user's profile.

5 The Treatment of Deformities

The treatment of these deformities are based on their diagnosis and they are usually in a form of an exercise. The treatment for each deformity is also defined in the medical references, the repetition and the timing of the exercise is based on the intensity of the deformity. The instruction for each exercise is given to the user in the beginning of the treatment phase. The motion capturing capability of Kinect device gave us the ability to control the user's movements and to clarify whether the user is doing the exercises correctly or not. Visual Gesture Builder is a software for defining a gesture or movement for Kinect camera. We used this software to teach Kinect these exercises as the correct movements that must be done by the user (Figs. 18,19).

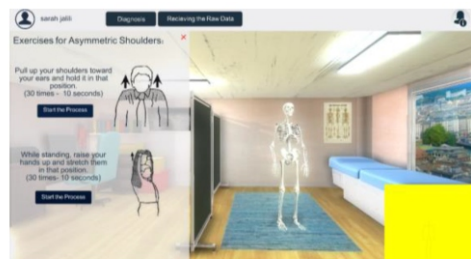


Fig.18: as the user enters the treatment of the asymmetric shoulders an instruction for the exercises will be given to the user

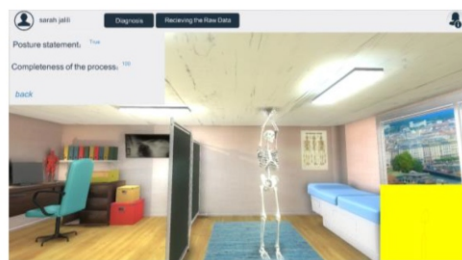


Fig.19: The monitoring section of the treatment phase has two parts, in the first part if the user does the exercise correctly the statement will be true and in the second part the completeness of the exercise that varies between 0 to 100 will be in the range of 80-100

6 The Raw Data Section

This section is created for doctors and medical purposes. In this section the user can have access to the data that the diagnosis of the deformities were done using it; this data consists of the Δx of knees, Δy of shoulders, the angle of knees, the slope of the shoulders, markers' coordination and the Δx of head and neck joints. We provided this data, so that the doctor would be able to see the information of the user's body himself/herself for any medical purposes (Fig.20).

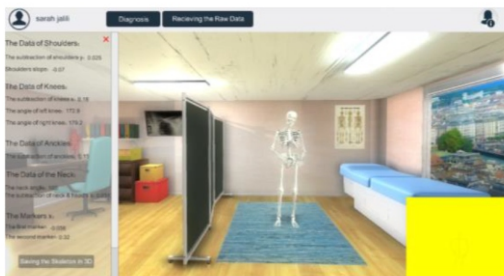


Fig. 20: The raw data panel will be opened as the user clicks on the receiving the raw data and the coordination of the markers are also shown on this panel

7 Results

To measure the accuracy of the system it was examined on 90 adolescence in the age of 16 between 18 (the examination was done on this age range because the deformities are more common in these ages). The results are shown on the chart below (Fig. 21).

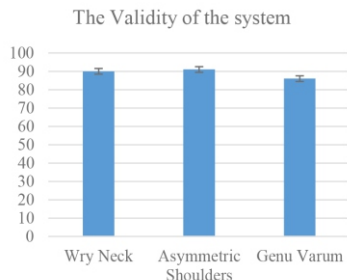


Fig.21: The results are compared in different deformities

The accuracy of wry neck was calculated 90 percent, for the asymmetric shoulders it was calculated 91 percent and the genu varum was about 86 percent; therefore, the validity of the system in average was about 89 percent.

8 Conclusions

Combining Kinect camera's features with the marker-based and averaging method gave us a system with the reliability for a medical diagnosis. This system can be practical in places that the environment often leads to the cause of these deformities such as schools and workplaces, also this system can be used instead of a doctor in places like disadvantaged areas in which there is a lack of medical workforces; it also can be used in any places with large number of users such as clinics, alongside these, any person having access to this system can go through the amelioration process individually. In all of these conditions, this system is going to be used for several years instead of hiring a doctor each time which leads to a reduction in the costs, also this system may absorb the user's interest for doing the amelioration process because of the game-like atmosphere of the system.

Acknowledgment

I would like to express my sincere gratitude to my supervisor, Hossein Azizinaghsh for helping and guiding me through this project. I also want to thank the head of the AYIMI institute for giving me opportunity to have my article in this journal.

References

[1] Solberg G., Postural Disorders & Musculoskeletal Dysfunction diagnosis, prevention, and treatment. Churchill Livingstone. 1st ed. Elsevier publisher; 25th October 2007.

[2] Viorica Petreanu, Aurelia-Mihaela Seracin. Risk factors for musculoskeletal disorders development: hand-arm tasks, repetitive work. National Research - Development for Health and Safety; Romania.

[3] Jana Kratenová, Kristyna Zejglicová Article. Prevalence and Risk Factors of Poor Posture in School Children in the Czech Republic. Journal of School Health. 2007. 77(3):131-7.

[4] Khoshelham, K. Accuracy Analysis of Kinect Depth Data. International Archives of the Photogrammetry, Remote Sensing and Spatial Information Sciences. 2011; Volume XXXVIII-5/W12. [2011ISPr3812W.133K:133-138](https://doi.org/10.1115/ISPr3812W.133K:133-138).

[5] Diana Pagliari, Livio Pinto. Calibration of Kinect for Xbox One and Comparison between the Two Generations of Microsoft Sensors. 2015; 15(11): 27569–27589.

[6] [Karen Otte, Bastian Kayser, Sebastian Mansow-Model, Julius Verrel, Friedemann Paul, Alexander U. Brandt, and Tanja Schmitz-Hübsch. Accuracy and Reliability of the Kinect Version 2 for Clinical Measurement of Motor Function. November 18, 2016; 11\(11\):e0166532.](https://doi.org/10.1111/e0166532)

Magnetic Field

Erfan Behrouz, Mashhad, Iran, erfanettn@gmail.com

ARTICLE INFO

Participated in ICYS 2018, Belgrade, Serbia
 Supervisor: Shayan Khajegi
 Accepted in country selection by Ariaian
 Young Innovative Minds Institute, AYIMI

<http://www.ayimi.org>, info@ayimi.org

ABSTRACT

In this research we can make electricity current and kinetic energy via magnetic fields which actually can be used in many places. Here three phenomena, which are caused and happened by magnetic fields are analyzed.

Key words *Magnetic fields, electricity, energy,*

1 Introduction

In magnet science, scientists achieved an extreme progress. We have many famous laws and famous scientists in this science, such as: Faraday's law, Lenz law, Joseph Henry (inductance), Hans Christian Oersted (magnetic fields).

There are motors which work via magnets and magnetic fields; but all of them use an external energy to meet the needs of themselves such as electricity or fossil fuels.

In mechanism that I've investigated and worked on, we can make electricity current and kinetic energy via magnetic fields. Actually, if we inspire and optimize this theory's consequences; we can use them in many places.

In this article, we analyze three phenomena as follows, which are caused and happened by magnetic fields:

a) to make electricity current by the means of magnetic field (Fig. 1)

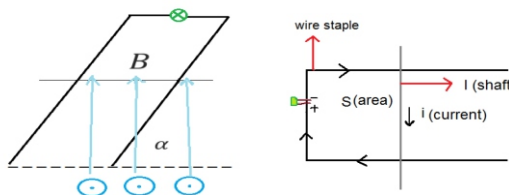


Fig.1: Current by magnetic field

b) making magnetic turbine by magnetic fields around the carrying current wire (Fig 2)

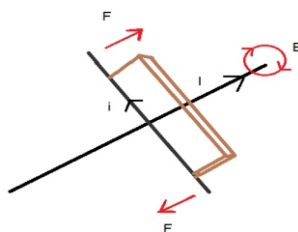


Fig.2: Magnetic turbine by magnetic field

c) magnetic engine: moving a round metal by magnet and heat (by magnifier) (Fig. 3)



Fig. 3: Magnetic engine

2 Experimental Setup

In a mechanism that I've investigated and worked on, we can make electricity current and kinetic energy via magnetic fields (Fig. 4). The main theories are explained to find the real and relevant parameters in our magnetic engine and also some equipment for our experimental setup such as:

- A conductive shaft (ferro alloy)
- Wire staple
- A diode
- Mag



Fig. 4: Experimental setup

Magnetic flux ($\varphi = \vec{B} \cdot \vec{A}$): it is the number of magnetic field lines passing through a surface (Fig. 5).

For increasing the flux, we can increase the A (area).

\vec{B} = constant

S = increasing area

\vec{B}' = magnetic field that is made by the induced current

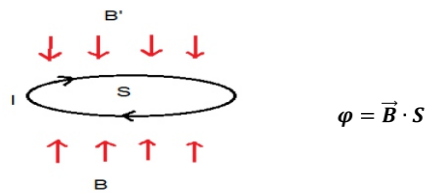


Fig. 5: Magnetic Flux

Faraday's law's details: if you want to make lots of EMF, then you have to find a way to change the flux near the conductor. Then more change the flux near the conductor, the more EMF you make (Eq. 1).

$$\epsilon = \frac{d\phi}{dt} \tag{1}$$

Lenz's law: As we know that the nature is against to the magnetic flux, by flux's changes, the induced EMF in the circle is opposite to the first EMF; because, the new magnetic field have to be made opposite to the first magnetic field (Eq. 2).

$$\epsilon = -\frac{d\phi}{dt} \tag{2}$$

In this process;

For making the drift velocity in wire, we use magnet to make magnetic field.

We imagine that the magnetic field which is made by the magnets, is constant. Because of the magnetic flux in the wire; it makes magnetic field to prevent the magnetic flux. By increasing the area (A), magnetic flux increases too; and more magnetic flux, more EMF. By shaft's falling down (because of the gravity); induced current will be made in the circle; this current causes the diode's lightness (Fig.6) (Eq. 3,4,5).

$$\phi = BS \cos\theta, \cos\theta = 1, S = Lx \tag{3}$$

$$\phi = BLx$$

$$\epsilon = -\frac{d\phi}{dt} \rightarrow \epsilon = -BL \frac{dx}{dt} \rightarrow \epsilon = -BLV \tag{4}$$

$$\epsilon = IR \rightarrow I = \frac{BLV}{R} \tag{5}$$

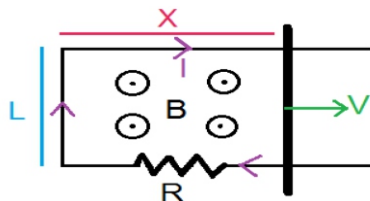


Fig. 6: Induced current

2-1 Magnetic Turbine

As shown in Figure (7), we have a main current inside wire ($I_2 \ll I_1$) and a vane which is on the main wire (1) and it has another wire (2) just under itself related to the main

wire.

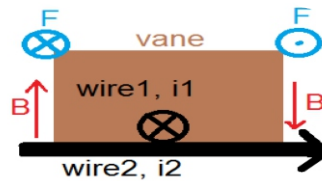


Fig. 7: Magnetic Field due to the current inside the wire

We know that electrical current which flows in wire makes magnetic field and according to the right-hand rule, we have two opposite forces which cause the vane's turning. According to the magnetic field we have some options to increase the force ($F = IL \times B$): $B = \frac{\mu I}{2\pi r}$
 - Increasing the (B) by increasing the (I),
 - Increasing the length of the wire (L) and increasing the current (I)

2-2 Curie Point Engine

The dipoles are aligned by external magnetic field. We define magnetic materials as small rings that an electron (e) rotates around it by the speed of (v) and angular acceleration (Eqs. 6-9).

$$\mu = IA = \frac{ev}{2\pi r} \times \pi r^2 = \frac{rev}{2} \tag{6}$$

$$\tau = \vec{\mu} \times \vec{B} = \frac{rev}{2} \times \vec{B} = \frac{revB}{2} \tag{7}$$

$$\tau = I\alpha \rightarrow \tau = \frac{mR^2}{2} \alpha = \frac{revB}{2} \tag{8}$$

$$\alpha = \frac{revB}{mR^2} \quad \text{angular acceleration} \tag{9}$$

For different metals, we have specific temperature (curie point); in this temperature, ferromagnetic metals, lose their permanent magnetism and their atoms convert to magnetic polarization (Fig. 8).

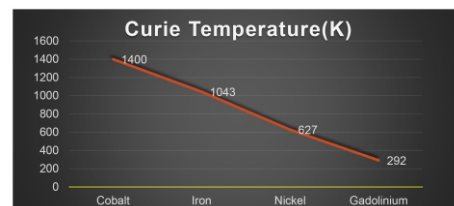


Fig. 8: Curie Temperature

When the temperature of a ferromagnetic material arrives to its curie point, they lose their magnetic basins and their dipoles will be free and unlimited and by getting the force which enters to them from the magnet, their magnetic polarizations will move and it causes the surface's moving (Fig. 9).

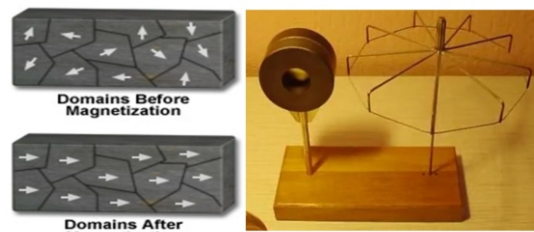


Fig. 9: Curie Point engine

3 Conclusion & Results

a) We can use this theory (Induced Current) to make electricity current.

By slopes we can save electricity such as the (U) which is used in amusement parks. People can play with them and at the same time the (U) makes electricity (Fig. 10).



Fig. 10: U makes electricity in amusement parks

b) In our cities, we have many cables and AC currents which can make magnetic turbines on them (Fig. 11).



Fig. 11: AC Currents and magnetic turbines

c) We found out that in this phenomenon, we can rotate something by bringing the temperature to the curie point. We can use magnifier instead of heaters and we don't need to use gas and fuels for doing this, we just need solar energy. And also we can use its turning for making electricity the same as turbines. And also we can use rewind around them and by moving the surface and rewind in magnetic field, we can make current and electricity (Fig. 12).

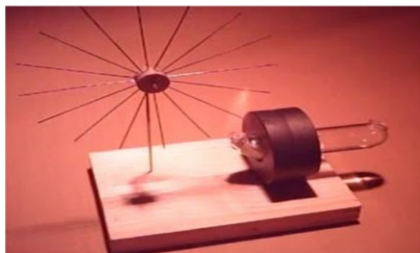


Fig. 12: rotating something by bringing the temperature to the curie point

References

- [1] Fundamental of physics (Halliday, Jearl Walker, Robert Resnick)
- [2] <https://www.nhn.ou.edu/~johnson/Education/Juniorlab/.../2013F-CuriePoint>.
- [3] hyperphysics.phy-astr.gsu.edu/hbase/electric/farlaw.html
- [4] <https://www.electrical4u.com/lenz-law-of-electromagnetic-induction/>

Epidemiology (Covid-19)

Artin Radmatin Grade 6, Valeh School, Tehran/Iran, artin.98.2.23@gmail.com

ABSTRACT

Coronaviruses are a large group of viruses. Some important coronaviruses are Mers, Covid-19 and Sars which these viruses cause Respiratory problems. But another important point in epidemiology is pandemic and epidemic and differences between them. Pandemic is an epidemic that has spread to a large area, for example on several continents or around the world, and affects a significant number of people. In this research we want to analyze some important epidemiologic data but our most important data is gender and infection between men and women doesn't have a lot difference but death in men is more.

Key words: *Coronavirus, Epidemic, Pandemic, Epidemiology*

ARTICLE INFO

Participated in IYNT / IMSEF 2021 and received Gold Medal in IMSEF.
Accepted in country selection by Ariaian Young Minds Innovative Institute, AYIMI

<http://www.ayimi.org>, info@ayimi.org

1 Introduction

Coronaviruses that can infect animals and humans and cause respiratory distress; these discomforts may be as mild as a cold or as severe as pneumonia. In rare cases, animal coronaviruses infect humans and then spread between them. You may remember the SARS virus from 2002 to 2003; The virus was an example of the corona virus, which was transmitted from animals to humans. Another important and newer breed of the virus is the coronavirus, which was discovered in the Middle East in 2012 and, according to scientists, the virus was first transmitted from camels to humans, and the new virus, Covid 19 or SARS Covid 2, which is an acute respiratory syndrome. A new branch of coronavirus discovered in 2019 in Wuhan, China. Pandemic is an epidemic that has spread to a large area, for example on several continents or around the world, but Pandemic not a widespread indigenous disease with a constant number of infected people. A pandemic occurs when a disease spreads to expectations around the world and people are not prepared for it. A pandemic is an epidemic that has spread to at least three WHO countries. An epidemic occurs when the number of cases of a disease, which of course can only be specific to a community or country, suddenly increases.

In this research we want to analyze some epidemiological data about controlling or strength of virus that our base virus is Covid-19 and some mutant covid-19 that again our base mutant virus is Delta Covid-19.

But a problem that researcher was thinking about it was how this virus transmit. According to the Centers for Disease Control and Prevention, person-to-person contact is thought to be the main route of transmission of the coronavirus. Suppose you are sitting in a meeting room with a person with a coronary infection and the patient suddenly sneezes or coughs. If the person does not cover their mouth and nose, they will be able to send breathing drops through your mouth or nose. In this case, the droplets that sit on you probably contain a virus. Or suppose you meet a person infected with the virus who has touched their nose and mouth with their hand. In this case, when you shake hands with this person, the viruses are transmitted from his hand to yours. In this situation, if you touch your nose or mouth with a dirty hand without rinsing, you may

accidentally provide a point for the virus to enter your body. A recent small study suggests that the virus may also be present in faces and may contaminate toilet stones or baths. But more research is needed to prove this claim.

2 Tests to Diagnose Covid-19

We have several tests such as PCR and antibody tests to diagnose covid-19.

An infectious disease test can tell you if you are currently infected with Covid-19- causing coronavirus. This is the same test that will be done if you are referred by your doctor based on symptoms and other factors for the Covid-19 test. In PCR the technician inserts a 15 cm cotton swab into either side of your nose and moves it for about 15 seconds. This movement will not hurt, but it may cause discomfort. The swab is then sent to a lab to test materials inside your nose.

An antibody test can show if you have ever been exposed to or infected with the Covid-19 virus, and if your body has made an antibody in an attempt to defend itself. It takes at least twelve days after exposure to the virus for the body to make enough antibodies to detect in the test. Blood or antibody tests (serology) look for antibodies. Your body makes antibodies when you have an infection. Covid-19 tests detect two types of antibodies:

- IgM, which the body builds for two weeks and then drops.
- IgG, which the body builds up more slowly (about 4 weeks) but usually lasts longer.

Swabs or sputum samples can only show the presence of the virus in the body at present, but a blood test will show if you have ever been infected with the virus, even if you have no symptoms. This is important in finding the prevalence of Covid-19 by researchers.

Aside from antibody tests, researchers are studying antibody therapies for Covid-19. The drug targets how the virus attaches to and enters the cell.

3 Methods

In this research we want to analyze epidemiological data such as age, gender, geographical spread and the most common symptoms of the disease.

3-1 Geographical spread

Many countries that have historically survived the widespread outbreak of infectious diseases had a younger population than others. According to scientific researches, young people are more likely to develop a mild form or without symptoms of infectious diseases. Young people are also less likely to develop underlying diseases that make Covid 19 worse.

The incidence of the new corona virus in Africa has been lower than in other continents. So far, only about 45,000 cases of the virus have been reported in Africa. 60% of Africa's population is under 25 years old (Fig.1). In contrast, the Italian population, in which the new type of corona virus is widespread, is considered to be older. The Italian population, in which the new type of corona virus is widespread, is considered to be older. The average age of Italians is over 45 years. The outbreak of Covid 19 has so far killed nearly 29,000 people in Italy (Fig. 2).

On the other hand, the immune system of young people is stronger than the elderly. This helps them fight the new corona virus in their body.

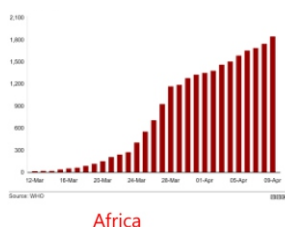


Fig. 1: Confirmed Coronavirus cases in South Africa

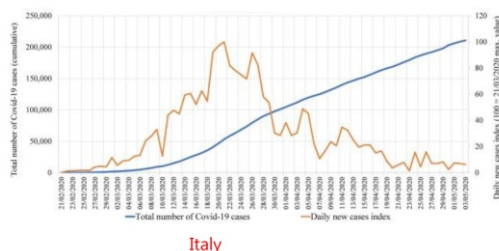


Fig. 2: The spread of Coronavirus in Italy

3-2 Cultural Factors

Specialists believe that cultural factors in some communities, including greater social distance, have helped them cope with the outbreak of the new coronavirus. Citizens in India and Thailand, for example, often greet each other by maintaining physical distance.

The use of masks during illness is also one of the effective cultural factors in preventing the spread of the new Corona virus. People in Japan and South Korea are accustomed to wearing masks when they are sick. However, the use of masks was not common in European countries before the outbreak of the new Corona virus. The continent of Europe has seen the highest mortality rate among the continents due to Covid 19 disease. Keeping the elderly at home instead of in a nursing home is another cultural factor influencing the spread of the new Corona virus. Countries with higher nursing home populations had higher mortality rates due to the outbreak of Covid 19 (Fig. 3).

3-3 Action of Governments Against the Spread of the Virus

Countries whose governments responded quickly to the outbreak of Covid 19 with quarantine and social distancing were less likely to be harmed in practice than other

countries. Vietnam and Greece are two countries that quickly adopted measures for social distance.

Of course, the speed of vaccine injection also helps to control the virus, and of course, the higher the speed of import or production of the vaccine, and of course the speed of injection, the lower the prevalence of the virus. Of course, there are different vaccines of different types with the required number of doses and, of course, different levels of effectiveness around the world, and we want to get information of this type.

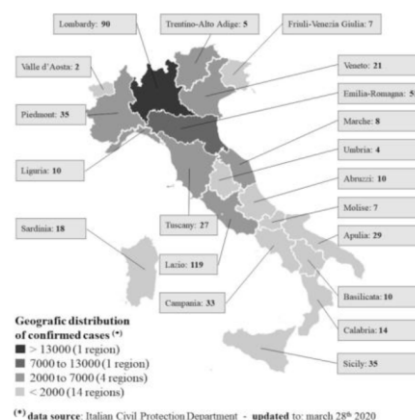


Fig. 3 : Geographic Distribution

There are different vaccines in the world with different effectiveness on covid-19 and mutant covid-19.

1- Pfizer Vaccine

Vaccine type: RNA proteins

Product: America and Germany

Confirmations: FDA License - Emergency Use License

2- Moderna Vaccine

Vaccine type: RNA proteins

Product: America

Confirmations: FDA approved

Efficiency percentage: more than 90%

3. Strazenka Vaccine

Vaccine type: Genetically modified virus

Product: England

Confirmations: FDA approval

Efficiency percentage: 76%

3-4 Weather conditions

Examining the areas where the new type of corona virus has become widespread, it can be cautiously concluded that the virus is less prevalent in hot and dry areas. Other types of coronavirus were less common in hot, dry areas in the past. The new corona virus spread late winter in countries with temperate climates such as the United States and Italy. In contrast, countries with tropical climates such as Chad and Guinea did not see the outbreak. However, scientists emphasize that it is not possible to rely solely on rising temperatures to deal with the corona. Brazil, for example, which has a tropical climate, is now the most important outbreak of Covid 19 in South America.

Scientists believe that the heat of summer, which leads to more people leaving their homes and indoor environments, may help reduce the transmission of the new corona virus. One of the effective factors in the spread of this virus is the long-term presence of people in closed environments with the infected person.

A study from a university in the US state of Connecticut shows that UV rays from direct sunlight can be effective in

in killing the new Corona virus. In this way, contact with surfaces exposed to direct sunlight is unlikely to transmit the virus.

3-5 Human Disease

3-5-1 Underlying Disease (both in delta Covid and Covid-19)

According to studies, the most common underlying diseases in people with Covid are 19 cardiovascular diseases and diabetes. In cases leading to death, the most common underlying diseases have been cardiovascular disease and diabetes.

A: Why are some people have a higher percentage of underlying diseases?

The results of a recent study show that high cholesterol, which most diabetics and heart patients suffer from, is associated with an increase in cell infection.

According to the Daily Mail, people with metabolic conditions such as diabetes and cardiovascular disease are more likely to have severe coronary heart disease. Chinese researchers are now investigating the cause in a recent study.

Most people with diabetes and cardiovascular disease have high cholesterol; For this reason, researchers at the Chinese Academy of Military Medical Sciences in this study examined the role of "good" cholesterol, known as high-density lipoprotein (HDL), in coronary heart disease.

In this study, the researchers specifically looked at the SR-B1 receptor, which binds to cholesterol molecules and is found in cells in the human body, including the lungs, which are targeted by the coronavirus.

The researchers found that SARS-CoV-2, which infects Covid-19, could not directly utilize the receptor, but could use the process of binding cholesterol to SR-B1 to penetrate cells.

The researchers found that SARS-CoV-2 uses cholesterol molecules in a taxi to penetrate cells to reach the cell surface; Then, when Covid-19 reaches the cell surface, its "spike" protein attaches to the ACE2 receptor and infects the cell. ACE2 is a receptor that allows the corona virus to enter human cells.

This study showed that the corona virus uses cholesterol molecules that bind to the SR-B1 receptor to enter the cell. The researchers then found that blocking the SR-B1 receptor and neutralizing it could prevent the infection. Targeting the SR-B1 receptor could be a potential way to develop therapies for coronation in the future, they say. The results of this study show that SR-B1, the SARS-CoV-2 cell binding procedure, facilitates the virus to enter cells and infect them. Thus, SR-B1 may be a potential therapeutic target for limiting SARS-CoV-2 infection (Fig. 4).

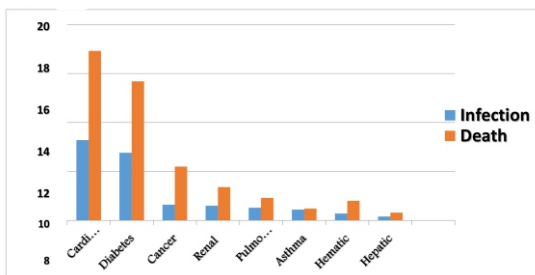


Fig. 4: Death and Infection data

3-5-2 Age

Most death in Covid-19 was in 70 to 79 years old group

and most infection in 50 to 59 years old and also in Delta covid infection is most in 1 to 14 years and the most death in 60 to 74 years old (Tables 1 and 2).

Table 1: Covid-19 Death and Infection data

Age	Covid 19 Death	Covid 19 Infection
0 - 9 years	0.1%	0.9%
10 - 19 years	0.9%	1.2%
20 - 29 years	0.9%	8.1%
30 - 39 years	3.4%	17%
40 - 49 years	6.6%	19.2%
50 - 59 years	14.4%	22.4%
60 - 69 years	23.1%	19.2%
70 - 79 years	28%	8.8%
80 - 89 years	19.6%	3.2%
90 and older	3.2%	

Table 2: Delta Covid Death and Infection data

Age	Delta Covid Infection	Delta Covid Death
<= 14 years	35%	1%
15-29	18%	3%
30-44	22%	11%
45-59	15%	32%
60-74	8%	39%
>= 75	2%	14%

3-5-3 Gender

Evidence suggests that although the incidence is the same between men and women, the mortality rate is higher among men than women. This may be due to differences in the immune responses of the two sexes or differences in different behavioural characteristics is gender. For example, the pattern and prevalence of smoking vary between the genders. But in general, differentiated data on gender are not enough.

But the findings that women are less likely to get sick or have a stronger immune system are not unique to Quid 19. In the case of other viral diseases, such as the flu or AIDS or hepatitis, it has been proven that women experience more severe episodes of the disease than men. What has been considered so far are some reasons

- 1- Excessive smoking by men compared to women
- 2- Differences in daily conditions and hygiene between men and women. More men in business and community than women
- 3- The role of two hormones, estrogen and testosterone

The female hormone estrogen is able to stimulate the immune system, while the male hormone testosterone is likely to do just the opposite.

Estrogens are a group of sex hormones that create and maintain female characteristics in the human body.

Testosterone is a hormone that is present in both women and men, but is found in smaller amounts in women and more in men (for example, hair growth in the body is one of the factors affected by the presence of testosterone in the body).

The question of what functions an extra X chromosome does in women (women have two X chromosomes and men have only one X chromosome that contains the female immune response) has long fascinated researchers. The answer to this question, according to many researchers, is that this chromosome is involved in the immune system.

* Stronger immune response in women, of course, has disadvantages, because women are more likely than men to develop autoimmune diseases such as arthritis, rheumatoid arthritis and lupus. In these diseases, the immune system attacks the body's own organs and tissues. 80% of people

have female autoimmune disease.

4 Cytokines and T Lymphocytes

What is a Cytokine?

When comparing male and female patients, the researchers found significant differences in the immune response in the early stages of infection. These differences included higher levels of different types of inflammatory proteins called cytokines in men.

Research has shown that severe cases of Covid-19 lead to a mysterious condition that disrupts the immune system; Instead of attacking only infected cells, the immune system attacks healthy cells as well. This condition is known as cytokine storm. Cytokines are used as part of the body's innate immune response. They are the first public counterattack to attack pathogens. However, in severe cases of Covid-19, the overproduction of cytokines, known as "cytokine storms," causes fluid to accumulate in the lungs, depriving the body of oxygen, and potentially causing shock, tissue damage, and lack of The proper functioning of different organs. Higher concentrations of cytokines earlier in men cause these symptoms to occur earlier. In contrast, scientists found that female T lymphocytes function more strongly than male T cells.

What is T lymphocyte?

It is a type of blood lymphocyte that is involved in the body's specific defences. T lymphocytes are initially made immaturely in the bone marrow. It then circulates to the thymus. There it is able to detect foreign factors, mature and return to the blood. Therefore, the site of bone T lymphocyte production and maturation is the thymus.

* The thymus is a gland in front of the trachea that is located behind the sternum.

T lymphocytes are responsible for cellular immunity. These cells have antigen receptors on their surface that are complemented by only one type of antigen. That is, they are able to specifically identify an antigen of cancer cells or virus-infected cells. When T lymphocytes are exposed to this cell, they multiply to form the following two types of cells:

1- Deadly T lymphocyte

After attaching to foreign target cells, these lymphocytes secrete a substance called perforin. Perforin is a protein that causes cavities in foreign cells when it comes in contact with them. As a result, lethal T lymphocytes can program to kill enzymes, enter the foreign cell, and eventually kill it.

2- Memory T cell

These cells are the body's immune memory. These T cells, like T lymphocytes, are sensitive to an antigen and play a role in the body's secondary immunity, meaning that when we are exposed to the same foreign cells for the second time, more deadly T lymphocytes and T cells are produced and the body produces more memory. Shows a faster immune response.

As a result, the poor response of T lymphocytes in men leads to worsening of the disease. Also, the lymphocyte T response in older men was significantly worse than in young male patients.

Researchers have now suggested that the treatment developed for Covid-19 should be such that, even with these differences, it can treat patients.

5 Results

According to the conducted researches in a determined period of time and a determined social community (during my research):

Infection : Men:57% , Women:43%

Death : Men: 59% , Women :41%

Acknowledgments

Special thanks to Mr. Arjmand as supervisor and Dr Izadi in AYIMI Institute.

References

- [1] <https://intermountainhealthcare.org/blogs/topics/live-well/2020/04/whats-the-difference-between-a-pandemic-an-epidemic-endemic-and-an-outbreak/>
- [2] <https://www.cdc.gov/careerpaths/k12teacherroadmap/epidemiology.html#:~:text=By%20definition%2C%20epidemiology%20is%20the,state%2C%20country%2C%20global>
- [3] https://www.who.int/news-room/feature-stories/detail/the-effects-of-virus-variants-on-covid-19-vaccines?gclid=CjwKCAjwtfqKBhBoEiwAZuesiHmNAYV5ng-16znL1qzk49sXYhXAnuwbPglh_DoPmUA-JnKCD4bwoRoCe7IQAvD_BwE
- [4] <https://www.cdc.gov/coronavirus/2019-ncov/covid-data/investigations-discovery/hospitalization-death-by-age.html>
- [5] <https://www.worldometers.info/coronavirus/-age-sex-demographics/>
- [6] https://www.who.int/news-room/q-a-detail/vaccines-and-immunization-what-is-vaccination?adgroupsurvey={adgroupsurvey}&gclid=CjwKCAjwtfqKBhBoEiwAZuesiNjKOWaPqstlHX_DvqM-
- [7] <https://www.frontiersin.org/articles/10.3389/fpsyg.2021.634863/full>
- [8] <https://medlineplus.gov/genetics/chromosome/text=The%20X%20chromosome%20is%20one,the%20total%20DNA%20in%20cells>
- [9] <https://www.frontiersin.org/articles/10.3389/fimmu.2020.01446/full>
- [10] <https://www.health.harvard.edu/drugs-and-medications/testosterone--what-it-does-and-doesnt-do>
- [11] <https://www.medicalnewstoday.com/articles/277177>
- [12] <https://www.cdc.gov/coronavirus/2019-ncov/symptoms-testing/symptoms.html>

Genotoxic and Cytogenic Effect of Four Loko in Human Cells

Laura Ivonne Herrera Reyes, Ameyalli Flores Herrera, Emilio André Vázquez Hernández, high school students from Centro Universitario México, ivonne.herrera@cum.maristas.edu.mx, 94190328@cum.maristas.edu.mx y. 94190314@cum.maristas.edu.mx

ABSTRACT

ARTICLE INFO

Gold Medalists in IMSEF/ISAC Olympiad 2021
Supervisor: Biol. Laura Ivonne Herrera Reyes
Accepted by: Ariaian Young Minds Innovative Institute, AYIMI

http://www.ayimi.org_info@ayimi.org

Four Loko® is a beverage which contains between 12% and 14% of alcohol, sugar, caffeine, taurine, wormwood and furfural, causing an intoxicated state accompanied with headaches, nausea, diarrhea, abdominal pain, general discomfort. For this reasons, one of the studies that must be realized is the toxicological test therefore in this project we evaluated the genotoxic effect of Four Loko® in lymphatic cells. Micronucleus are chromosomes fragments which are left out of the nucleus and can be caused by clastogen agents such as radiation that breaks chromosomes and aneuplodogen agents which damage mitotic spindle such as vincristine.

Key words: *Micronucleus, Four Loko®, giemsa, lymphocytes, clastogen, aneuplodogen*

1 Introduction

1-1 Justification

Four Loko® is an energetic beverage consumed by young people in parties and social events, it contains 12% alcohol, wormwood, furfural and taurine between others. This beverage has been banned in several countries for its secondary effects. The deputy Maria Mercado Sánchez requested Cofepris to realize toxicologic studies for this beverage since many young people have been hospitalized by drinking it, and even launched an inciative to withdraw it of the Mexican market. Students from the CUM made a research to determine the lethal dosis of Four Loko® in *Drosophila melanogaster*, yet the higher concentration which could be tested was of 40% because the alcohol levels of the beverage exceed the tolerance levels of the fly. The SMART test revealed around 11 mutations with mwh and flare3 markers (Ferral, et al, 2019, P: 3-5). For this reason we decided to continue with the Project, evaluating its genotoxicity in lymphatic human cells using the micronucleus (MN) technique employed by Castillo and Fujita in 2011, which allows to determine the damage in cellular DNA (Fig.1).

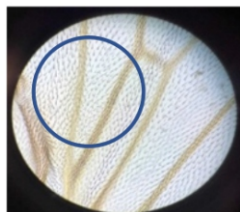


Fig. 1: Mutations in flies' trichrome

1-2 Problem Statement

Many alcoholic beverages that are sold in convenience stores like Four Loko® don't have preliminary toxicologic studies which confirm a secure intake, furthermore, they are sold unrestrictedly to minors which turns them into a health risk. This is the reason which lead us to raise the next project where we evaluate the genotoxic effect of Four Loko® in lymphatic cells by the determination of micronucleus (Fig. 2).



Fig 2: Four Loko Black

1-3 Hypothesis

If Four Loko® contains cutogenic and/or genetic substances, then we will observe in the lymphatic cell the presence of MN, if they are small then it will have clastogenic compounds and if they are big then it will have aneuploidogenic substances.

1-4 Research Purpose

- Evaluate the genotoxic and cytogenic effect of Four Loko® in lymphatic cells.
- Observe the behavior of the lymphatic cell which were exposed to the different Four Loko® concentrations.

2 Theoretical Framework

Four Loko is mainly consumed by Young people between 15 and 24 years old because of it easy access and unrestricted sale in 24 hours convenience stores. This sweet beverage has caused important reactions in the young people who drink it and some have even been emergency admitted to hospitals. In the section of "Nación" in the Mexican newspaper "El Universal" (07/17/2019) it says: Cofepris analyzed the content of this beverage and as a result of their analysis in batches L19338354 and L1751338 it was detected the presence of furfural in quantities outside de Official Mexican Norm NOM-142-SSA1/SCFI-2014 Alcoholic Beverages.

Furfural is an ethanol metabolite which in high quantities can cause: headache, nausea, diarrhea, abdominal pain and malaise in general, the preliminary results in reproductive studies and of feeding in mice and rats demonstrate the possibilities of birth and reproductive defects (Rivera, S. M. y Aguilera, R. J., 2000).

Micronucleus are spherical cytoplasmic corpuscles which are detected in the interphase, smaller and with the same characteristics of the cell nucleus; they are origintaed by the loss of chromosomic fragments or entire chromosomes

surrounding the cellular division and they have value in the diagnosis of genotoxicity (Castillo, Guevara-Fujita y Fujita, 2011, P: 1) (Fig. 4).

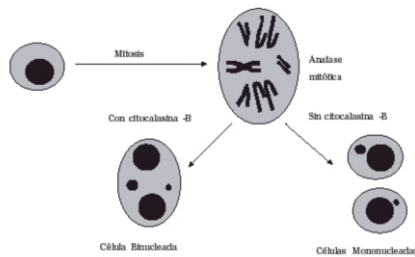


Fig. 3: Micronucleus formation by the loss of an entire chromosome and chromosomal acrocentric fragments in mitotic anaphase. The scheme shows the blockade with cytochalasin-B and the resulting formation of binuclear cells

Micronucleus may be caused by clastogenic agents (such as radiation that breaks chromosomes) and by aneuploidogenic agents that damage the mitotic spindle such as vincristine. Micronuclei are known in the field of hematology as Howell-Jolly bodies and their shape is generally round or almond-shaped, with a diameter of 0.4 to 1.6 microns. If the compound studied is a clastogen then a small micronuclei will be formed; however, if a large micronucleus is formed it will be an aneuploidogenic. (Zúñiga, G. G. & Gómez, M. B, 2006, P: 1- 3). The year 1999 was crucial for the MN test since the technique was validated worldwide and considered as an effective biomarker of DNA damage. In order to validate the technique an international human micronucleus program (HUMN: Human Micro Nucleus Project) was created to collect the basal frequencies of MN obtained in different laboratories around the world. (Zalacain, M., Sierrasesúmaga, L. y Patiño, A., 2005, P: 3,4).

3 Methodological Process of the Project Development

The research took place from October 7, 2019 to March, 3 2020 at the CUM’s laboratory. The independent variable was the concentration of a commercial beverage known in the market as Four Loko® and the dependent variable was the presence of micronucleus in lymphocytes. 5 ml of peripheral blood were extracted from 3 healthy donors and between the ages of 15 and 18 years old (Fig. 4).



Fig. 4: Blood Extraction

0.5 ml of heparin were added to the blood sample and this was collocated in centrifuge tubes (Fig. 5).



Fig. 5: Tubes with Heparin

The samples were centrifuged for 30 minutes at 3000 rpm

to separate the components by density (Fig. 6).

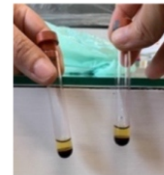


Fig. 6: Blood separation by density

The lymphocyte interface was separated and 5 ml of PBMAX (gibco) were added; then it was incubated at 37°C for 48 hours (Fig. 7).



Fig. 7: Addition of the culture medium

After 48 hours, 6 samples of Four Loko® black were formed and the concentration was added. In the first sample, 0.5 ml at 100%, in the second 0.5 ml at 80%, in the third 0.5 ml at 60%, in the fourth 0.5 ml at 40%, in the fifth 0.5 ml at 20%, and finally, the sixth where as positive control, mitomycin C (MMC-Sigma MO503) was used and, as negative control, ethyl alcohol at 12% was added (Fig. 8).



Fig. 8: Four Loko concentrations are added

After 24 hours, 2 drops of colchicine were attached and it was incubated at 37°C for another 24 hours. 96 hours later, all the tubes were centrifuged at 3000 rpm for 5 minutes. The overlying was decanted and one drop from the beaker was collocated on a clean glass slide doing a smear (two repetitions in each sample).



Fig. 9: Tubes ready for the final decantation. The lymphocytes buttons are observed

The samples were set for 5 minutes with an acetic acid solution and methanol 1:1. Then, they were dyed with giemsa colorant at 5% for 8 minutes and they were looked through with a microscope at 100X using immersion oil.



Fig. 10: Staining of samples

IDN of binucleate cells was calculated, for genotoxicity the number of cells were divided with a micronucleus for concentration between the total cells quantified. For cytotoxicity the number of nuclei per multinucleated cells between the number of total cells.

4 Results

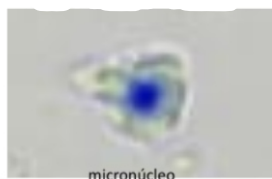


Fig. 11: Mononucleated cell, alcohol with water

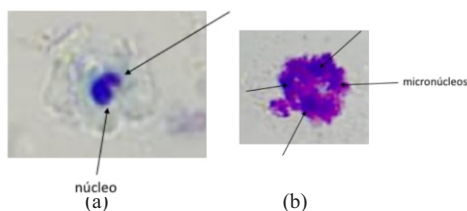


Fig. 12: a) Binucleated cell, b) Multinucleated cell, 100% concentration

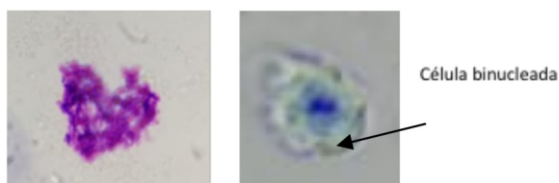


Fig. 13: On the left, cell with cromatine and on the right, binucleated cell with a 50% concentration

Table 1: Four Loko effect in human lymphocytes

Concentración	No. de células totales	Promedio por muestra	Células con núcleo alterado	Genotoxicidad	Citotoxicidad	IDN
Mitomicina C						
(+)	780	195	500	0.70512821		1.617
100%	436	109	280	0.64220183	0.800	0.823
80%	400	100	200	0.50000000	0.589	0.588
60%	450	113	150	0.33333333	0.432	0.441
40%	420	105	125	0.29761905	0.341	0.367
20%	370	92	98	0.26486486	0.250	0.288
(-)	400	100	34	0.085	0.090	0.100

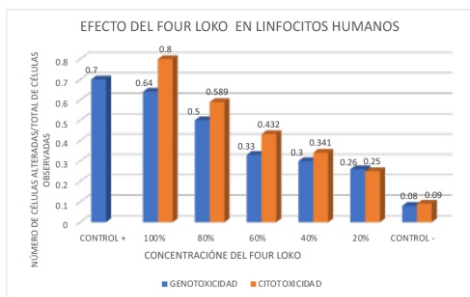


Fig. 14: Genotoxic and cytogenic effect of Four Loko

5 Analysis and Discussion

Photographs of the experiment allow to appreciate different micronucleus; the smaller correspond to clastogens substances and the bigger to aneuploidogens. (Fig. 14) shows that the genotoxic and cytogenic of Four

Loko® effect is observed in lymphocytes. We confirm our hypothesis since the presence of micronucleus in lymphocytes reveals the damage that Four Loko® causes to cellular DNA In Table (1), IDN concentration in this beverage is very high; it is almost 50% of mitomycin. This is a substance highly mutagenic. We would like to make a spectrophotometric of gases to verify the real content of the substances included in this beverage and analyzed them separately.

5-1 Future Research Lines

This project opens an important line of investigation concerning people’s health care. It is important that any food or product (medical or cosmetic) complies with the quality standards established by the norm to guarantee the safety of the consumers. Young population is considered a vulnerable group due to the tendency they have to follow "trending stuff" and "fashions" that could represent an irreparable damage to their reproductive and medical health since, nowadays, genotoxicity is being linked to some severe diseases such as cancer.

6 Conclusions

In all tested concentrations it is shown that Four Loko® is a toxic substance that alters cell division causing the rupture of mitotic spindle or the fragmentation of chromosomes generating multinucleated cells. Lymphocytes exposed to the different concentrations of Four Loko® present MN in all of the concentrations, therefore it contains aneuploidogenic and clastogenic substances which cause DNA cellular alterations. Four Loko® is a genotoxic substance, the presence of micronucleus demonstrates it and the concentration of the beverage is related to them since the higher the concentration, the bigger the number of multinucleated cells. Therefore, we accept our hypothesis, and we propose to make similar studies for every Four Loko® component.

We recommend to take it out of the market until further research is conducted, and to put all of its ingredients on its nutritional label for the public.

7 Acronym List

- Cofepris – Federal Commission for Protection Against Sanitary Risk
- MN – Micronucleus
- mwh – multiple wing hairs. Flies line with cellular marker of trichomes in wings
- flr3 – phenotype resistant
- ADN – Deoxyribonucleic Acid
- HUMN – Human Micro Nucleus Project
- CUM – Centro Universitario México
- SMART – Somatic Recombination and Mutation Test
- NOM – Mexican Official Norm
- IDN – Nuclear Division Rate

References

[1] Castillo, E., Guevara-Fujita, M. y Fujita, J. (2011). Optimización del test de micronúcleos en linfocitos cultivados usando una metodología de gradiente y frotis. *Revista Perú Biología*. 18(2): 261- 263.

[2] Countryman, P. y Heddle, J. (1976). The production of micronuclei from chromosome aberrations in irradiated cultures of human lymphocytes. *Mutat Res* (41), pp 321.332.

[3] Fenech, M. y Morley, A. (1985). Measurement of micronuclei in lymphocytes. *Mutat Res* (147), pp 29-36

[4] Ferral, A., Martínez, D., Portillo, D., Vidales, D. y Herrera, I. (2019). Efecto mutagénico del Four Loko en *Drosophila*

melanogaster. Recuperado de https://www.feriadelasciencias.unam.mx/antteriores/feria27/feria05601_efecto_mutagenico_del_four_loko_en_drosophila_mela.pdf

[5] Lobo, T. y Bolaños, A. (2014). Micronúcleos: biomarcador de genotoxicidad en expuestos a plaguicidas. *Revista Salus*. volumen 18 (2), pp 18-26.

[6] Mostafalou, S. y Abdollahi, M. (2013). Pesticides and human chronic diseases: evidences, mechanisms, and perspectives. *Toxicol Appl Pharmacol*; 268: 157-77.

[7] Rivera, M. y Aguilera, J. (2000). Propiedades físicas y termodinámicas del furfural. *Revista Tecnología química*. Volumen XX (1), pp 83

[8] Rodríguez-Gómez, A. y Frias, S. (2014). La mitosis y su regulación. *Acta Pediátrica de México*. Volumen 35 (1), pp 55-86.

[9] Torres -Bugarin, O. y Ramos, M. (2013). Utilidad de la prueba de Micronúcleos y anormalidades nucleares de células exfoliadas de mucosa oral en la evaluación del daño genotóxico y citotóxico. *International Journal of Morphology*. Volumen 31 (2), pp 1-6.

[10] Torres-Bugarin, O., Zavala, M., Macriz, N., Flores, A. y Ramos, M. (2013). Procedimientos básicos de la prueba de micronúcleos y anormalidades nucleares en células exfoliadas de la mucosa oral. *Revista Medigraphic:El residente*. Volumen 8 (1), pp 4-11.

[11] Zalacain, M., Sierrasesúmaga, L. y Patiño, A. (2005). El ensayo de micronúcleos como medida de inestabilidad genética inducida por agentes genotóxicos. *Anales del sistema Sanitario de Navarra*. Volumen (28), pp 1-10.

[12] Zuñiga, G. y Gómez, B. (2006). La prueba de micronúcleos. *Revista de divulgación científica y tecnológica de la universidad Veracruzana*. Volumen 11(1), pp 1-3.

[13] El Universal.com. (2019). Ya analizaron que tiene el Four loko y este es el resultado. www.eluniversal.com.mx/nacion/sociedad/profeco-ya-analiza-que-tiene-four-loko-yeste-fue-el-resultado

[14] Frias, C. (2010). Alertan sobre el licor Four Loko, un peligroso 'desmayo en una lata'. Recuperado de <https://www.elnuevoherald.com/vivirmejor/salud/article2009864.html#storylink=cy>

Augmented Reality as a Didactic Tool in Education

Myrahis Yurizahan Sanluis Cerezo, Armando Palma Lima, Escuela Secundaria Técnica, "Ing. Guillermo González Camarena", Mexico
myurisc@gmail.com

ABSTRACT

ARTICLE INFO

Gold Medalists in IMSEF/ISAC Olympiad 2021
Supervisor: Armando Palma Lima
Accepted by: Ariaian Young Minds Innovative Institute, AYIMI

http://www.ayimi.org_info@ayimi.org

Augmented Reality as a didactic tool in education is a project that aims to support teachers in their teaching practice using augmented reality technology. This technology allows combining the real and virtual world by adding layers of visual information about the world that surrounds us, this helps to generate experiences that provide relevant knowledge about our environment and in this way the educational content is in different basic education school topics. In the process these tools were used: Aumentaty Creator, which allows to create AR projects easily and quickly; Augmented Scope to visualize AR projects; and Tinkercad for 3D modeling and animation.

Key words: *Augmented reality, education, Aumentaty, Technology*

1 Introduction

At present, information and communication technologies (ICT) have allowed a new form of interaction in the teaching-learning processes. The rapid evolution of computers and the growing use of mobile devices is making both students and teachers use new media and resources to enhance and acquire knowledge and thus facilitate learning.

One of the many tools that can be used in education to enhance knowledge is Augmented Reality (AR). AR is a technology that uses virtual objects (created by computer) for the user to perceive the real environment "augmented".

For example, with AR applications, in geography the parts that make up a volcano can be shown to the student, how the DNA of human beings is made, some math problems can be exemplified. All of this by using 3D models that are more attractive, visual, and fun.

The purpose of this project is to create an AR application that uses 3D models to enrich certain contents in 3 subjects of the secondary education curriculum: Geography, Science and Mathematics.

1-1 Justification

This project has been designed with the aim of favoring the development of disciplinary competencies and active learning, facilitating secondary education students the appropriation of disciplinary knowledge and transfer it in subjects related to Mathematics, Science I and Geography.

This will undoubtedly update the old didactic means of teaching science in which there are only images through sheets or, at best, with an explanatory video.

On the other hand, both students and teachers will benefit, as long as they know the benefits of AR technology, such as the use of three-dimensional models and the experimentation, as well as the generation of Learning Objects (LO) through the available tools, favoring the use of ICT and the development of future research on its impact on the teaching-learning process, and the design of strategies that can incorporate AR as a teaching resource.

1-2 Problem Statement

Most of the academic material that serves as a complement to the teaching material in the classes is based on the use of text that incorporates images, video,

animations, and sound. When using this type of resources, students become more interested, however, more visual and attractive media are needed so they allow them the ability to analyze, making them participate in a more collaborative and motivating environment.

Therefore, it is necessary to gradually provide teachers with innovative AR resources that allow students to understand a concept, content, or procedure, based on the exploration of knowledge with the body, since AR helps the learning process of students among other reasons due to the high degree of interaction it provides.

This form of teaching is the "learning by doing" approach, also known as active learning and "learning by playing", in this way it contributes to the achievement of the constructivist approach that allows the user to be able to modify, build, test ideas, and get actively involved in problem solving.

In addition, the use of AR in the classroom, and specifically, the use of mobile devices, overcomes the limitation of time and space in learning environments.

1-3 Objectives

Choose topics from the Geography, Science I and Mathematics subjects where 3D models can be used to generate an AR application that works on mobile devices.

Find, download, and optimize 3D Aumentaty Creator models to use in the AR application.

Create simple 3D models using the Tinkercad tool to use them in the AR application.

Use the RA Aumentaty platform to develop the augmented reality application and view the content on a mobile device.

2 Theoretical Framework

2-1 What is Augmented Reality

Augmented reality is the technology that complements the real environment with computer-generated information, in this way reality is combined with virtual elements, providing a mixed or augmented reality in real time. (Fig. 1).

For an application to be defined as an AR application, it must meet the following requirements:

- a) Combine virtual objects with the real world.
- b) Be interactive in real time.
- c) Present virtual objects in three dimensions.

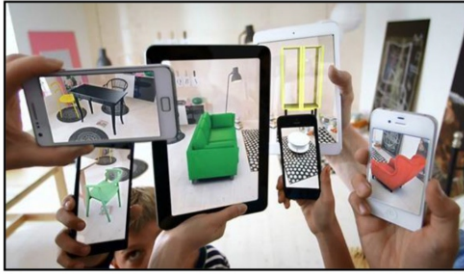


Fig. 1 :Textbook with augmented reality

2-2 Types of Augmented Reality

There are basically two types of AR, Augmented Reality based on markers or images and Augmented Reality based on position.

2-2-1 Augmented Reality Based on Markers or Images

This type of Augmented Reality uses markers or images, in which some type of information (images, 3D objects, video) is superimposed when they are recognized by a certain software(Fig.2).



Fig. 2: Augmented Reality based on markers

2-2-2 Augmented Reality Based on Position

In this type of applications, Augmented Reality browsers are used, these applications use the hardware of smartphones (GPS, compass and accelerometer) to locate and superimpose a layer of information on points of interest (POI) in our environment.

When the user moves the smartphone capturing the image of their surroundings, the navigator, based on a data map, shows the nearby POI. (Fig. 3).

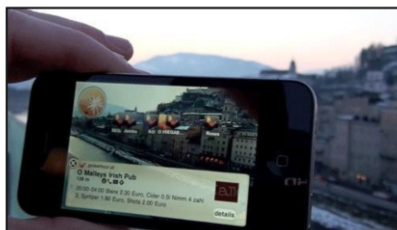


Fig. 3: Augmented Reality based on position

2-3 How Augmented Reality Works

In any augmented reality system, four fundamental tasks are necessary to carry out the augmentation process.

1. Scene capture

2. Scene identification
 3. Mixed reality and magnification
 4. Visualization.
- 2.4 Uses of the Augmented Reality.

Due to its benefits, AR can be used in an infinity of areas and topics of interest such as:

- Mobile marketing
- Online searching
- Tourism
- Medicine
- Architecture
- Interior design
- Science
- Education
- Videogames

Figure (4) shows an example of an AR application in video games.



Fig. 4: Augmented Reality in videogames

2-4 Augmented Reality in Education

The applicative possibilities of AR, with respect to the elaboration of didactic materials and learning activities, are multiple and heterogeneous in practically all subjects. It can provide learning experiences outside the classroom, more contextualized, displaying links between reality and the learning situation in which students participate. Any physical space can become a stimulating academic setting. For example, students of Archeology, History or Anthropology, could have applications that reconstruct exceptional historical sites (Fig. 5).

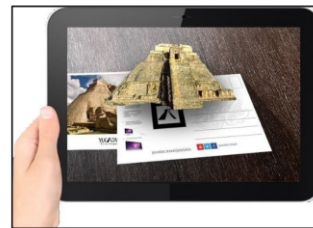


Fig. 5: Augmented Reality in a history class

2.5 Aumentaty

Aumentaty is a free software that allows users to create augmented reality scenes, it is the ideal Augmented Reality content generation tool for those who do not know how to program, but it does not have an editor or creator of 3D models(Fig.6).

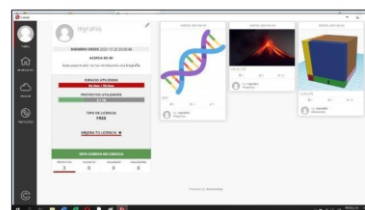


Fig. 6: Environment of Aumentaty development

Aumentaty Creator is the desktop version of Aumentaty to create our augmented reality applications. It is currently only available for Windows. Once the project is created, the Scope application is needed on our mobile device to view the AR. To start using creator, follow these steps:

1. Register at Incentaty.com
2. Verify your email
3. Click on new project and fill in your project information
4. Add files to your project
5. Choose what type of QR code to launch your file
6. Add what type of AR element you want to carry that marker
7. Publish the project

Aumentaty Scope is the Aumentaty application that allows you to view all the AR projects that have been created with the Creator tool. To use it, simply access the Android store. Once downloaded, you can enter the app as a guest without registration or you can register. Within the application, you can search for the project in the section searches, or scan with the camera in search of the project.

The application allows you to save the projects so that it is not necessary to search for them every time you want to view them, it also tells you if there is a new update to it and gives you the option to download the new version.

3 Methodological Design

3-1 Construction of the Target Image



To make use of Aumentaty Creator it is necessary to register on its portal and verify the registration by means of an email that the app sends you.

The next step is to download the software and install it, and then log in with your registration data (Fig.7).

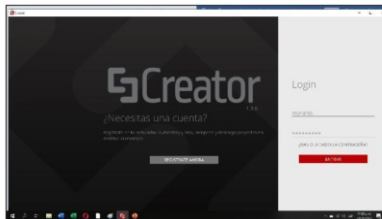


Fig. 7: Aumentaty Creator log in

Once logged in, we find on the left side a vertical menu with four options: profile, news, search, and projects. The latter is where the applications that can be made with this tool are built (Fig. 8).

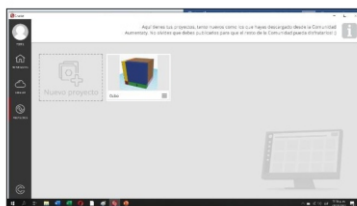


Fig.8: Aumentaty Creator log in

The process of creating projects in Aumentaty begins

when you click on new project and enter a name and description(Fig. 9).

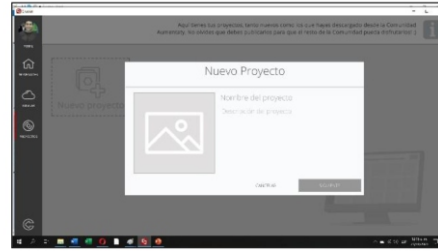


Fig. 9: Aumentaty Creator new project

Then the necessary files that the project will carry are added, they work by using different types of markers which can be: QR code type, image type or geolocation type (figure 10). For the three projects we carried out, files with image type makers were used.

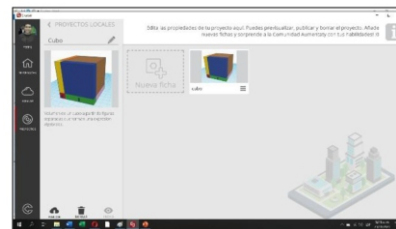


Fig. 10: Adding files to a project

The next step is to add elements to our scene which can be:

- Image
- Text
- Video
- 3D Models
- Link

In the case of the math project, the scene consists of 4 elements: one 3D model, two images, and one video (Fig. 11).

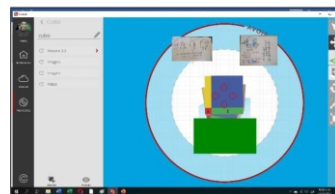


Fig. 11: "Cube" project elements of the mathematics subject

The options on the right-side menu are used to place each element in the desired position, as well as to modify its dimensions.

Once we have finished adding files and elements, we proceed to the publication of the project, for this we return to the main screen of the project and click on the publish button (Fig.12).



Fig.12: Publication of the finished project

Figures (13) and (14) show the other two projects related to the subjects of Science and Geography, in each of them we incorporate elements such as the 3d model, videos and images.

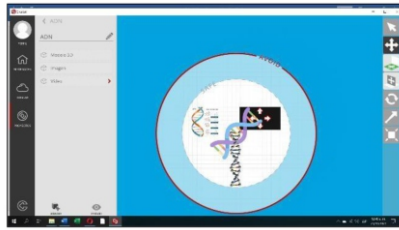


Fig. 13: DNA Project for the science subject

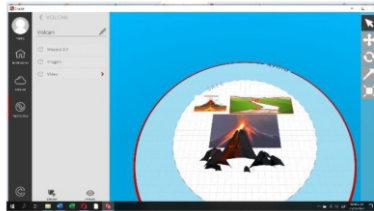


Fig. 14: Volcano project for the geography subject

3-2 How to Use Tinkercad.

This application is very good to make 3d models and animations. To start using it, you must first enter its website and then sign in with your Google or Apple account(Fig. 15). Once logged in, on the left side there is a vertical menu with several options from which we will occupy three, 3d designs, circuits, and code blocks (Fig. 16). In the latter you can make 3d animations.

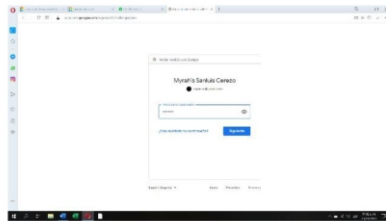


Fig.15: Tinkercad log in

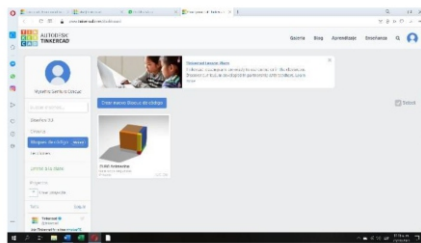


Fig. 16: Tinkercad main page

3-3 Creation of 3D Animations

The procedure to make animations is when you click on Create new Code Block (Fig. 17). Immediately, you will find a box that gives you the option to choose a design or make a new design. For the animations of the "Cube" and "Rotation and Translation" projects, the option of "a new design" was used.

Consequently, the animation is made with code blocks which are found on the left side (Fig. 18), these give us tools to:

- Form

- Modify
- Control
- Mathematics
- Data
- Mark

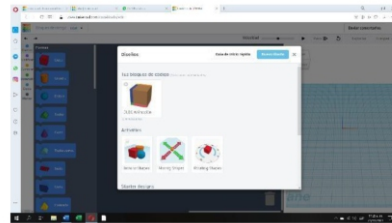


Fig. 17: Choosing 3D design

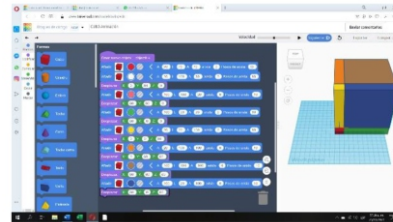


Fig. 18:Code blocks for the Cube animation

When our animation has already accomplished what we wanted to achieve, we will proceed to save it as a video and then use it in Aumentaty Creator. For this, you click on the share button which is in the upper right part. Next, a box will appear where you will click on Animated Gif, button at the bottom right (Fig. 19).

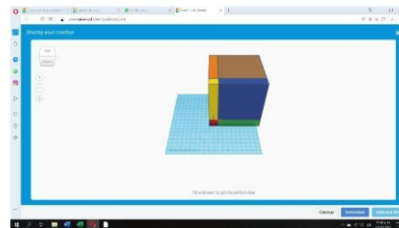


Fig. 19: Saving the Cube animation

Later the gif will be downloaded automatically.

3-4 How to Use Scope Aumentaty

This is a mobile application which helps us to visualize the figures in 3D, figure 20. To use it you must first download it, then open it, you can enter with your user or enter as a guest, then you will find the initial page where you will find the following:

- Marker
- Browser
- Searcher
- Downloads

Next, to visualize the Cube Project, we will open the search magnifying glass and then enter the name of the project, once found, you click on the image, then the project will appear and then at the bottom you click on download. (Fig. 21).

Afterwards, you click on the open button, then on the lower left button that shows a camera in order to focus on the marker and observe the 3D figure, along with the images and videos (Fig. 22).

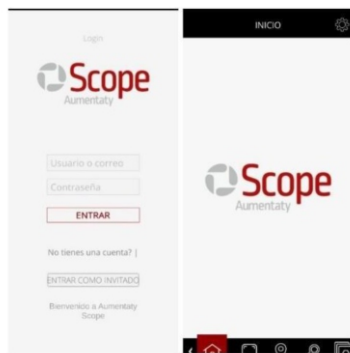


Fig. 20: Aumentaty Scope log in

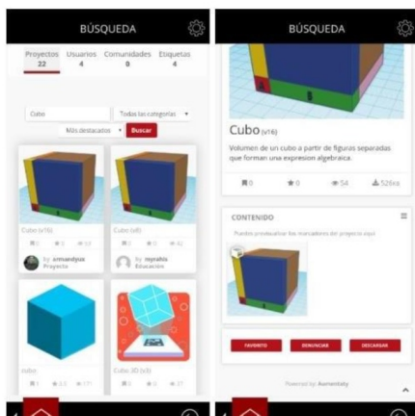


Fig. 21: Searching and downloading the Cube project

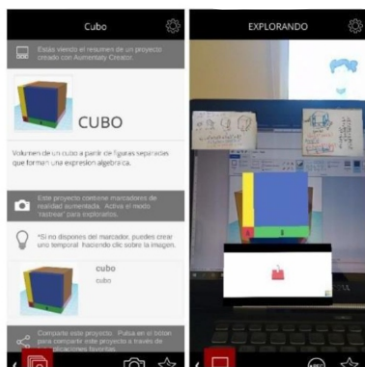


Fig.22: Verify Cube Project on AR

4 Results

To verify the acceptance of the application, a survey of 9 questions was applied using a Google form and the following results were obtained (Figs.23 -30).

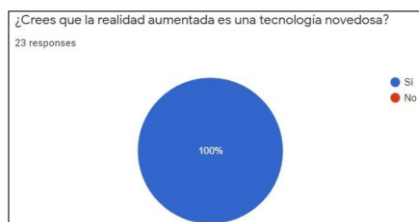


Fig. 23: Do you think that Augmented Reality is an innovating technology?



Fig. 24: Do you consider that Augmented Reality can be applied in education?

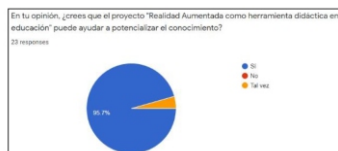


Fig. 25: In your opinion, Do you think that the project "Augmented Reality as a didactic tool in education" can help to enhance knowledge?

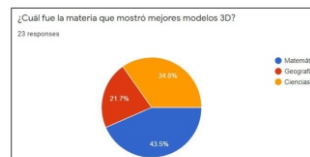


Fig. 26: Which subject showed the best 3D models?

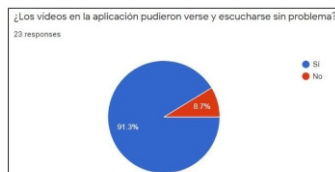


Fig. 27: Did the videos in the application reproduce without problems?



Fig. 28: Were the images in the Project legible?

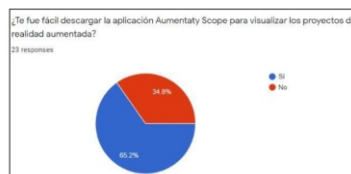


Fig. 29: Was it easy to download the Aumentaty Scope app to visualize the projects in Augmented Reality?

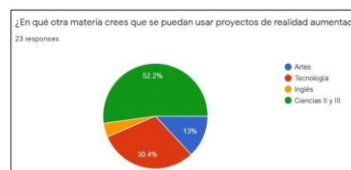


Fig. 30: Which other subjects can use the Augmented Reality projects?

5 Conclusions

After the completion of this project, we were able to conclude that:

- Augmented Reality is very useful and can be used as a pedagogical tool in basic education.
- Teaching materials are needed to promote active student

learning, and AR projects can help to achieve this.

- The Aumentaty platform provides the possibility to create AR applications in a quick and easy way.

- The people who tested the application we developed like it and there were comments and observations that will undoubtedly help to improve it in some respects and create future versions.

5-1 Future Lines of Research

Based on the observations and recommendations that teachers and students shared with us, in future versions of the project it is proposed to use better designed and more detailed 3D models, for this we must use specialized tools for the creation of those models

This also raises the possibility of using a development tool such as Unity 3D to develop mobile applications so as not to depend on an online platform.

Acknowledgment

To my parents, from whom I have always received their unconditional support, protection and love.

To my teacher, who has been my guide throughout my secondary education.

To the organization of Expociencias Mexico, who motivated me and provided me with all the facilities to enjoy the 1st Online International ISAC Olympiad experience.

References

[1] Universidad Politécnica de Madrid, Gabinete de Tele-Educación, Realidad Aumentada en Educación. http://oa.upm.es/45985/1/Realidad_Aumentada_Educacion.pdf

[2] Heras L., Villareal J. L., La realidad aumentada: una tecnología en espera de usuarios, Departamento de Visualización, DCI, DGSCA, UNAM.

[3] J. Lorenzo, Mega Tutorial TinkerCAD, cómo utilizarlos paso a paso. Revisión a fondo y opinión. <https://of3lia.com/tinkercad-tutorial-completo/>

[4] Blázquez A, Manual de Aumentaty, herramienta de realidad aumentada., Universidad politécnica de Madrid Gabinete de Tele-Educación.

[5] De Miguel R., Realidad Aumentada para potenciar la capacidad de innovación del alumnado. <https://www.educaciontrespuntocero.com/noticias/usos-realidad-aumentada-aulas/>

[6] Muñoz, S, Merino C, Espinosa I, Delgado A, Arrien P. Aplicaciones la realidad aumentada en la educación. España 45 – 73p.

The Effect of Salt on Ice Melting

AmirAli Safari, Grade 6, Valeh School, Tehran/Iran, Amiralisafari185@gmail.com

ARTICLE INFO

Participated in IYNT / IMSEF 2021 and received Gold Medal in IMSEF
Supervisor: Ahmadreza Arabani Mostaghim
Accepted in country selection by Ariaian Young Minds Innovative Institute, AYIMI

<http://www.ayimi.org>, info@ayimi.org

ABSTRACT

According to the scientific exploration, some questions are raised about the happenings while sprinkling salt on ice. Then, some theories have been developed. Some experiments were conducted to prove the presented theories. The rate and speed of ice melting depend on some factors like size of the ice, the temperature of the room, shape of the ice, etc, which were examined with the experiments. It was found by increasing the concentration of salt, the speed of ice melting will increase and type of salts are more useful for melting ices which include: NaCl-KCl-MgCl₂ and CaCl₂.

Key words: Colligative properties, Salt, Ice cubes, Melting

1 Introduction

This problem tries to tell us how salt can melt ice and what are these factors can affect this phenomenon. It relates to our daily live, for example in winter when it snows, we need to know which materials are better in terms of various criteria such as the availability of material or the speed and strength of melting snow and ice. First, we have to know salt is a mineral composed primarily of sodium chloride (NaCl), a chemical compound belonging to the larger class of salts; salt in the form of a natural crystalline mineral is known as rock salt or halite. Also, there are different types of salts categorized into monovalent, bivalent and other categorized according to the periodic table.

Colligative properties is the ratio of the number of solute particles to the number of solvent particles in a solution. These properties do not depend on the nature of the chemical species but the number of soluble particles affects the boiling point, freezing point, and vapor pressure. The higher the number of solute particles in a solution, the faster the dissolution. It is an important factor especially when we are comparing the salts based on their concentration. The next factor is the surface-to-volume ratio that checks the rate of one surface in which its volume helps us especially when we are comparing the speed of ice melting based on their size. In chemical reactions where a solid is in contact with a solution, the ratio of surface to volume is an important factor in reactivity. Consider a pot and a jug, the pot has a bigger surface than the jug. However, the volume of the pot is more than the jug. Therefore, if you fill both of them with water and return them simultaneously, you will see that the time for the jug to be empty will be shorter than the time needed for the pot. It means the surface-to-volume ratio of the jug is less than the surface-to-volume ratio of the pot (Fig. 1).

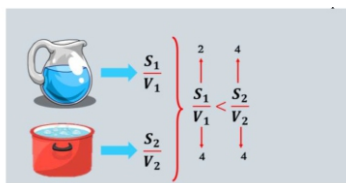


Fig. 1: Surface to volume ratio

Therefore, these rules can affect on our experiments. At

first when the experiment starts, we can see temperature drops down for a time and then it is constant. The main factors are:

- 1- Concentration of salts
- 2- Size and shape of the ices
- 3- Different types of the salts

According to our experiments it is found NaCl is the most useful salt for melting the ice with smaller cubes (Fig. 2).

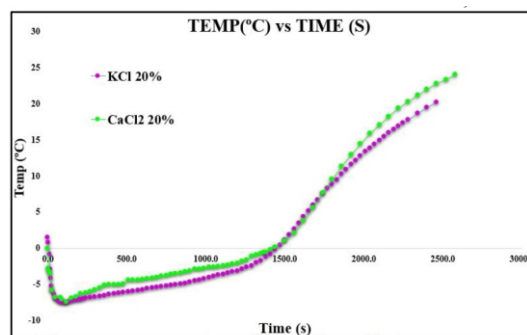


Fig. 2: Comparing two types of salt affecting on ice melting, KCl 20% and CaCl₂ 20%

2 Experiments and Methods

At first, it was observed that salt can melt ice in 2 forms when we sprinkle the salt on ice or dissolve it in water at room temperature. Then, some questions were asked and some hypotheses were assigned accordingly.

The first hypothesis was the rate and speed of the melting have a relationship with the size and shape of ices. Second hypothesis was the rate and speed of the melting have a relationship with the concentration of salts and the last one was the type of salts and other factors like room temperature or shape of containers that can affect this phenomenon.

Different determined parameters included:

- Concentration of salts
- Shape, size, and color of containers
- Different types of salts
- Room temperature
- Shape and size of ices

First Experiment: the distilled water had been put in two different ice molds and not just for once because the number of ices was a lot and put them in the freezer to make

ices. Then with a digital scale, the amount of salt was chosen (20% and 40%). The ice molds were divided into crushed ice and ice cubes which was the variable parameter and the melting ice was measured in different times (Fig. 3).

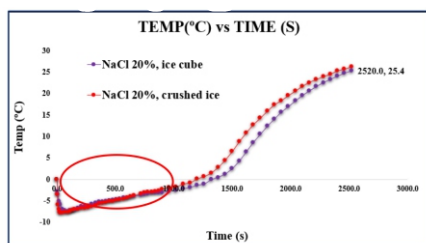


Fig. 3:Temperature versus time in ice melting by sodium chloride 20%

It's clear that starting point of each line is 0 °C (because the temperature of the water was 0 °C and one of the fixed parameters) and also both of the lines have a minimum which is lower in the crushed ice .Then the temperature is getting higher and higher but in the part that shows in a chart with the red circle, the fluctuations are low. This part is calling the latent heat. We have different latent heat, like latent heat of fusion, latent heat of vaporization, etc., however, the duration of the latent heat of the salts are the same. These experiments have been done with 20% and 40% of sodium chloride for both crushed and ice cube with the same results (Fig. 4).

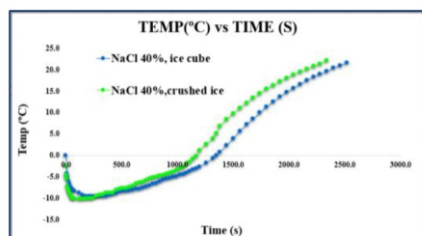


Fig.4:Temperature versus time in ice melting by sodium chloride 40%

Also, these experiments were done with two types of salts which were Calcium chloride (CaCl₂) (20% and 40%) in order to make sure that the results are the same for each type of salts and concentration (Fig. 5).

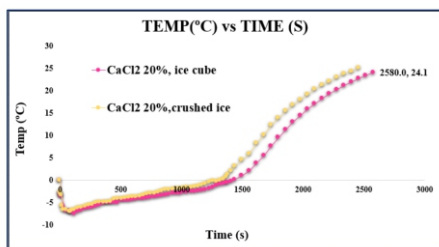


Fig. 5: Calcium chloride (20%) on ice melting.

Second Experiment: The second experiment is about salt concentration affecting on ice melting, requirements for doing these experiments were the same as the previous section only four types of salt are used (NaCl -KCL-MgCl₂ and CaCl₂) . The results for 0/2/4/6 and 8 % of sodium chloride in one diagram are compared with each other better (Fig.6).

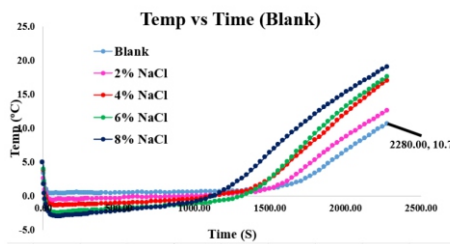
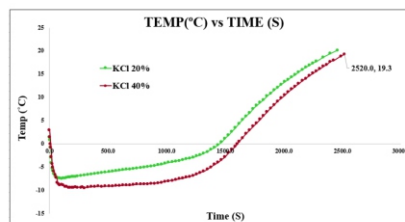
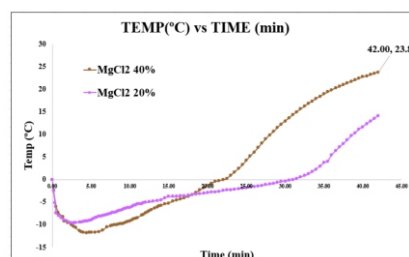


Fig.6: Sodium Chloride on ice with different concentration

According to the different concentrations of salt, the temperature gradient is different which is more in 8% sodium chloride salt compared to the other percentages. It is repeated again for other kinds of salt (Figs. 7 a,b,c).



(a)



(b)

Fig.7: a)Potassium Chloride and b) Magnesium Chloride on ice with different concentration

Third Experiment: In this experiment, monovalent and bivalent salts (Fig. 8) at a same concentration are compared in ice melting.

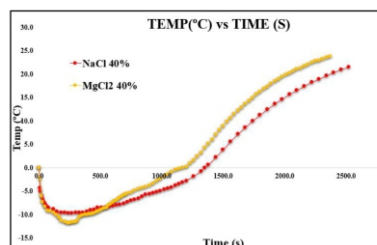


Fig. 8: Comparing between monovalent and bivalent salts in ice melting

In this case, according to the periodic table, monovalent salts are in one column & bivalent salts are in one column and according to the colligative properties the salts in one column in general form has the same structure and molecules so in this case, monovalent and bivalent salts are used together.

3 Discussion and Results

In our experiments, when the size of ice gets smaller, it can melt earlier and faster. Because by increasing the size

size of ices, the molecules of ice get more because they have more volume and they can have more overlap with water and hydrogen molecules, therefore, they would melt faster.

In all diagrams all lines start at 0.5 °C & all had a negative gradient in temperature due to the heat energy from the overlap of ice molecules with salt, which generates heat and lowers the temperature. According to the different concentrations of salt, this gradient is different, which by increasing of salt concentration, it becomes more severe. This gradient in 4% is twice more than 2% or 8% is four times more than 2% because of colligative properties. By increasing the concentration of salts, the time of latent heat decreases and then temperature increases.

According to these properties, the higher the number of particles in the ingredient, the more it reacts with other molecules. In this case, more concentrated salt would overlap and overheat faster which leads to produce energy and the ice melts faster and the latent heat lasts less. After latent heat, the slope of the sodium chloride diagram in 8% is higher because more heat is generated and therefore, the temperature rises more.

In the monovalent section, sodium locates above potassium, and in each column in periodic table, the more we go down, the more will be metallic characteristic. Potassium has more metallic features than sodium due to its position so the temperature gradient of potassium is more than sodium and the latent heat of that is shorter too. But, according to this, the overlap of potassium salt with ice is more exothermic and releases more heat. Therefore, it would reach the exothermic point sooner and after that, it is less inclined to continue the reaction due to the production of stable ions. For this reason, sodium chloride can act more than potassium chloride.

The negative gradient temperature for magnesium is more than sodium, because magnesium is bivalent and sodium is monovalent. Therefore, the number of MgCl₂ atoms is higher than NaCl so it overlaps with more molecules of ice.

Due to the higher number of particles, we consider the latent heat for magnesium runs out sooner but, the time of latent heat is the same too which of these two salts reaches a temperature of °C sooner? Sodium chloride. In Mendeleev's table, the more we move from left to right, the higher mass of the metal will be. After the latent heat, Magnesium salt which has the less metallic features does not tend to continue the overlap since more heat is generated and the time of latent heat for sodium makes less or the same as magnesium, and temperature increases for sodium to get more. Therefore, sodium is more effective in ice melting.

According to the table of solubility of salts in water (25 °C) in ambient temperature, for example, NaCl dissolves only 35.9 grams in 100 cc of 25 °C water, but magnesium can be dissolved up to 52.9 g, which means that when we do this with 40% concentration of these salts, some of the NCL salt is precipitated and its molecules are not released so that they can overlap with the ice molecules.

Due to the overlap of (water, hydrogen) molecules with ions and electrons of salt, ice melts by produced heat. Actually, the time and speed of ice melting belongs to the following factors:

- o Ambient temperature
- o Level of the ambient light
- o The amount of solvent (cc)
- o Salt concentration
- o ice material

- o type of salt
- o shape and size of ices
- o the place and wheatear
- o the type of water

We concluded that although the size of ice gets smaller, the amount and speed of melting the ice increases. According to the colligative properties, when the number of Solvent molecules gets more, it can react with non-metal such as ice.

Type of salts can affect this phenomenon and with NaCl (sodium chloride) we could melt more ice and also it is the most available salt in the world that we use in our daily lives. So according to the following order salts can be used on ice melting as: **NaCl>KCl>MgCl₂>CaCl₂**

Acknowledgment

Thanks to Mr. Arabani as my supervisor and leader to solve this problem and Dr Izadi in AYMI institute.

References

- [1] Sails, Andrea, and Barry W. Ninham. "Models and mechanisms of Hofmeister effects in electrolyte solutions, and colloid and protein systems revisited." *Chemical Society Reviews* 43.21 (2014): 7358-7377.
- [2]. Hua, Wei, et al. "Cation effects on interfacial water organization of aqueous chloride solutions. I. Monovalent cations: Li⁺, Na⁺, K⁺, and NH₄⁺." *The Journal of Physical Chemistry B* 118.28 (2014): 8433-8440.
- [3] Yatsenko, O. B., and I. G. Chudotvortsev. "Ice melting and crystallization in binary water-salt systems." *Inorganic materials* 38.9 (2002): 907-913.
- [4] Almeida, Nalinda, Leela Rakesh, and Jin Zhao. "Monovalent and divalent salt effects on thermogelation of aqueous hypromellose solutions." *Food Hydrocolloids* 36 (2014): 323-331.
- [5] Thorat, Alpana A., et al. "Effects of Chloride and Sulfate Salts on the Inhibition or Promotion of Sucrose Crystallization in Initially Amorphous Sucrose-Salt Blends." *Journal of agricultural and food chemistry* 65.51 (2017): 11259-11272.

Slope Warning System

Zeren Kaynak, Karşıyaka Efe Afyonlu, Ozel Eraslan Anadolu Lisesi, Izmir/Turkey,

zerenkaynak@gmail.com, muhammet.coruh@eraslan.k12.tr

ABSTRACT

ARTICLE INFO

Gold Medalist in IMSEF 2021 Izmir, Turkey, and in ISAC Olympiad 2021, Tehran, Iran

Advisor: Muhammet Coruh

Accepted by Ariaian Young Innovative Minds Institute, AYIMI

<http://www.ayimi.org>, info@ayimi.org

Accidents experienced by motorcycle drivers on curvy roads are among the most frequently encountered news. The vast majority of these accidents occur when the rider loses control of the motorcycle while cornering as a result of excessive leaning while cornering. Based on these findings, it is aimed to develop a warning system that can prevent motorcycle accidents in corners and inform the user about the slope of the vehicle. "Arduino" card and MPU6050 acceleration sensor were used in the warning system produced in the study. By developing the system, it is also aimed to produce a product that will notify the driver of whether the tipper is open or closed in dump trucks.

Key words: *Motorcycle accidents, Arduino, warning system*

1 Introduction

Accidents experienced by motorcycle drivers on curvy roads are among the most frequently encountered news. The vast majority of these accidents occur when the rider loses control of the motorcycle while cornering as a result of excessive leaning while cornering. Based on these findings, it is aimed to develop a warning system that can prevent motorcycle accidents in corners and inform the user about the slope of the vehicle.

"Arduino" card and MPU6050 acceleration sensor were used in the warning system produced in the study. The MPU6050 acceleration sensor can measure the angle and thus gives the motorcycle user information about the angle of the engine with the ground momentarily. In case the engine leans 8, 16, 24, 32 or 40°, it warns the driver with changing lamp colors such as blue, yellow and red and increasing sound. In this way, the driver will be aware of the degree of incline while cornering, thanks to the colored signals and audible warning, and will be able to prevent a possible accident by taking immediate action according to the danger situation.

By developing the system, it is also aimed to produce a product that will notify the driver of whether the tipper is open or closed in dump trucks. In addition, it is aimed to find a solution to the overturning problem as a result of the work machines that we hear frequently when they reach a certain slope while working.

2 Entrance to the Problem

Many traffic accidents occur every day in Turkey. According to the Turkish highway accident statistics published by TURKSTAT for the years 2009-2018, thousands of people lose their lives due to traffic accidents every year. The leading causes of these accidents are fast entering the bends, skidding on the bends, and tilting on the bends (www.kgm.gov.tr/).

The accidents caused by the engines in the corners are frequently mentioned in the newspapers and news. When the statistics of the motor accidents that occur, it is obvious that the motor accidents that occur in the corners should not be underestimated. According to 2018 data, approximately 16% of the accidents in our country occur on bends (Table 1). Curves are one of the most important issues and problems for highways. In terms of road safety, the

geometric standards of the bends should be adjusted very well. It is very important to raise the awareness of the drivers in the bends that may create an accident hazard for the drivers to reduce the accident rates. Entering the bend at a high speed will cause the vehicles to skid on the bends (<http://ogmmateryal.eba.gov.tr/>). Drivers need to be aware of the incline of their engines and trucks while cornering and whether the grade of the incline is dangerous for them.

Table 1: Statistics of the motor accidents (2018)

horizontal path	residential area		out of town		Total	
	number of accidents	%	number of accidents	%	number of accidents	%
straight road	125674	89.82	30808	66.1	156482	83.89
bend	12096	8.64	10020	21.5	22116	11.86
dangerous bend	2152	1.54	5782	12.4	7934	4.25
Total	139922	100	46610	100	186532	100

Figure (1) also shows the rate of the issues which cause motorcycle problems. It is seen that 38.2% of the motorcycle accidents are the result of over-shooting bends and not knowing the danger of the slope.

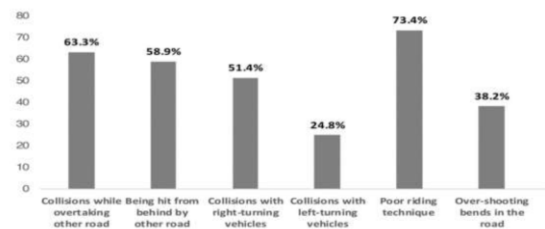


Fig.1: Motorcycle problems

When the measures taken to prevent these accidents were investigated, it was seen that some of the bends were inclined to support the rider in case of losing control, but this configuration was not a solution to prevent motorcycle accidents. We decided that ignoring this problem will allow the increase in accident and death rates. So that an effective, applicable, innovative, and cost-effective solution should be produced as soon as possible.

In addition, especially in recent years, many accidents have occurred because truck dumpers are often left open and these accidents have caused loss of life and property. There is no solution to prevent these accidents due to the

absent-mindedness of the driver. Similarly, no system can warn the construction equipment operators in case of danger of tipping due to excessive bending while working. To prevent the user from losing control and causing an accident while the motorcycle is turning as it is leaning on the bend, a system has been developed to determine the inclination of the motorcycle and warns the rider with visual and auditory signals. While developing this system, the principles of rotational physics (Fig. 2) were taken into account (Giancoli, 2009).

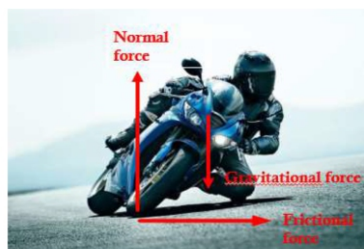


Fig. 2: The force on the motorcycle in a rotational road

The produced light and audible warning system warns the rider of the slopes of the motorcycle to the right or left during the journey, and riders will be informed about the degree of inclination of their motorcycle and whether that slope is dangerous or not, with colored signals and an auditory warning system, thus taking immediate action in a dangerous situation, the rider can prevent an accident.

3 Material and Method

Firstly, motorcycle users were interviewed to determine the root cause of the accidents on curvy roads.

Motorcycle users mentioned that they tilted the engine while turning the corners and that the engine skidded because they did not know the slope.

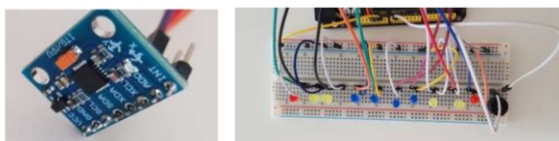


Fig. 3: MPU6050 acceleration sensor and circuit

Based on this, the hypothesis that "the driver knows the slope of the engine while driving around the bend and the driver is warned in case the slope reaches dangerous points prevents possible accidents" was established. While developing a prototype, the MPU6050 acceleration sensor included in the "Arduino" coding kit was used (Fig. 3) In addition, 10 mushroom LEDs and 1 buzzer were used for the warning system. The codes, inspired by open-source codes and optimized for prototype circuits.

4 Results and Discussion

The created circuit informs the right or left inclination of the motor. The first blue lamp lights up when the motor tilts 8° to the right from the vertical axis. When tilted at 16° , two blue lamps are on.

When the engine is tilted at 24° , two blue and one yellow lamp are on. At the same time, the buzzer starts to beep intermittently. When the engine leans 32° to the right, two blue and two yellow lamps are on and the buzzer beeps intermittently. When the engine leans 40° to the right, two blue, two yellow, and one red lamp are on. In addition, the buzzer beeps continuously when the red lamp is on.

As explained above, the light and sound warning system

work effectively on slopes to the right, as well as on slopes to the left. Thus, a system was produced that informs the motor driver how many degrees the motor is tilted to the right or to the left (Fig. 4).



Fig. 4: The produced warning system and integrated system on a prototype

By establishing a similar system, the tipper clearance warning system for dump trucks and the rollover warning system of the construction equipment will be developed. In addition to the materials used in the system we have developed for the tipper and construction equipment, a screen will be added so that the user can see the angle of the tipper and construction equipment with the horizontal.

There is no other product produced to prevent or reduce the accidents caused by motorcycles on bends.

No system indicates whether the truck dumpers are open or not and informs the inclination of the construction equipment. A viable, innovative, and cost-effective solution has been developed that will prevent many fatal accidents and property damage. A system to be developed similarly will be integrated into trucks, and a possible accident will be prevented by measuring whether the tipper is open or not and warning the rider by measuring the angle of the tipper. With the same system, the tipping problem will be solved by informing the user of the slope of the work machine while it is operating.

References

- [1] Giancoli, D. C., 2009, Fen Bilimcileri ve Mühendisler İçin Fizik. Çev.: Gülsen Öngüt. Ankara: Akademi Publishing
 - [2] www.kgm.gov.tr/SiteCollectionDocuments/KGMdocuments/Trafik/TrafikKazalariOzeti2018.pdf Last time accessed : 05.06.2021
 - [3] <http://ogmmateryal.eba.gov.tr/panel/upload/etkilesimli/kitap/fenlisesifizik/12/unite1/files/ba-sic-html/page77.html> Last time accessed: 05.06.2021
- <http://ogmmateryal.eba.gov.tr/panel/upload/etkilesimli/kitap/fenlisesifizik/12/unite1/files/ba-sic-html/page77.html>
Last time accessed: 05.06.2021

The Effect of Biofilters on Water Quality Parameters and Efficiency in Aquaponic System

Sena Ocak, Giresun Science High School, Turkey/Giresun, senaocak5328@gmail.com

ABSTRACT

ARTICLE INFO

Gold Medalist in IMSEF 2021 Izmir, Turkey, and Bronze medalist in ISAC Olympiad 2021, Tehran, Iran
Accepted by Ariaian Young Innovative Minds Institute, AYIMI

<http://www.ayimi.org>, info@ayimi.org

Aquaponic systems are ecological systems suitable for sustainable agriculture. With the reuse of water in the system, the fertilizer needs of plants are met with natural fish waste and water consumption is minimized. In our project, a control and experiment group consisting of 2 pilot aquaponic systems consisting of a fish tank and a hydroponic vegetable tank working in parallel has been established. In addition, Biofilters is designed for the Experimental group. Koi fish was used in the fish tank and Kale was used in the vegetable tank. Blue LEDs were used due to insufficient sunlight.

Key words: *Aquaponics, Biofilter, Water quality, Koi, Black cabbage*

1 Introduction

In today's world, a lot of inorganic fertilizer is given to the environment to get more products from the unit area to meet the nutritional needs. However, the introduction of chemical fertilizers has caused environmental pollution and serious health problems. Organic fertilizers used as a solution provide significant efficiency increase in yield and quality (Badr ve Fekry, 1998; Arisha ve ark., 2003).

Aquaponic systems are an ecological system conducive to sustainable agriculture. By reusing water in the system, natural fish waste meets the fertilizer needs of plants and water consumption is minimized. 2 Pilot aquaponic systems were operated simultaneously and in parallel with each other, including control and experimental group. During the process of our project, 3 different contents filter were prepared. Our aim is to investigate the effect of 3 filters with different contents on water quality and efficiency in the aquaponic system.

Water quality is the sum of all physical, chemical, biological and aesthetic properties that affect the beneficial use of water. (Tepe ve Boyd, 2002). It is important to identify various factors that change the quality of water in terms of aquaculture. Fish are stressed when exposed to situations other than these values. Water quality parameters followed during the project process temperature, pH, dissolved oxygen, total hardness and alkalinity, salinity, conductivity, oxidation ORP, TDS, TAN.

Akdogan (2014) reported that fish farm water increases yields in the aquaculture system. Güzel et al. (2014), in a research project on the cultivation of carp and lettuce in the aquaponic system; they stated that fish and lettuce can be grown together, water is cleaned and reuse and provides better performance according to the system. Tyson (2007) stated that the appropriate pH range is 7.5-8.0 in his study on determining the appropriate pH range in biological filtration of ammonia in aquaponic environment. Trang and Brix, (2012) examined the function of the biofilter placed in the integrated aquaponic system within the system. Lorena et al. (2008) in her study for the production of sturgeon and lettuce in an aquaponic system reported that throughout the entire study, water parameters remained within optimal limits to ensure optimal growth.

2 Methods

The trial assembly of our project was created in August 2021 in Giresun Science High School Biology laboratory and ended on January 15, 2021. Made with 3 repeaters.



Fig. 1: Pilot-1 and Pilot-2 aquaponic systems

In the aquaponic system; In the pilot-2 group designated as the experimental group, the effect of 3 biofilters on water quality parameters and efficiency was investigated in different characteristics in which wastewater from the fish tank was filtered. In our project, an aquaponic system was created for the fish tank using koi fish (*Cyprinus rubrofasciatus*) and vegetable bed Cabbage (*Brassica oleracea*) plant. In the trial groups, a total of 30 pieces weighing an average of 5-6 g were placed in each fish tank (2 in total, 1 control, 1 experimental group) (Fig.2).



Fig. 2: Koi fish and Cabbage

In our project, Filled Environment, Tank System was preferred from aquaponic designs. The equipment used in this system is small and the resulting product is lower (Fig.3).

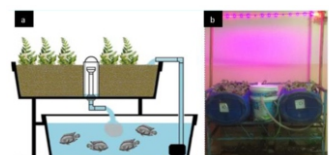


Fig. 3: Filled Media Tank System

2-1 Fish Tanks and Vegetable Tanks

Pilot-1 control group (Fish tank and vegetable tank) aquaponic system was accepted, while pilot-2 system was determined as Experimental group (Fish tank, vegetable tank and Biofilters) (Fig. 4) (Table 1).

Table 1: Group symbols and contents

Trial Group symbols	Trial group contents
KS-1	Control Vegetable Tank
KB-1	Control Fish Tank
DB-2	Experimental Fish Tank
DS-2	Experimental Vegetable Tank
F-2	Experimental Biofilter

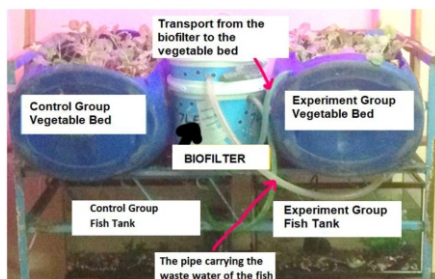


Fig. 4. Our aquaponic system

In the design of the aquaponic system, the rack system is used in the profile iron structure (Fig. 5)



Fig.5 : Metal Rack system

In our aquaponic system, vegetable bed 1 and 2 were obtained by using 50 liter volume PE canisters (60x35x25)cm³ for vegetable growing environment (Fig. 6).



Fig. 6.: Vegetable Tank design

For fish tanks, 2 50x20x30 cm³ and 30L volume aquariums were used (Fig.7).

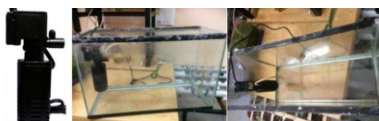


Fig.7: Internal Filter and Fish tank

Waste water is sent to the biofilter with the aquarium internal filter motor in fish tanks (Fig. 8).



Fig.8: Hydrotone

Styrofoam was used for the placement of violas (Fig.9).



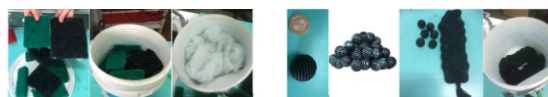
Fig.9: Styrofoam

2-2 Biofilter Design

In addition to Figure(10) and Table (2), Sponge, Fiber, Activated Carbon, internal filter motor was used when preparing biofilters.

Table 2: Types and Contents of Biofilters

Symbol	Biological External Filter
Biofilter-1	Plastic Bioball
Biofilter-2	Plastic Bioball and Zeolite
Biofilter-3	Ceramic Ring and Zeolite



a-Biological Filter Sponge and Fiber

b- Plastic Bioball



c- Ceramic Ring



d- Activated Carbon and Zeolite



e- internal filter and biofilters

Fig.10: External filter materials (a,b,c,d,e)

2-3 Operation of the Aquaponic System

In our project, two simultaneous and parallel pilot aquaponic systems were operated. In the Pilot-1 aquaponic system, the wastewater control group is pumped into the vegetable tank with the help of an internal filter motor from the control group fish tank. In the Pilot-2 aquaponic system, the experimental group fish tank waste water is sent to the biofilter system designed with the help of the internal filter engine and the filtered water is transferred to the experimental group vegetable tank with the help of the biofilter motor and after being used by Cabbage, it is transmitted back to the fish tank with the pipe system and the turnover is ensured.

2-4 Oxygen Requirement

Oxygen in air motor and air stone are saturated in the fish tank and vegetable bed (Fig.11).

2-5 Light Source and Feeding of Fish

A blue strip LED was used as the light source. Daily feed was given as 3% of the weight of the fish (Fig. 12).



Fig.11: Air motor and Air Stone



Fig.12: Strip Led and Fish Food

2-6 Arduino System

With the Arduino system, pH, temperature and water level were measured daily. If the data from the sensors is appropriate, the green LED will light up and alert if not.

2.1.2. Dissolved Oxygen, Saturation, ORP, TDS, E.C. and Salinity measurement. Orp, TDS, E.C. and Salinity were measured with The Hach brand measuring device with Dissolved Oxygen, Saturation and YSI pro1030 multiparameter device (Fig.13).

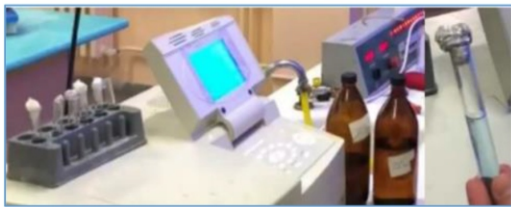


Fig.13:TU-1810 UV-VIS Spectrophotometer

2-7 TAN Analysis

TAN 1 and TAN 2 solutions were used to determine total ammonia nitrogen. 635 nm wavelength reading was made. TU-1810 UV-VIS model Spectrophotometer was used.

2-8 Height Tracking in a Vegetable Tank

A total of 40 cabbages were grown and height measurements were made for 20 control and 20 experimental groups in vegetable tanks.

2-9 One-Way Variance Analysis (ANOVA)

It was made with ANOVA in SPSS 22 program in comparison of plant sizes.

3 Results

3-1 Temperature, Dissolved O2 and Saturation

The findings of pilot-1 and pilot-2 system are given below.

According to the results of 93 measurements, Biofilters caused an increase in Dissolved O2 and an increase in Biofilter-1 and Biofilter-2 Dissolved O2 in Fish tanks (Table 3). The water temperature was found to be between 16.18 and 16.28. It is seen that there is an inverse ratio between temperature and Dissolved O2. Saturation Pilot-2 gave the highest result of Filter-2 in both vegetable tank and fish tank. Accordingly, according to the water pollution control regulation, the quality of the water is 1st class (Fig. 14-17).

Table 3: Dissolved O2 and Saturation

Biofilter-1 Process				
Name	Akuaponic component	Temperature	CO	% Saturation
Pilot-1	Control Group Vegetable Tank	16,70	9,28	97,88
Pilot-1	Control Group Fish Tank	16,65	9,10	95,63
Pilot-2	Biofilter-1 Mounted Experimental Group Fish Tank	16,85	9,50	100,05
Pilot-2	Biofilter-1 Mounted Experimental Group Vegetable Bed	16,90	9,61	100,75

Biofilter-2 Process				
Name	Akuaponic component	Temperature	CO	% Saturation
Pilot-1	Control Group Fish Tank	15,89	10,24	103,35
Pilot-2	Biofilter-2 Mounted Experimental Group Fish Tank	15,94	10,29	104,47
Pilot-2	Biofilter-2 Mounted Experimental Group Vegetable Bed	16,08	10,37	105,39

Biofilter-3 Process				
Name	Akuaponic component	Temperature	CO	Saturation
Pilot-1	Control Group Vegetable Tank	16,38	10,13	101,20
Pilot-1	Control Group Fish Tank	16,35	10,10	100,75
Pilot-2	Biofilter-3 Mounted Experimental Group Fish Tank	16,28	10,10	104,10
Pilot-2	Biofilter-3 Mounted Experimental Group Vegetable Bed	16,03	10,25	104,20

Measurement of water samples from Biofilter Output				
Name	Akuaponic component	Temperature	CO	% Saturation
Pilot-2	Biyofilter 1	16,65	9,87	102,40
Pilot-2	Biyofilter 2	15,91	10,43	105,58
Pilot-2	Biyofilter 3	15,95	10,25	104,15

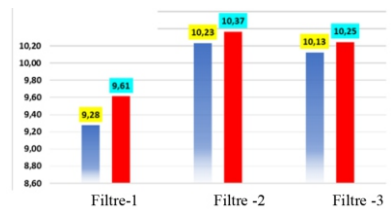


Fig. 14: A Control Group Vegetable Tank Trial Group Vegetable Tank

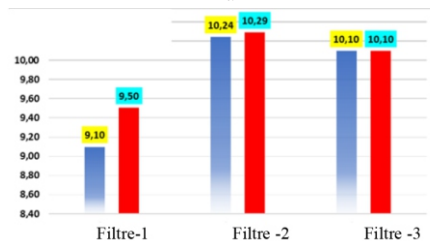


Fig. 15: B Control Group Fish Tank Trial Group Fish Tank

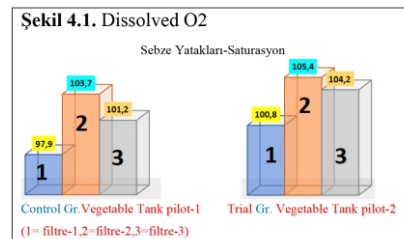


Fig. 16: Dissolved O2

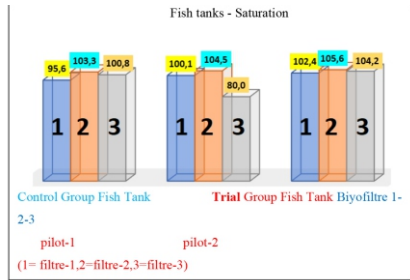


Fig. 17: Saturation

3-2 Alkalinite, Hardness and pH

Filter-3, Pilot-2 While increasing alkalinite in the vegetable tank and fish tank; Filter-2 increased hardness in the Vegetable tank and Fish tank (Table 4, Fig.18). The Alkalinity and Hardness values of the biofilter output water samples are smaller than the values of the Experimental group Vegetable tanks from which this water is poured. Filter-3 has been shown to cause the pH values of the Vegetable tank and Fish tank to decrease. During Filter-2, the pilot-2 pH value was found to average 7.84 and pilot-1 pH averaged 7.79, but during Filter-3, the pilot-2 pH value was 7.65 and pilot-1 pH averaged 7.60 (Figure 4.3). In the light of these results, it shows that the quality of the water is 1st class according to the water pollution control regulation.

Table 4: Alkalinity and Hardness

	Filter 2- Alkalinite	Filter 3- Alkalinite	Filter 2- Hardness	Filter 3- Hardness
Control Gr. Vegetable tank pilot-1	208	192	287	338
Trial Gr. vegetable tank pilot-2	208	198	309	312
control Gr. Fish tank pilot-1	207	209	294	342
Trial Group Fish Tank pilot-2	199	218	308	335
Biyofiltre pilot-2	199	177	305	302

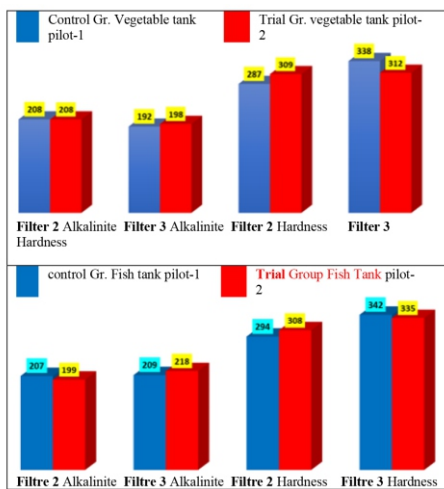


Fig. 18: Alkalinite and hardness results

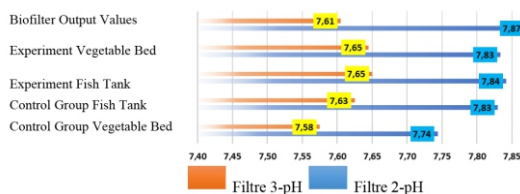


Fig. 19: pH results

3-3 TAN

Biofilter-2, control group vegetable tank TAN value was found to be 30.6% lower than Control Group Fish Tank and reduced vegetable tank TAN value. Biofilter-2 reduced the experimental group Fish Tank TAN from 0.121 mgL-1 to 0.115 mgL-1, but the Vegetable tank TAN increased to 0.153 mgL-1. In the biofilter-3 process, the Control Group Vegetable tank TAN value is 91.2% lower than the Control Group Fish Tank and the vegetable tank decreases the TAN value. Biofilter-2 Experimental group Fish Tank increased the value from 0.188 mgL-1 to 0.193 mgL-1 and the Vegetable tank reduced the TAN value by 38.03% to 0.140 mgL-1 (Table 5 and Fig. 20).

Table 5: Alkalinite and Hardness results

TAN ORTALAMALARI			
		BIYOFILTRE-2	BIYOFILTRE-3
Pilot-1	Kontrol Grubu Balik Tankı	0,136	0,224
Pilot-1	Kontrol Grubu Sebze Yatağı	0,104	0,117
Pilot-2	Biyofiltre takılan Dency Grubu Balik Tankı	0,121	0,188
Pilot-2	Biyofiltre Çıkış Değerleri	0,115	0,193
Pilot-2	Biyofiltre takılan Dency Grubu Sebze Yatağı	0,153	0,140

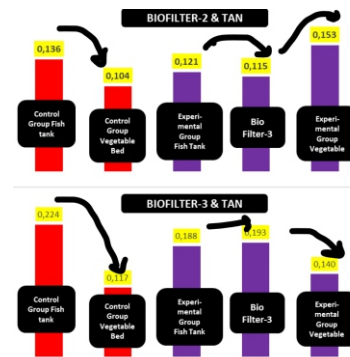


Fig. 20: Filter 2 and Filter 3

3-4 TAN result Electrical conductivity (E.C.), TDS, ORP and Salinity (Table 5).

Table 5: E.C. Results

GROUP	Filter 1	Filter 2	Filter 3
Control Group Vegetable Bed	473,0	522,6	563,0
Control Group Fish Tank	406,0	519,6	564,5
Experiment Fish Tank + Biofilter	489,3	549,0	583,5
Experiment Vegetable Bed +Biofilter	490,5	550,1	583,8
Biofilter Output Values	500,0	551,8	585,8

Table 4.6. TDS Results

GROUP	Filter 1	Filter 2	Filter 3
Control Group Vegetable Bed	365,0	407,5	449,5
Control Group Fish Tank	315,3	399,5	450,8
Experiment Fish Tank + Biofilter	377,5	422,4	463,6
Experiment Vegetable Bed +Biofilter	378,0	426,0	463,3
Biofilter Output Values	387,5	431,4	464,5

Table 4.7. ORP Results

GROUP	Filter 1	Filter 2	Filter 3
Control Group Vegetable Bed	118,5	166,0	185,5
Control Group Fish Tank	116,0	159,1	192,3
Experiment Fish Tank + Biofilter	115,3	154,9	192,5
Experiment Vegetable Bed +Biofilter	114,5	152,6	192,8
Biofilter Output Values	117,5	149,3	188,8

Table 4.8. SAL Results

GROUP	Filter 1	Filter 2	Filter 3
Control Group Vegetable Bed	0,3	0,3	0,3
Control Group Fish Tank	0,3	0,3	0,3
Experiment Fish Tank + Biofilter	0,3	0,3	0,3
Experiment Vegetable Bed +Biofilter	0,3	0,3	0,3
Biofilter Output Values	0,3	0,3	0,3

E.C., TDS, ORP values are highest in biofilter-3 and lowest result is seen in Biofilter-1. Salinity values were not changed in all ambient conditions and were 0.3. In light of these results, the quality of water according to the water pollution control regulation is 1st class (Table 5).

3-5 Cabbage Size Measurements

Control and experimental groups : There were 5 seedling losses in 7 experimental groups in the Control group of 20 cabbage seedlings preferred in the Vegetable tank. head of Project and end-of-project size measurements for each of the 28 seedlings are seen in Table (6).

Table 6: Cabbage Size Measurement results

	Control Group Vegetable Bed		Experiment Vegetable Bed	
	First measurement (cm)	Last measurement (cm)	First measurement (cm)	Last measurement (cm)
1.	13	13,5	15	24,5
2.	15	15,5	15	15,5
3.	14,5	14,5	17,5	19
4.	12	12,5	13	14
5.	17	20	13,5	14,5
6.	15	15,5	13	14
7.	16,5	18,5	17	20,1
8.	11	11	13	16
9.	16	17	12,5	16
10.	13,5	15	13	14
11.	12	14	14,5	14,5
12.	13	13	14	16
13.	14,5	16	14,5	16
14.			13,5	14
15.			14	15
Average	14,07	15,07	14,20	16,2

4 Discussions

In our project, in the Aquaponic system containing Koi fish and cabbage plant; In the pilot-2 group, the effect of 3 biofilters on water quality parameters and efficiency was investigated in different characteristics in which wastewater from the fish tank was filtered. Pilot-1 aquaponic system While the control group (fish tank and vegetable tank), Pilot-2 aquaponic system Experimental group (fish tank, vegetable tank and Biofilter) was accepted. When the temperature results were evaluated, the ideal water temperature values for Koi fish in aquaponic systems were 15-20 degrees and a total of 93 measurements were made during our project and the water temperature was determined to be between 16.18 and 16.28. Unsuitable water temperature conditions regrow the growth of fish, larvae can not get feed or feed. Dissolved oxygen is one of the important parameters for aquaponic systems. In the measurements, it was seen that ventilation was sufficient. Pilot-2 All Biofilters in vegetable tanks led to an increase in Dissolved O₂ and an increase in Biofilter-1 and Biofilter-2 Dissolved O₂ in Fish tanks. According to the saturation results, Pilot-2 gave the highest result of Filter-2 in both vegetable tanks and fish tanks. In the light of these results, it shows that the quality of the water is 1st class according to the water pollution control regulation.

The appropriate pH range for plants and fish in aquaponic systems is 7-8. In the Pilot-2 Aquaponic system, Filter-3 increases alkalinity, while Filter-2 increases hardness. When looking at the pH results, it is seen that Filter-3 causes the pH to decrease. During Filter-2 for Pilot-1 and Pilot-2, the pH value was 7.84 and 7.79, respectively, but Filter-3 was 7.65 and 7.60. According to the measurements made, the pH range in the system is

suitable. When we look at the studies in the literature, the pH value of an aquatic environment should not endanger living life and should not exceed the limit value of 6.5-8.5 in order for this water source to be used for fish farming purposes (Kara and Potteryoglu, 2004). Passing water through activated carbon filters reduces pH and hardness. The total alkalinity desired in the aquaculture environment is between 20-300 mg/L as CaCO₃. Low alkaline waters with a total alkalinity of less than 20 mg/L and high alkaline waters of more than 300 mg/L are not conductive. Alkalinity; plays a role in increasing the effect of toxic substances in terms of aquaculture (Göksu, 2003). From this point of view, alkalinity and hardness values were appropriate for fish life (Boyd, 1990). literature.

Total ammonia nitrogen (TAN) is the sum of ionized ammonium with non-ionized ammonia found in water. When tan results were evaluated, in the biofilter-2 process, on average, the Control Group reduced the value of vegetable bed TAN from 0.136 to 0.104, despite falling from 0.121 to 0.153. However, during biofilter-3, it decreased from 0.188 to 0.140. In light of these results, it shows that the nitrification process was more successful in the Biofilter-3 (Ceramic Ring and Zeolite) process. In addition, the lack of oxygen in the Biofilter-3 process compared to Biofilter-3 indicates that dissolved oxygen is used by microorganisms in the nitrification process. Pilot-1 The decrease of the average of the fish tank TAN by 30.5% in the Biofilter-2 process and by 91.2% in the Biofilter-3 process indicates that there is a cost-free removal by Cabbage in the aquaponic system. Pilot-2 Fish tank TAN average decreases by 33.92% in biofilter-3 process indicates a cost-free removal by Cabbage in aquaponic system.

Electrical conductivity is an important parameter in studies related to water quality. In the Pilot-1 aquaponic system, the average electrical conductivity values were 519.5 mS/cm in the Vegetable Bed and 496.7 in the fish tank. In the Pilot-2 aquaponic system, the values of Biofiltre1, Biofiltre2, Biofiltre3 were 489 mS/cm, 549 mS/cm, 584 mS/cm and 490.5 mS/cm, 550.1 mS/cm, 583.8 mS/cm, respectively, in the Fish Tank. Biofilter3 containing Ceramic Ring and Zeolite gave the best result with an average of 583.8 mS/cm. It is reported that there are no fish shelter in waters with an electrical conductivity value exceeding 1000 μ S/cm at 25°C, and the conductivity of the water to be grown should be in the range of approximately 12.50-1800 μ S/cm (Göksu2003).

In the pilot-1 aquaponic system, the mean TDS values were 407.3 mg/L in the Vegetable Bed and 388.5 mg/L in the fish tank. TDS values of Pilot-2 aquaponic system Biofiltre1, Biofiltre2, Biofiltre3 were 377.5 mg/L, 422.4mg/L, 463.6 mg/L and 378 mg/L, 426 mg/L, 463.3 mg/L for vegetable bed, respectively for Fish Tank. Biofilter3 containing Ceramic Ring and Zeolite gave the best result with an average of 463 mS/cm. The highest results of E.C., TDS, ORP values are seen in Biofilter-3 and lowest results are in Biofilter-1 Salinity values were not changed in all ambient conditions and were 0.3. It has an inverse relationship between salinity concentration of water and oxygen solubility, and as salinity increases, the amount of dissolved oxygen decreases (Tepe and Mutlu, 2004). In the light of these results, it shows that the quality of the water is 1st class according to the water pollution control regulation.

According to the results of cabbage size measurement of 28 seedlings in vegetable tanks, pilot-1 vegetable tanks (control group) averaged 14.07 cm in initial height and

harvest size average was 15.07 cm; Pilot-2 Vegetable tanks (Experimental group) was found to have an average initial height of 14.2 cm and a harvest size average of 16.2 cm. In the aquaponic system where biofilter is applied, cabbage lengthening is thought to be greater, but in the absence of sufficient elongation, ambient temperature and lack of sunlight due to winter season negatively affect. As a result of the one-way variance analysis, no significant difference was found between stations statistically ($p < 0.05$).

Our project tyson (2007) stated that the appropriate pH range in biological filtration of ammonia in an aquaponic environment is 7.5-8.0, Trang and Brix, (2012) examined the function of the biofilter placed in the integrated aqua aquaponic system, Lorena et al. (2008) reported that water parameters remained within optimal limits to ensure optimal growth throughout the aquaponic system study, and Graber and Junge (2009) reported that aquaculture waste it supports its work, which shows that it can be used in ebze cultivation, and the study of Güzel et al. (2014), which the aquaponic system states allows water to be cleaned and reused.

References

- [1] Akdogan, B., 2014. Effects of Fish Farm and Treatment Plant Wastewater on The Yield and Quality Characteristics of Curly Leaf Salad in Systems (Master's Thesis, Unpublished). Gaziosmanpasa University, Institute of Science, Tokat.
- [2] Arisha, H.M.E., A.A. Gad and S.E. Younes, 2003. Response to some pepper cultivars to organic and mineral nitrogen fertilizer under sandy soil conditions. *Zagazig J. Agric. Res.*
- [3] Badr, L.A.A. and W.A. Fekry, 1998. Effect of intercropping and doses of fertilization on growth and productivity of taro and cucumber plants. Vegetative growth and chemical constituents of foliage. *Zagazig J. Agric. Res.*, 25: 1087-101.
- [4] Boyd, C. E. (1990). Water quality in ponds for aquaculture.
- [5] Graber A., and Junge R., 2009. Aquaponic Systems: Nutrient recycling from fish wastewater by vegetable production. *Desalination* 246: 147–156.
- [6] Güzel, Ş., Sen, F., Kankaya, E., Paruğ, Ş., Ş., Gültekin, A., 2014. A Study on The Cultivation of Carp (*Cyprinus carpio*) Fish and Lettuce (*Lactuca sativa*) in Aquaponic Systems, Centennial University Scientific research project final report, Van.
- [7] Lorena, S., Cristea, V. and Oprea, L. 2008. Nutrients dynamic in an aquaponic recirculating system for sturgeon and lettuce (*Lactuca sale*) production. *Zootehnie si Biotehnologii*, 41(2): 137-143]
- [8] Hill, Y. and Boyd, C.E. 2002. Sediment Quality in Arkansas Bait Fish Minnows Ponds. *Journal of World Aquaculture Society*. Vol.33, No.3.
- [9] Trang, N.T.D. and Brix, H., 2012, Use of planted biofilters in integrated recirculating aquaculture-hydroponics systems in the Mekong Delta, Vietnam, *Aquaculture Research*, 2012, 1–10. doi:10.1111/j.1365-2109.2012.03247.x.
- [10] Tyson, R.V., Simonne E.H., White, J.M., & lamb, E.M. (2004). Reconciling water quality parameters impacting nitrification in aquaponics: the pH levels. *Proc.Fla.State Hort. Soc.*

Nephron Model For Course Teaching Material Purpose

Müşerref Şeyma Şahin, Giresun Science High, School Turkey/Giresun, mseymasah@gmail.com

ABSTRACT

ARTICLE INFO

Gold Medalist in IMSEF 2021 Izmir, Turkey, and Encouragement Medalist in ISAC Olympiad 2021, Tehran, Iran

Accepted by Ariaian Young Innovative Minds Institute, AYIMI

http://www.ayimi.org_info@ayimi.org

A successful science education aims to provide individuals with the knowledge and skills they will need in their daily lives. In biology teaching, both educational situations and abstract and complex biology concepts lead to students having difficulty understanding some topics and learning by memorizing them without understanding them. The aim of our project is to prepare visual material that will facilitate the understanding of the structure and function of Nephron by students in Biology courses from the subjects belonging to the excretory system.

Key words: *Nephron, Kidney, Material, STEAM, Biology*

1 Introduction

The main purpose of today's education is; It should be to raise people who can ask questions, say no, take critical decisions, use initiative, have sufficient communication skills, cope with new environments and establish new relationships. Today's individuals are not "knowledge memorized" individuals who grew up in the traditional school; must be "learning individuals" (Okutan, 2004).

Today, science education focuses on improving the science literacy of individuals. A successful science education aims to provide individuals with the knowledge and skills they will need in their daily lives (Anderson, 2010). Since science literate individuals have the skills to access and use the information they need to solve the problems they encounter, they have more advanced problem-solving skills (Kaptan, 1998).

Biology is very difficult to teach and learn because it includes complex relationships between foreign and abstract concepts. In biology teaching, both educational situations and the abstract and complex nature of biology concepts cause students to have difficulty in understanding some subjects and to learn by memorizing without understanding (Kılıç ve Sağlam, 2004). In order to solve this problem, the use of educational technologies in biology lessons is extremely important. Well-prepared pictures, three-dimensional models, animated animations, interactive environments, etc. It makes it easier to understand the targeted information (Çömlekçioğlu ve Bayraktaroğlu, 2001).

In order to convey learning and teaching in a real sense, technology has a great importance as well as the use of tools and equipment in biology education. Tools in the learning-teaching process are generally used to support teaching, well-prepared tools enrich the teaching process. It is known that meaningful learning occurs when the concepts are modeled or visualized as much as possible, and even when videos explaining the related concept are used in the science lesson (Coştu, Beler, Coştu, 2017).

Recent studies in the cognitive field show that students learn better when their minds are actively engaged in research, moving from (traditional) teaching and learning to exploratory learning (Harris et al, 2001).

The lack of importance given to laboratory activities in schools and the difficulties in preparing materials related to

11th grade human physiology make it difficult to teach concepts. Therefore, it is important to prepare and use the material of the nephron model, which is the basic part in understanding the excretory system.

The aim of our project; To prepare visual materials that will facilitate students' understanding of the structure and function of the Nephron, which is one of the subjects of the excretory system, in the 11th grade Biology course of secondary education.

1-1 Constructivist Approach in Education

The reorganization of the curricula according to the constructivist approach in the Turkish Education System can be described as the biggest change. Curriculums are based on student-centered and active participation teaching activities rather than teacher-centered teaching (Arslan ve Özpınar, 2009; Peker ve Halat, 2008). However, in studies on new curriculums in Turkey, teachers' opinions are frequently encountered regarding "significant disruptions in the implementation of the curriculum due to the lack of structures, tools, materials and materials" (Akça, 2007, Peker ve Halat, 2008, Şahin, 2010).

Constructivism is based on the understanding that learning is a process that takes place in the mind of the individual. For this reason, information cannot be stored by transferring it to the human mind, and the human mind is not an empty place where all information is stored (Yaşar, 1998, s.69). Therefore, constructivism is the meaning that an individual produces in his mind as a result of perceiving, processing, evaluating and reasoning about the events in the outside world (Ersoy, 2003). Constructivism is concerned with solving problems that best fit real-life situations. This theory requires students to make choices about what and how to learn. Students learn by working collaboratively in groups and achieve success by trying solutions to problems and developing a presentation, not just as the teacher conveys (Kaptan ve Korkmaz, 2000).

The main feature of constructivist theory lies in defining the role of students. In this process, the student actively constructs his/her ideas and perceptions, instead of passively receiving them from other sources or teachers. Structuring means that the learner uses their thoughts and perceptions shaped by their previous experiences to associate and expand their new experiences. This can be

associate and expand their new experiences. This can be achieved through mental activities or sometimes through physical activities, that is, by doing and living (Harlen, 2000).

1-2 Material Development and Model Teaching Method

With the developing and changing conditions, educators and those who need other presentation technologies can easily find the teaching tools and materials they need in the market. However, these can sometimes be difficult, time-consuming and expensive to achieve. In these cases, teachers can prepare some of the tools and materials they need themselves, or they can have students prepare by guiding them (Şahin Yanpar-Yıldırım, 1999; İşman, 2008). What makes the use of materials in education so valuable is the linear relationship between learning and sense organs. Students learn 83% of their learning by sight, 11% by hearing, 3.5% by smell, 1.5% by touch and 1% by taste. In addition, people remember 10% of what they read, 20% of what they hear, 30% of what they see, 50% of what they see and hear, 70% of what they say and 90% of what they do and say (Ergin, 1995; Kılıç, 1997). The effect of seeing and hearing on learning at this rate makes the design of visual materials extremely important.

Model Teaching Method; It is a teaching method applied with the help of examples of real objects made of the same or other material, and objects brought to the classroom from their natural environment. Models can be larger or smaller than the original object, or they can be exactly the same size and structure as the real object they replace (Çilenti, 1985).

Models are recognizable imitations of the real object. It may or may not be in working condition like the real object. However, the original is similar in everything except size. In addition, there are models that are visible inside or very simplified ones that are free of all details (Okan, 1993).

Concept education is basically providing the formation of cognitive schemas of the concepts to be learned and the winners by the students. It aims for students to acquire concepts from abstract to concrete, from complex to simple, according to their accessibility or descriptive order (Baba & Öksüz, 2015). Concept training is done with methods and techniques to reach a concept in the easiest and most meaningful way. Especially in the field of science, it is important for students to acquire concepts that are difficult to reach, dangerous, inaccessible even though they are abstract or concrete, both visually, audibly and descriptively by using models in the classroom environment and by making use of today's technology (Gülen, 2018; Tömen, Akdeniz, Odabaşı Çimer ve Gürbüz, 2013).

1-3 Filtration Unit "NEFRON" in Kidney

When the microscopic structure of the kidney is examined, structures called nephron are seen. The most important structural-functional unit of the kidney is the "filtration unit. The nephron, located in the shell region of the kidney, forms the core region of the kidney (Fig. 1).

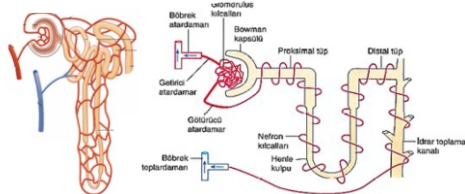


Fig. 1: Parts of the Nephron

The Malpighi body is the end or beginning of the nephron, the Bowman's capsule. The transmitting artery entering the Bowman's capsule divides into capillaries that form the glomerulus tuft. These capillaries join and exit the Bowman's capsule as the efferent artery. This ascending artery divides into renal capillaries, surrounds the nephron canals, and then joins together to connect to the renal vein. The nephron canal consists of three parts: Proximal tube, loop of Henle and Distal tube. In addition, urine collection channels open into the pool.

1-4 Renal Vessels

The renal artery enters the kidney from the pit and divides into thinner branches. Dirty in terms of O₂ rich residue; however, metabolic waste products, except CO₂, are abundant in his blood (Urea, NH₃, uric acid and other chemicals to be excreted). Renal vein is clean in terms of CO₂-rich residue.

I. Glomerulus capillary system (First capillary cyst): The branches entering the kidney are divided into thinner branches in the core and shell region and form the glomerulus capillaries.

II. Efferent Artery: Carries blood from the glomerulus to the 2nd blood system.

III. Second capillary system: The efferent artery emerging from the glomerulus divides into renal capillaries and forms the "second capillary system" that surrounds the nephron canals.

IV. Renal vein: These capillaries separate from the nephron canals and form the renal vein.

2 Materials and Methods

In our project, we designed a teaching material in order to make the structure and function of the Nephron, which performs the filtering-reabsorption-secreting function in the kidney, which is one of the subjects of the 11th grade biology course, excretory system unit, more understandable.

Material development method was used in the study. This method is used in educational materials developed based on the sensory, cognitive and psycho-motor characteristics of the student (Karamustafaoğlu, 2006).

Our project was carried out in the biology laboratory of our school. The construction stages of our project are as follows.

2-1 Ground Preparation of the Nephron Model

An upright floor was obtained by using 80 cm long and 50 cm wide chipboard and Styrofoam of the Nephron model (Figs. 2 and 3).

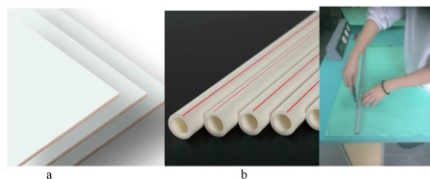


Fig. 2: a)hardboard b)PVC pipe c)styrofoam



Fig. 3: final state

2-2 Nephron Model and Placement with PVC Pipe

The Nephron Model was designed using a PVC pipe with a diameter of 2 cm and a length of 155 cm used for water installation (Figs 4 and 5).



Fig. 4: Glomerulus design stage

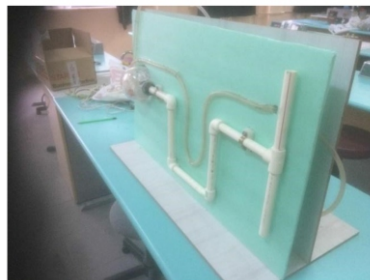


Fig. 5: Preparation of PVC pipe in appropriate dimensions

2-3 Placement of Blood Vessels Around the Nephron Model

For the blood vessel display in the nephron model, a 1 cm diameter and 220 cm long transparent tube shown in figure 3.5 was preferred. The transparent pipe was fixed to the Styrofoam floor with copper wires (Fig. 6).

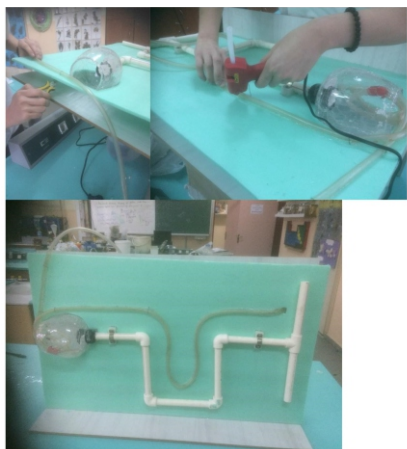


Fig. 6: Fixing the transparent tube for blood vessels to the model

2-4 Ensuring Blood Flow in the Transparent Tube

In order to ensure the movement of blood in the transparent tube, the aquarium in a container filled with red acrylic paint placed at the back of the nephron model was moved with the help of an internal filter motor. The functions of the parts of the nephron, which are shown blood flow, are pasted on the Styrofoam as notes (Fig. 7).



Fig. 7: Ensuring Blood Flow in the Transparent Tube

2- 5 Representation of Absorption Percolation Zone in the Nephron Canal

A glass sugar bowl was used for the Malpighi body filtration Bowman capsule. Glomerulus is shown with a transparent tube filled with red acrylic paint. One-way filtration occurs from the glomerulus capillaries to the Bowman capsule (Fig. 8).



Fig. 8: Malpighi body

3 Conclusions

In order to symbolize the absorption of water, glucose, amino acids, vitamins, ions and urea absorbed from the filtrate in the proximal tube, a transparent tube filled with yellow acrylic paint was preferred. In addition, the syringe used was used to symbolize the absorption of suction from the proximal tube into the blood. In order to symbolize the absorption of the water absorbed from the filtrate into the blood in the descending arm of Henle, a transparent tube filled with green acrylic paint was preferred. In addition, the syringe used was used to symbolize the absorption of suction from the Henle descending arm into the blood. A transparent pipe filled with black acrylic paint was preferred in order to symbolize the absorption of salt absorbed from the filtrate into the blood in the arm leading out of Henle. In addition, the syringe used was used to symbolize the absorption of suction from the arm of Henle into the blood. In order to symbolize the absorption of water, Na, Cl and HCO₃ absorbed from the filtrate in the distal tube, and the reabsorption of water and urea from the urine collection canal, a transparent tube filled with blue colored acrylic paint was preferred. In addition, the syringe used was used to symbolize the absorption of suction from the Distal tube and urine collection channel into the blood (Fig.9).

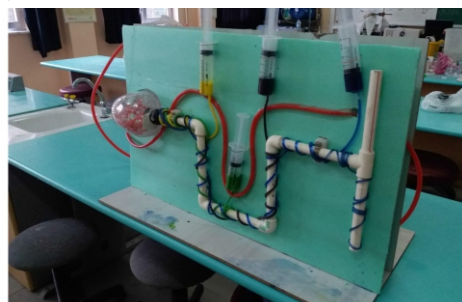


Fig. 9: Malpighi Bodies

4 Discussions

A successful science education aims to provide individuals with the knowledge and skills they will need in their daily lives (Anderson, 2010). Since science literate individuals have the skills to access and use the information they need to solve the problems they encounter, they have more advanced problem-solving skills (Kaptan, 1998). In biology teaching, both educational situations and the abstract and complex nature of biology concepts cause students to have difficulty in

understanding some subjects and to learn by memorizing without understanding (Kılıç & Sağlam, 2004). In order to overcome this problem, well-prepared three-dimensional models in biology lessons enable the knowledge to be grasped more easily (Çömlekçiöğlü & Bayraktaroğlu, 2001). In studies on new curricula in Turkey, teachers' opinions are frequently encountered regarding "significant disruptions in the implementation of the curricula due to the lack of structures, tools, materials and materials" (Akça, 2007, Peker & Halat, 2008; Şahin, 2010). Model teaching method; It is a teaching method applied with the help of examples of real objects made of the same or other material, and objects brought to the classroom from their natural environment (Çilenti, 1985).

In our project, the teaching material describing the structure and function of the Nephron, which performs the filtration-reabsorption-secretion function in the kidney, which is one of the subjects of the 11th grade biology course, excretory system unit, was designed with the "material development method". Chipboard and Styrofoam were used for the background of the nephron model. For the demonstration of the nephron canal, a PVC pipe with a diameter of 2 cm and a length of 155 cm, which is used for plumbing, was used. A transparent tube with a diameter of 1 cm and a length of 220 cm was used for blood vessel display in the nephron model. In order to ensure the movement of blood in the transparent tube, the aquarium in a container filled with red acrylic paint placed at the back of the nephron model was moved with the help of an internal filter motor. Glomerulus capillaries with glass sugar bowl and transparent tube filled with red acrylic paint were shown in Bowman capsule design to demonstrate infiltration in Malpighi corpuscle. Transparent tubes and syringes filled with acrylic paint were used to symbolize the parts of the nephron where absorption and secretion from the blood occur (Proximal tube, descending and ascending limb of Henle, Distal tube and urine collection duct). In addition, the functions of the parts of the nephron, showing blood flow, were pasted on the Styrofoam as notes.

Acknowledgment

I would like to thank my Consultant Murat KODAT, who guided me with her knowledge and experience at all stages of our project and provided all kinds of scientific support.

References

- [1] Akça, S. (2007). İlköğretim 5. sınıf 2005 matematik programının öğretmen, yönetici ve ilköğretim müfettişleri görüşleri doğrultusunda değerlendirilmesi (Afyonkarahisar ili örneği). Yayınlanmamış yüksek lisans tezi, Afyon Kocatepe Üniversitesi, Sosyal Bilimler Enstitüsü, Afyonkarahisar.
- [2] Anderson, C. W. (2010). Perspectives on science learning. S. K. Abell, & N. G. Lederman (Dü.) içinde, Handbook of Research on Science Education (s. 3-56). New York: Routledge.
- [3] Arslan, S. ve Özpınar, İ. (2009). İlköğretim 6. sınıf matematik ders kitaplarının öğretmen görüşleri doğrultusunda değerlendirilmesi. Dicle Üniversitesi Ziya Gökalp Eğitim Fakültesi Dergisi, 12, 97-113.
- [4] Baba, M., ve Öksüz, Y. (2015). The effect of the use of concept cartoons in gaining of citizenship consciousness of primary school students. International Periodical for the Languages, Literature and History of Turkish or Turkic, 10(15), 119-136. DOI Number: <http://dx.doi.org/10.7827/TurkishStudies.8866>
- [5] Coştu, F., Beler, Ş., ve Coştu, B. (2017). Fotosentez konusunda öğrencilerin grafiksel becerileri ve karşılaştıkları güçlükler. Scientific Educational Studies, 1(1), 41-63.
- [6] Çilenti, K. (1985). Fen Eğitimi Teknolojisi. Kadıoğlu Matbaası, Ankara
- [7] Demirel, Ö., Altun E. (2007). Öğretim Teknolojileri ve Materyal Tasarımı, Ankara: Pegem A Yayıncılık.
- [8] Ergin, A. (1995). Öğretim Teknolojisi ve İletişim. Pegem Yayınları, Ankara.
- [9] Ersoy, Y. (2003). Fen Bilimleri Öğretiminde Yeni eğilimler ve Öğretmen Eğitimi, <http://www.geocities.com/ioffes2002/yersoy.html>, Erişim tarihi: 06.11.2003.
- [10] Gülen, S. (2018). Using volume of concept in the class environment. Journal of Technology and Science Education, 8(4), 205-213. <https://doi.org/10.3926/jotse.362>
- [11] Harlen, W. (2000). Teaching Learning Assessing Science 5-12, London: Paul Chapman Publishing Co.
- [12] Harris, K., Marcus, R., Mc Laren, K., Fey, J. (2001). Curriculum Materials Supporting Problem-Based Teaching. School Science & Mathematics, 101(6), 9-310.
- [13] İşman, A. (2008). Öğretim Teknolojileri ve Materyal Geliştirme. Pegem A Yayıncılık, Ankara.
- [14] Kaptan, F. (1998). Fen bilgisi öğretiminin niteliği ve amaçları. S. Yaşar (Dü.) içinde, Fen Bilgisi Öğretimi (s. 13-30). Anadolu Üniversitesi, Açıköğretim Yayınları.
- [15] Kaptan, F. ve Korkmaz, H. (2000). Yapısalcılık (Constructivism) Kuramı ve Fen Öğretimi, Çağdaş Eğitim Dergisi, 265, 22-27. _____ (2002). Fen Eğitiminde Proje Tabanlı Öğrenme Yaklaşımının İlköğretim Öğrencilerinin Akademik Başarı, Akademik Benlik Kavramı ve Çalışma Sürelerine Etkisi, Hacettepe Üniversitesi Eğitim Fakültesi Dergisi. 22, 91-97.
- [16] Karamustafaoğlu, O. (2006). Fen ve teknoloji öğretmenlerinin öğretim materyallerini kullanma düzeyleri: Amasya ili örneği. Bayburt Eğitim Fakültesi Dergisi, 1(1), 90-101.
- [17] Kılıç, R. (1997). Görsel Öğretim Materyalleri Tasarım İlkeleri. Millî Eğitim Dergisi, Sayı 136, 74
- [18] Okan, K., 1993, Fen Bilgisi Öğretimi. Okan Yayınları, Ankara.
- [19] Okutan, M. (2004). Bilgi Toplumunun Öğretmeni Nasıl Olmalıdır? Eğitimde Çağdaş Yaklaşımlar. Samsun (8 Mayıs 2004)
- [20] Peker, M. ve Halat, E. (2008). İlköğretim I. kademe matematik programının eğitim durumları boyutunun öğretmen görüşleri doğrultusunda incelenmesi. Selçuk Üniversitesi Ahmet Keleşoğlu Eğitim Fakültesi Dergisi, 26, 209-225.
- [21] Rıza, E. T. (2003). Eğitim Teknolojileri Uygulamaları ve Materyal Geliştirme. (6.Baskı). İzmir: Birleşik Matbaası
- [22] Şahin Yanpar, T. ve Yıldırım, S. (1999). Öğretim Teknolojileri ve Materyal Geliştirme. Anı Yayıncılık, Ankara.
- [23] Yaşar, Ş. (1998). Yapısalcı Kuram ve Öğrenme-Öğretme Süreci, Anadolu Üniversitesi Eğitim Fakültesi Dergisi 8 (1-2), 68-75.

The Coefficient of Restitution of Rebounding Capsules

Sadra Dindar, Rahe Roshd School, sadra.dindar1384@gmail.com

ABSTRACT

This research has been done to solve one of the 34th IYPT problems. The question statement is as follows: “A spherical ball dropped onto a hard surface will never rebound to the released height, even if it has an initial spin. A capsule-shaped object (i.e. Tic Tac mint) on the other hand may exceed the initial height”. To find the relevant parameters qualitative analysis by *Newtonian* and *Lagrangian* mechanics has been done.

Key words: *Rebounding Capsule, Newtonian Mechanics, Lagrangian Mechanics*

ARTICLE INFO

Participated in IYPT 2021, Tbilisi, Georgia
Accepted in country selection by Ariaian
Young Innovative Minds Institute, AYIMI

<http://www.ayimi.org>, info@ayimi.org

1 Introduction

When tablets collide during manufacturing and handling operations they rebound with a force and velocity that is determined by the collision conditions and the properties of the materials. This collision rebound behavior of solid bodies can be described using a parameter known as the “coefficient of restitution” (CoR). The CoR varies with the mechanical properties of both colliding bodies and is lower for more plastic collisions and higher for elastic collisions.

2 Basic Theories

The coefficient of restitution, e , is a parameter that quantifies the energy losses during collision and is defined as (Eq. 1):

$$e = \frac{-V_r}{V_i} \quad (1)$$

where V_r and V_i are the rebound and impact relative velocities of the colliding objects. The collision is said to be perfectly elastic if $e = 1$ and completely inelastic if $e = 0$. For a freely falling object under the influence of gravity, Eq. (1) simplifies to the form [1](Eq. 2):

$$e = \sqrt{\frac{h_2}{h_1}} \quad (2)$$

To solve this problem the capsule-shaped object is divided by 2 hemispheres, then integrating them in each axis ($\dot{x}, \dot{y}, \dot{z}$) and summing up would be the main approach (Fig.1).

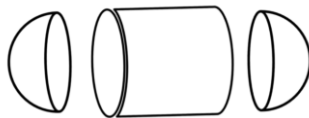


Fig. 1: capsule-shaped object is divided into 2 hemispheres

Defining force as a function of momentum-time, gives (Eq. 3):

$$F = \frac{dP}{dt}, \frac{mv_0^2}{2} = mgh_0 \rightarrow v' = \sqrt{2gh_0}; \text{ then} \quad (3)$$

$$m\Delta v = N\Delta t = m(v'_1 - v'_0)$$

and for calculating N^{th} height of the capsule, it is released

with: $v_{\text{initial}} = 0$ then :

$$E_1 = mgh_1 = amgh_0 \rightarrow h_1 = ah_0 \mid h_2 = \alpha^2 h_0 \mid h_n = \alpha^n h_0 \quad (4)$$

where α is $0 < \alpha < 1$.

If we assume the second restitution as an ideal parabola (neglecting air drag), Then for the second height being greater than the initial height, $v^2 \sin^2 \theta > h_{\text{initial}} \cdot \sin^2 \theta$ in $\frac{\pi}{2}$ will be maximized; but $v = \omega \cdot r$ and if $\theta = \frac{\pi}{2}$ then the angle (ϕ), between the radius (r), the geometric center and impact ground and ($r \sin \phi$) would be equal to 0; so:

$$\tau = rN \sin \phi = 0$$

Since there is waste force acting upon the capsule then it wouldn't reach the initial height. In this case:

$$v = -gt + v_0 \quad v_0 = e\sqrt{2gh} \quad (5)$$

where e is the coefficient of restitution ($e = \frac{v_{\text{rebound}}}{v_{\text{impact}}}$). So, the ideal angle (ϕ, θ) would be $\pi/4$.

Now three different shapes are analyzed:

a) Cylinder

$$I_z = \frac{mr^2}{2} \quad I_y = I_x = \frac{1}{12}m(3r^2 + h^2) \quad (6)$$

b) Capsule

$$I_x = I_y = \frac{1}{12}m_1(3r_1^2 + h_1^2) \quad (7)$$

$$I_z = \frac{1}{2}m_1r_1^2 + \frac{2}{10}m_2r_2^2 + \frac{2}{10}mr^2 \quad (8)$$

c) Sphere

$$I_x = I_y = I_z = \frac{2}{10}mr^2 \quad (9)$$

Lagrangian Mechanics (Released Height – Impact Ground):

$$L = T - V \quad \frac{1}{2}I\dot{\theta}^2 + \frac{1}{2}m\dot{x}^2 - \frac{1}{2}kx^2 + mgx \quad (10)$$

Acquiring the equation of motion by the Euler-Lagrange method:

$$\frac{d}{dt} \left(\frac{\delta L}{\delta \dot{x}} \right) - \left(\frac{\delta L}{\delta x} \right) = 0 \quad (11)$$

$$m \frac{d^2x}{dt^2} - kx + mg = 0 \tag{12}$$

In our 3D model the capsule is made out of two hemispheres and one cylinder where ($\xi = x^2$) [2], then we write our impact ΣF as followings:

$$m \frac{d^2y}{dt^2} = \left(-k\Delta y^{\frac{3}{2}} - \delta \left(\Delta \dot{y}^{\frac{3}{2}} \right) \right) \tag{13}$$

$$m \frac{d^2x}{dt^2} = \left(-x\Delta y^{\frac{3}{2}} - \delta \left(\Delta \dot{x}^{\frac{3}{2}} \right) \right) \tag{14}$$

$$\frac{d^2\theta}{dt^2} = -N \frac{\theta}{|\theta|^2} \cos(\phi) \tag{15}$$

$$\Delta y = \left(y - \frac{\theta}{|\theta|^2} \sin(\phi) - r \right) \tag{16}$$

$$\Delta x = \left(x - \frac{\theta}{|\theta|^2} \cos(\phi) - x_{point} \right) \tag{17}$$

3 Experiments

For finding the ideal height for $h_2 > h_1 | h_4 > h_3 | h_3 > h_1$ we would write the PDF (Probability Distribution Function). When the capsule hit the ground it starts gong up and down but with two different motions linear and rotational. We need to know why this phenomenon happens (Figs. 2 and 3).

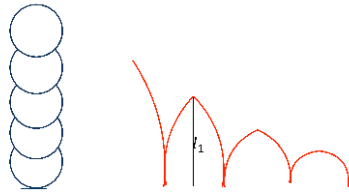


Fig.2: Capsule hits the ground without considering friction

$$t_1 = amgh_0$$

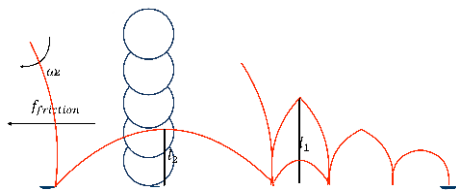


Fig.3: Capsule hits the ground with considering friction

$$t_2 = amgh_0$$

$$t_1 > t_2$$

In linear and rotational motion , total energy will be:

$$\Sigma E = \frac{mv^2}{2} + \frac{I\omega^2}{2} + mgh \tag{18}$$

$$mgh = amgh = mgh_1 + \frac{I\omega^2}{2amgh_0} \tag{19}$$

$$= mgh_1 + \frac{I\omega^2}{2} \tag{20}$$

$$\alpha(mgh_0 + \frac{I\omega^2}{2}) = mgh_1 + \frac{I\omega^2}{2} \tag{20}$$

$$mgh + \frac{I\omega^2}{2} = amgh_1 + \alpha \frac{I\omega^2}{2} \tag{21}$$

$h_0 = \text{dropheight}$
 $h_1 = \text{reboundheight}_0$
 $h_2 = \text{reboundheight}_1$

$$h_2 = \alpha h_1 + \frac{I}{2mg} (\alpha\omega^2 - \alpha_2^2) \tag{22}$$

$$\alpha\omega_1^2 - \omega_2^2 > \frac{2mgh(1-\alpha)}{I} \tag{23}$$

$$\omega_1 > \sqrt{\frac{\omega_2^2}{\alpha} + \frac{2mgh_1}{I} + \frac{1-\alpha}{\alpha}} \tag{24}$$

When the capsule collide the ground the coefficient restitution which is a function of the velocity before and after hitting will be as follows:

$$e = \sqrt{\frac{KE_{after}}{KE_{before}}} = \sqrt{\frac{\frac{1}{2}mv^2}{\frac{1}{2}mu^2}} = \frac{v}{u} \tag{25}$$

$$\text{PotentialEnergy} \simeq 0$$

$$v^2 = u^2 + 2gh \tag{26}$$

$$a = \frac{v+u}{\text{CollisionTime}} \tag{27}$$

By Euler - Lagrangian equation:

$$L = T - V = \frac{1}{2}m\dot{x}^2 + \frac{1}{2}I\dot{\omega}^2 - mg(x) \tag{28}$$

$$\frac{\delta L}{\delta x} - \frac{d}{dt} \left(\frac{\delta L}{\delta \dot{x}} \right) = 0 \tag{29}$$

$$m\ddot{x} - mg = 0 \tag{30}$$

The components of forces in two directions , x and y:

$$y - l\sin(\theta) - r = y_{point} \tag{31}$$

$$\Delta y = \left(y - \frac{\theta}{|\theta|^2} \sin(\theta) - r \right) \tag{32}$$

$$\Delta x = x - \frac{\theta}{|\theta|^2} \cos(\theta) - x_{point} \tag{33}$$

$$m\ddot{y} = \left(-k\Delta y^{\frac{3}{2}} - \delta \left(\Delta \dot{y}^{\frac{3}{2}} \right) \right) \tag{34}$$

$$m\ddot{x} = \left(-k\Delta x^{\frac{3}{2}} - \delta \left(\Delta \dot{x}^{\frac{3}{2}} \right) \right) \tag{35}$$

$$I\ddot{\theta} = -N \frac{\theta}{|\theta|^2} \cos(\theta) \tag{36}$$

The angular velocity in x, y and Z (Fig. 4):

$$\omega = \frac{\Delta\theta}{\Delta t} \tag{37}$$

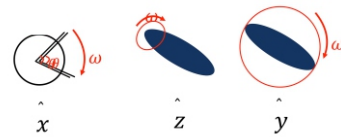


Fig. 4: Angular velocity of the capsule in x, y and z directions

$$I_z = \frac{1}{2}mr^2 + \frac{2}{10}mr^2 \tag{38}$$

$$I_x = I_y = \frac{1}{12}m(3r^2 + h^2) + \frac{2}{10}mr^2 \tag{39}$$

$$I_z = \frac{1}{12}m(3r^2 + h^2) + \frac{2}{6}mr^2 \tag{40}$$

For finding the ideal height several experiments are done in different heights.

4 Results and Conclusions

To write the PDF (Probability Distribution Function), the capsule-shaped object is spined 10 times in different angular velocities in 10 different heights according to the experimental setup (Figs.5,6, 7 and 8).

$h_1 = 10$	$P(x)_1 = 0$	$h_6 = 35$	$P(x)_6 = \frac{3}{10}$
$h_2 = 15$	$P(x)_2 = 0$	$h_7 = 40$	$P(x)_7 = \frac{3}{10}$
$h_3 = 20$	$P(x)_3 = \frac{1}{10}$	$h_8 = 45$	$P(x)_8 = \frac{1}{10}$
$h_4 = 25$	$P(x)_4 = \frac{1}{10}$	$h_9 = 50$	$P(x)_9 = \frac{3}{10}$
$h_5 = 30$	$P(x)_5 = 0$	$h_{10} = 55$	$P(x)_{10} = \frac{1}{10}$

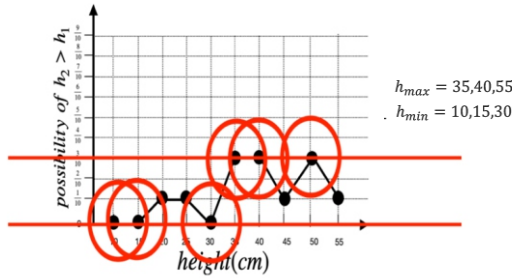


Fig.5: Probability versus height

$p(h_2 > h_1) = 35, 40, 55 \text{ cm}$

$h_1 = 10$	$P(x)_1 = \frac{4}{10}$	$h_6 = 35$	$P(x)_6 = \frac{2}{10}$
$h_2 = 15$	$P(x)_2 = \frac{1}{10}$	$h_7 = 40$	$P(x)_7 = \frac{2}{10}$
$h_3 = 20$	$P(x)_3 = \frac{2}{10}$	$h_8 = 45$	$P(x)_8 = 0$
$h_4 = 25$	$P(x)_4 = \frac{1}{10}$	$h_9 = 50$	$P(x)_9 = \frac{2}{10}$
$h_5 = 30$	$P(x)_5 = 0$	$h_{10} = 55$	$P(x)_{10} = \frac{1}{10}$

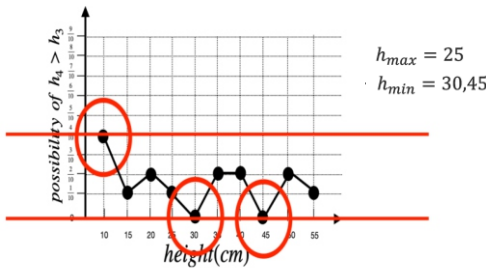


Fig.6: Probability versus height

$p(h_4 > h_3) = 25 \text{ cm}$

$h_1 = 10$	$P(x)_1 = 0$	$h_6 = 35$	$P(x)_6 = \frac{1}{10}$
$h_2 = 15$	$P(x)_2 = 0$	$h_7 = 40$	$P(x)_7 = \frac{2}{10}$
$h_3 = 20$	$P(x)_3 = 0$	$h_8 = 45$	$P(x)_8 = 0$
$h_4 = 25$	$P(x)_4 = \frac{1}{10}$	$h_9 = 50$	$P(x)_9 = \frac{3}{10}$
$h_5 = 30$	$P(x)_5 = 0$	$h_{10} = 55$	$P(x)_{10} = 0$

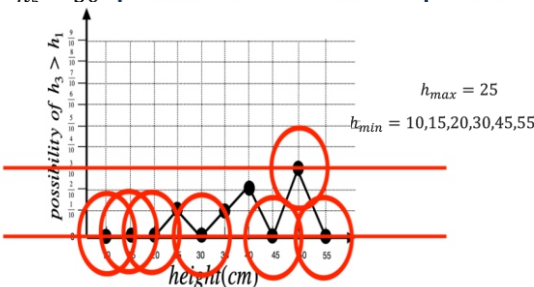


Fig.7: Probability versus height

$p(h_3 > h_1) = 25 \text{ cm}$

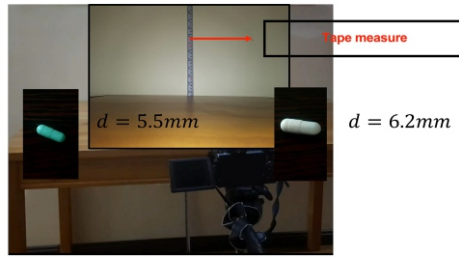


Fig. 8: Experimental Setup

Maximum and minimum of the angular velocities in our experiment are calculated in different collision times as shown in figure (9).

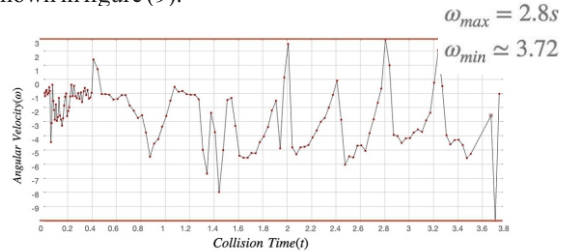


Fig. 9: Angular Velocity versus collision time

References

- [1] Bharadwaj R., Carson S., Bruno C. H., (2010), ‘The coefficient of restitution of some pharmaceutical tablets/compacts’. , International Journal of Pharmaceutics, Elsevier 402 (2010) 50–56.
- [2] Fesharaki, A., 2020, “Investigation of parameters in Oscillations of Newton’s Cradle”, Lat. Am. J. Phys. Educ. Vol. 14, No. 3, Sept. 2020

ZEPHYROS a Habitat on Mars

^aZoe Konstantinidou, ^bPolyxeni Panou, ^cAndrianna Solomonidou, ^dIoanna Petridi, Anatolia College, Greece/Thessaloniki,

^a20171069@student.anatolia.edu.gr, ^b20137058@student.anatolia.edu.gr, ^c20191127@student.anatolia.edu.gr,

^d20191116@student.anatolia.edu.gr

ABSTRACT

This research is about a space station which has been designed by considering some important affecting parameters. The habitat is on Mars surface but to protect it from hurricanes and dust storms (which occur often on Mars) we have found a series of processes.

ARTICLE INFO

Gold Medalists in ISAC Olympiad 2021, Tehran, Iran

Supervisor: Apostolos Michaloudis

Accepted by Ariaian Young Innovative Minds Institute, AYIMI

<http://www.ayimi.org>, info@ayimi.org

Key words: *Mars, Space Station, Designing*

1 Introduction

The main aim of this research is to find how we can find a place to live in space and what parameters should be considered as the most important ones.

What is ZEPHYROS ?

2 Explanation

The name Zephyros sparked our interest because Zepher is the ancient Greek God of Spring. We felt that this name is perfect for our house on Mars because this is a new idea that will bloom just like a flower in Spring. Zephyr was also the God of the winds, which often symbolize change, new ideas and environments, literally and figuratively.

We let the wind of inspiration take us to a place of ambition and hope, which lead to us designing this ideal habitat on Mars.

With this wind leading us to do the unexpected, we finally maintain our standards and achieve our goals. Our Mars habitat is well designed and thought through, and if someday we achieve to make it a reality, we can assure that it will be 100% safe and livable.

To explain the ZEPHYROS, it is started from its different parts.

For safety reasons, we will locate our shelter inside a crater on Mars' surface. That is because the radioactivity levels are lower and since the shape of the crater is proper for protecting the habitat from hurricanes and dust storms (which occur often on Mars). The lower level of the habitat, which includes the bedroom, the space toilet, the shower unit and the H₂O and O₂ tanks will be built underground where radioactivity protection is maximized, while the other two floors will be above the surface of the ground.

The shelter consists of three floors, which, because of the gravitational acceleration on Mars (3.69m/s²) will be 7,25 m each. The greenhouse will be 9,63 m tall. The underground (-1 level) floor's area will be 23m², while the other two floors will be 25m², which means that the total area of the house will be 72m² and the greenhouse will be 17m². Our shelter will approximately accommodate 3-6 people and more beds will be designed accordingly. One local Mars resource we will use (and the most important one) is the soil from Mars' surface we will use to construct the outer casing of the upper floor. A series of processes will

create a hard consistency that forms a brick. Most materials will be 3D-printed using a static construction rover and the rest will be gathered from the surface of the Red Planet (Martian soil to make bricks). We decided to place two airlock doors, one that connects the external environment with the airlock area and one that connects the airlock area with the internal environment, as an entrance to prevent loss of oxygen or pressure. The astronaut-helmet structure of the building (Extra vehicular Visor assembly) will provide protection from radiation, along with the housetop, which will be made of bricks of Martian soil. The aerogel Insulation Layer which will be applied to the house's human-interfacing surfaces will function as an extremely effective insulator, protecting from infrared radiation and ensuring thermal comfort. The residents' rooms will be on the -1 level, while they will be exercising at the gym on the ground floor. Working needs can be covered by the communication system and proper facilities, which will be installed in the living room area.

In order to ensure safe, reliable, long-lived power systems to provide electricity and heat for the residents, we will combine three different power sources for the shelter:

solar panels,

NASA RTG (Radioisotope Thermoelectric Generator, which converts heat directly into useable electrical energy),

and fuel cells, which produce electricity by chemical reactions.

There will be two main sources for water; the first one is related to the process of collecting all the liquids such as sweat and mostly urine and converting them, via the space toilet, to water. The second source is the water that will be provided through the fuel cells, as water production could be a by-product of power generation. The food source will mostly be planted vegetables that will be growing constantly in the habitat's greenhouse. More specifically foods that can be cultivated on Mars are: Dandelions because, they grow quickly, every part of the plant is edible and they have high nutritional value. Other nutritional foods that will thrive are micro greens, lettuce, arugula, spinach, peas, garlic, kale and onions. They could serve up to 3100 per day for 3-6 astronauts over a 600 day excursion to the Red Planet. Last but not least, the waste will be disposed via an airlock into space.

disposed via an airlock into space .

3 Several parts in Zephyros (Figs. 1):

1- Airlock front door: two doors separated by a short corridor to create airlock

2- Window wall: made from high temperature polysulfone plastic (like in astronauts' helmets). Inner visor, made of ultraviolet-stabilized polycarbonate. filters ultraviolet rays and rejects infrared rays. Outer visor filters visible light and rejects ultraviolet and infrared rays . Together, they form an effective thermal barrier.

3- Housetop: made out of Martian Soil.

4- Aerogel Insulation Layer: applied to the house's human interfacing surfaces to ensure thermal comfort.

5- Greenhouse: vegetables will be grown with Martian soil, LEDs will ensure that the plants get enough sunlight and sheets of silica aerogel will make plant growth feasible.

6- Silica Aerogel

7- Small Greenhouses

8- Fuel Cells: used for providing extra electricity, heat, water, and CO_2 . The fuel will be the H generated from the electrolysis.

9- Solar Panels: to generate energy

10- Radioisotope Thermoelectric Generator (RTG): to convert heat directly into useable electrical energy

11- UHF Antennas: close range antennas functioning like walkie-talkie compared to the long range of the low gain and high gain antennas

12- Pneumatic (Vacuum) Elevator

13- Kitchen

14- Living Room

15- Spacesuit Storage

16- Home Gym (gravity on Mars being 38% of Earth, humans could run the risk of muscle wastage and other health issues.

17- Bedroom

18- UWMS (space Toilet): will feed pre-treated urine into a regenerative system, which recycles water for further use

19- Shower Unit

20- Oxygen Tanks: will be generated with electrolysis by running electricity through water, water will be separated into H and O_2 gas.

Floor height: 1 level: 7,15 meters

0 level: 7,25 meters

-1 level: 7,25 meters

Greenhouse height: 9,636 meters

Waste disposal: via an airlock into space

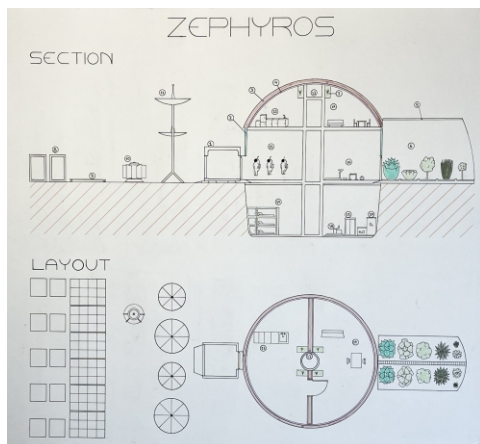


Fig. 1: Several parts of Zephyros

A New Sampler Invention

Saina Ahmadi, Nazanin Azizi, Farzanegan I high school, Tehran/ Iran , saina17121382@gmail.com

ABSTRACT

The unit of volume in a micropipette is microliter, so the slightest error causes the largest variations in the test results. Most of the time, the researcher does not notice the error that changes the overall result of the experiment. At best, the researcher realizes the error and has to repeat the experiment, resulting in a waste of materials and time. Accordingly, this error became the basis for this project and an attempt was made to solve this problem by providing a simple, creative and low-cost model that is available to all laboratories. We made a counter sampler using a magnet B/sensor and an electrical counter, which were installed in the piston and body of micropipette.

Key words: *Micropipette, Laboratories, Errors, Creative model*

ARTICLE INFO

Gold Medalists in IMSEF 2020, Izmir, Turkey

Supervisor: Maryam Davoodi

Accepted by Ariaian Young Innovative Minds Institute, AYIMI

<http://www.ayimi.org> , info@ayimi.org

1 Introduction

If you are a researcher in biology laboratories, you are definitely familiar with micropipette as one of the most important equipment. Human error is an inseparable part of an experiment. One of the most common human errors that occurs when working with a micropipette is that the sampled well is lost in a 96-well plate due to the proximity of the wells, low transfer volumes ($<1000\mu\text{l}$), adding a colorless solution (which prevents visual control of the sampling process), environmental factors (such as noisy devices and overcrowded rooms), and mental states of the operator (work stress, fatigue, and lack of concentration). The unit of volume in a micropipette is microliter, so the slightest error causes the largest variations in the test results. Most of the time, the researcher does not notice the error that changes the overall result of the experiment. At best, the researcher realizes the error and has to repeat the experiment, resulting in a waste of materials and time. Accordingly, this error became the basis for this project and an attempt was made to solve this problem by providing a simple, creative and low-cost model that is available to all laboratories. We made a counter sampler using a magnet B/sensor and an electrical counter, which were installed in the piston and body of micropipette. Installation of the sensor into the body has caused the counter can count the number of sampling only when piston button was pressed to the second step. So, drawing up liquid is not included in the count. Low price, portability, and being user friendly are the advantages of our plan.

1-1 Pipette

Working in laboratories and doing experiments is one of the most important parts of a research. Among the various instruments which are used to perform laboratory test, some equipment such as pipettes and samplers are very useful. Pipettes are mostly used in a few fields like genetics, chemistry, microbiology and pharmacology. A range of pipettes with different accuracy is manufactured and designed based on their applications. They can be a non-standard piece of glass or plastic designed to transfer a single volume of liquid or can be precious instruments with more complex structures for transferring a couple of volumes (Fig. 1).



Fig. 1: Pipettes

1-2 Micropipettes

Micropipettes, also called samplers, are the most accurate pipettes which are widely used to collect and transfer a very little amount of volumes in microliters. They are favourable instruments for many researchers working on some precious researches, especially in the field of cell-molecular biology, chemistry and pharmacy. Moreover, lab technicians are likely to learn to use it in the first steps of their experiments and to spend most of their time on using it. Accordingly, samplers can be classed based on their different characteristics, some of which are mentioned below.

1-2-1 Adjustable and Fixed Micropipette

Adjustable pipettes are those that can be adjusted to a range of specific volumes. These pipettes usually have such labels as "10-100 microliters" that indicate the desired volumes by which can be transferred. In fact, this type of samplers can only draw the adjusted volumes; However, the pipetting system will be disrupted if users use sampler out of the defined ranges.

On the other hand, fixed volume micropipettes are those whose volume is unchangeable. Compared to adjusted samplers, there are fewer moving parts in the structure of fixed micropipettes, therefore, their mechanism of action is simpler, which makes them enable to transfer a specific volume more accurately. These kinds of samplers are mostly used in laboratories with routine daily works with a need of transferring some specific volumes (Fig. 2).



Fig. 2: Variable (A) and fixed (B) samplers

1-2-2 Single-Channel Samplers and Multi-Channel Samplers

There is a difference between single-channel and multi-channel samplers depending on the number of channels attached to their pistons. Most researchers sometimes prefer a multi-channel pipette to a single one, e.g. filling some wells of a 96-well plate at the same time, so that one-by-one filling in using a single-channel sampler will take a long time during an experiment.



Fig. 3: Single-channel samplers and multi-channel samplers

1-2-3 Electronic Samplers

The electronic micropipettes were designed by reducing the required force to improve the ergonomics of the micropipettes. Manually moving the piston is replaced by a small electric motor powered by a battery. The work steps are set and displayed on a small screen. In addition, electronic pipettes can reduce the risk of RSI-type injuries (Fig. 4).



Fig. 4: Electronic samplers

The main components of a sampler and mechanism of its action are as shown in figures (5 and 6).

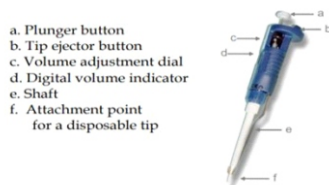


Fig. 5: Components of a sampler

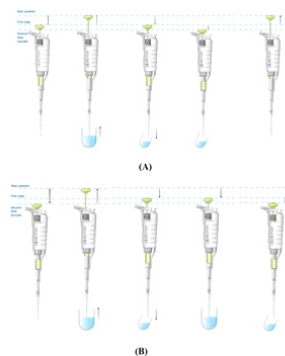


Fig. 6: The schemes of (A) the direct and (B) the reverse pipetting methods.

2 A problem Statement

Since laboratories are complex systems consisting of different people and devices, the presence of errors in there is undeniable. Basically, laboratory errors are classified as pre-analytical, analytical and post-analytical errors. On the one side, pre-analytical errors may occur in the procedure of requesting a test, collecting a sample, and transferring it to the laboratory. On the other side, analytical errors may occur during a test in response to either uncalibrated equipment or tired, careless technician with high workload. Besides, post-analytical errors are present after a test during data collection, analysis and reporting.

Since the samplers are usually used for doing an experiment, driven errors are analytical. As mentioned, poor calibration and quality controls along with technical errors of users can be the main sources of this errors. Due to the calibration program for most laboratory devices is scheduled, some researchers believe that the role of technicians in occurring this error might be greater. As a result, the awareness of the technicians is the most important factor to prevent the occurrence of this type of error, which is usually less noticed.

3 The Main Aims

The error related to a sampler can be caused by various factors, including using an uncalibrated sampler, contaminated sampler, unsuitable tips, a broken sampler and so on. These errors can be largely eliminated by properly training staff and creating a regular program to calibrate. However, error is always an integral part of human action; as a result, efforts should be made to identify drastic errors that have been overlooked in the testing process and to take actions to correct them.

The error in counting sampling number is one of the most common human errors which can be occurred during a work set with sampler. Some environmental factors, such as working in a noisy workplace with high workload or having a bad working day and getting exhausted, can disrupt the focus of technicians, which let them to make mistake. In addition, running a test into 96-well plates might be another source of analytical errors. That's why their wells are too small and close to each other, resulting in missampling especially when the transferred volume is very small and its visually tracking is practically impossible. For example, the researcher forgets in which well he has sampled or in which step of adding a solution to a mixture s/he has been. On the other hand, the sampler transfer volumes in the microliter range, so any error in transferring equals more deviation in results. In fact, researchers usually do not pay attention to these errors, which lead to erroneous results and reports. Occasionally, a researcher recognizes the error and has to repeat the experiment, resulting in a waste of material and time. Sometimes it is practically impossible to repeat the experiment due to a limitation of budget, time and materials. For example, the ELISA test is usually one of the final stages of a test series; thus, if for any reason the researcher makes a mistake in pouring the sample into the ELISA plate wells, all the cost and time spent on the series of experiments will be wasted.

As a result, in this study, an attempt was made to design a sample with the ability to count the number of sampling in order to increase the efficiency, accuracy, precision and reproducibility of the results by reducing user errors, so that it could save materials and time in the laboratory.

4 Methods

4-1 Solution 1:

Installing the Counter on the Piston Button of a Sampler

The first scheme was to install the counter on the plunger button. Thus, when the experimenter wanted to do sampling, he/she had to push the counter which led the number on counter to increase by one unit.

There were some disadvantages in this idea; the major problem was that it counted each sampling twice because the button was pushed one time for filling the disposable tip and the other time for discharging the solution. Moreover, the other problem was that the surface of the counter's button is slippery and non-user friendly (Fig. 7).

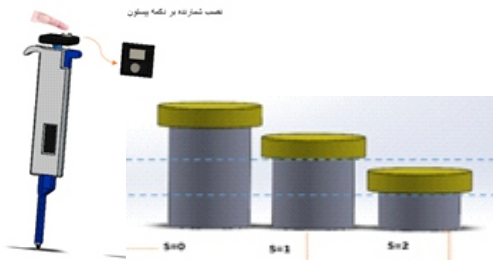


Fig. 7: Solution 1

4-2 Solution 2:

Installing of the (Diode-Receiver-Transmitter) on Piston Base and Piston Button

In this idea, two diodes were used that one of them was attached on the plunger rod and the other was placed in front of the tip ejector. While the experimenter pushed the plunger button, the plunger rod went towards other diode. Consequently, an electrical current was triggered and the number on counter increase by one unit (Fig. 8).

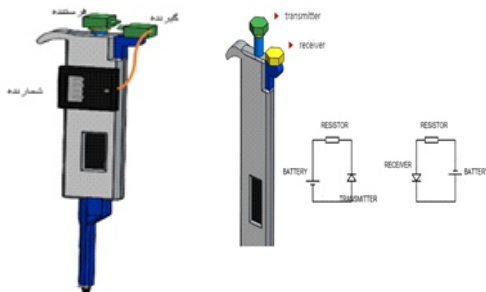


Fig. 8: Solution 2

To be honest, this idea was practically impossible so that it would not be user-friendly.

4-3 Solution 3:

Installing both Receiver and Transmitter on Piston Base and Piston Button, Respectively, Along with Adding a Shiny Reflective Ring to the Piston Rod

In this idea, both receiver and transmitter were placed on the same place (i.e. in the front of the tip ejector) and a shiny ring was attached on the plunger rod. The mechanism was that the transmitter sent a beam of light as soon as the technician pushed the plunger, then these beams got reflected by the shiny ring and the receiver received them. Consequently, an electrical current added a number to the counter. This idea was easier than our 2nd solution but still there were some problems. The diodes were expensive and needed more energy sources. In addition, the shiny ring was able to be destroyed after several uses (Fig. 9).

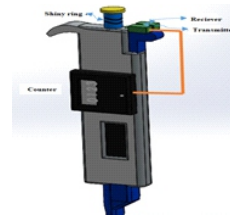


Fig. 9: Solution 3

4-4 Solution 4:

Micro-Switch

In this idea, when the experimenter is doing the samplings and pushes the plunger button until the second step (the step of sampling, which should be count), the plunger button hits the micro switch, the counter counts.

The mechanical touch, between the plunger button and the switch makes the device not to be able to work for a long time. Also, a switch as small as needed wasn't found (Fig. 10).

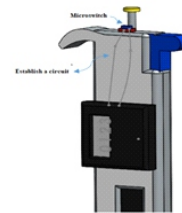


Fig. 10: Solution 4

4-5 Solution 5:

Copper Wire and Ring

In this solution, a ring was attached under the plunger button, and 2 wires were attached from the counter to the sampler body. When the experimenter pushed the plunger button for sampling, the wires reached the ring and the counter counted.

The disadvantages of this solution was that the copper wires and the ring had mechanical connection which let to make damage to them after several sampling (Fig. 11).

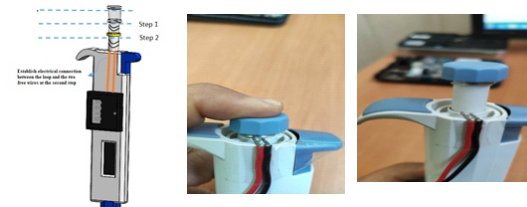


Fig. 11: Solution 5

4-6 Final Solution

Magnet/ Magnet key

In this idea, a magnet was put in the plunger rod hole and a magnet sensor was put on the sampler body, attaching by 2 wires to the counter which is also put on the sampler body, with a short distance of the sensor. The mechanism was that when the experimenter pushed the plunger button till the second step of sampling, the magnet became close to the sensor; consequently, an electrical pulse was induced which led to adding a number to the counter.

This idea had the most advantages. It was user-friendly and easy to use. Moreover, it was simply placed on the

other hand, the battery of counter consumed the least amount of energy, so it was not able to be destroyed even for several years. Furthermore, there was no mechanical connection between its component and it could work for years (Fig. 12).

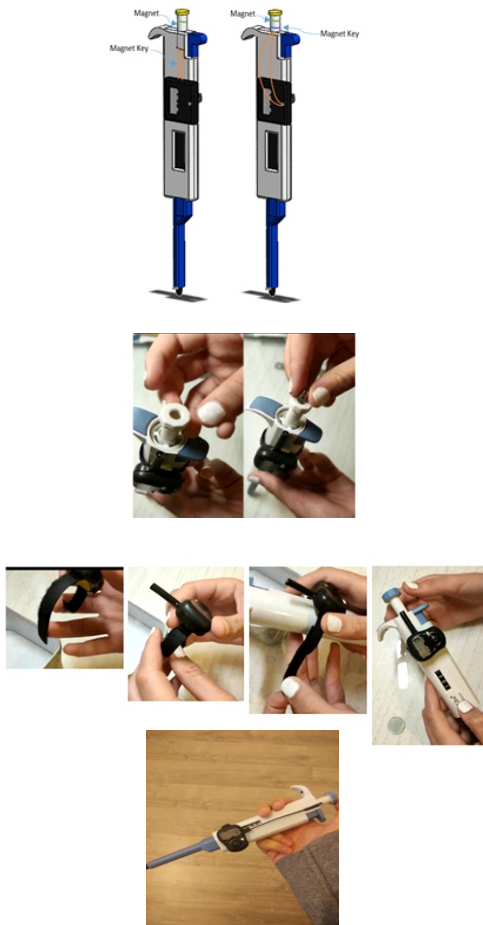


Fig. 12: Final Solution

We also did a 3D print for covering the counter in order to look better (Fig. 13).



Fig. 13: Final Design

5 Suggestion

There are some suggestions to expand this work. A program could be designed in order the counter be able to save the data. It may also be applied in other samplers by the sampler companies.



Ariaian Young Innovative Minds Institute, AYIMI
Unit 14, No. 32, Malek Ave., Shariati St.
Post Code: 1565843537
Tel - Fax: +9821-77522395, 77507013
Tehran/ Iran
URL: <http://www.ayimi.org>
<http://journal.ayimi.org>
Email: info@ayimi.org